NAVAL POSTGRADUATE SCHOOL
Monterey, California

THESIS

ROUNDOFF ALGORITHIMS FOR DIGITAL
PHASE SHIFTERS THAT
MINIMIZE BEAM SHIFT

by

Stanley E. Engle
Lieutentant, United States Navy
B.S., University of Kentucky, 1984

March, 1992

Thesis Advisor: D. C. Jenn
Second Reader: LCDR. H. J. Rood

**Approved for public release
distribution unlimited.**

REPORT DOCUMENTATION PAGE

Form Approved
OMB No 0704-0188

1a REPORT SECURITY CLASSIFICATION: UNCLASSIFIED	1b RESTRICTIVE MARKINGS
2a SECURITY CLASSIFICATION AUTHORITY	3 DISTRIBUTION / AVAILABILITY OF REPORT: Distribution unlimited; Approved for public release
2b DECLASSIFICATION / DOWNGRADING SCHEDULE	
4 PERFORMING ORGANIZATION REPORT NUMBER(S)	5 MONITORING ORGANIZATION REPORT NUMBER(S)
6a NAME OF PERFORMING ORGANIZATION: Naval Postgraduate School; 6b OFFICE SYMBOL (If applicable): EC	7a NAME OF MONITORING ORGANIZATION
6c ADDRESS (City, State, and ZIP Code): Monterey, CA 93943-5000	7b ADDRESS (City, State, and ZIP Code)
8a NAME OF FUNDING / SPONSORING ORGANIZATION; 8b OFFICE SYMBOL (If applicable)	9 PROCUREMENT INSTRUMENT IDENTIFICATION NUMBER
8c ADDRESS (City, State, and ZIP Code)	10 SOURCE OF FUNDING NUMBERS: PROGRAM ELEMENT NO; PROJECT NO; TASK NO; WORK UNIT ACCESSION NO

11 TITLE (Include Security Classification)

ROUNDOFF ALGORITHMS FOR DIGITAL PHASE SHIFTERS THAT MINIMIZE BEAM SHIFT

12 PERSONAL AUTHOR(S)
ENGLE, Stanley E.

13a TYPE OF REPORT	13b TIME COVERED	14 DATE OF REPORT (Year, Month, Day)	15 PAGE COUNT
Master's Thesis	FROM _____ TO _____	1992 March	161

16 SUPPLEMENTARY NOTATION
The views in this thesis are those of the author and do not reflect the official policy or position of the Department of Defense or the U. S. Government

17 COSATI CODES			18 SUBJECT TERMS (Continue on reverse if necessary and identify by block number)
FIELD	GROUP	SUB-GROUP	roundoff; beam shift; phase shifters; bitsize; pointing error; null depth; sidelobe

19 ABSTRACT (Continue on reverse if necessary and identify by block number)

The performance of a phased array antenna depends upon the phase and amplitude distribution across the aperture. A continuous linear phase distribution is required for an efficient focussed beam, but practical phase shifters are digital devices and can only provide an approximation to a linear phase distribution. Consequently some type of roundoff criteria must be established. The method of roundoff affects the radiation pattern characteristics such as beam location and sidelobe level. Accurate target tracking requires that a radar have a small beam pointing error. Low sidelobes are also desirable to prevent jamming and the illumination of clutter. Therefore the goal was to select a roundoff criterion that provides a phase distribution across the aperture to minimize both the beam shift and the sidelobe levels, while simultaneously maximizing the gain. The methods examined are referred to regular roundoff, weighted random roundoff, running sum roundoff and symmetric running sum roundoff. The first two are in common use, but the third and fourth are new methods examined in this paper. It was demonstrated that the latter two have the minimum beam shift ofthe four roundoff methods, without significantly degrading the other pattern properties.

20 DISTRIBUTION / AVAILABILITY OF ABSTRACT	21 ABSTRACT SECURITY CLASSIFICATION
[X] UNCLASSIFIED/UNLIMITED [ ] SAME AS RPT [ ] DTIC USERS	UNCLASSIFIED
22a NAME OF RESPONSIBLE INDIVIDUAL: D. C. Jenn	22b TELEPHONE (Include Area Code): (408) 646-2254; 22c OFFICE SYMBOL: EC/Jn

Approved for public release; distribution is unlimited.

Roundoff Algorithms for Digital Phase Shifters that Minimize Beam Shift

by

Stanley E. Engle
Lieutenant , United States Navy
B.S., University of Kentucky

Submitted in partial fulfillment
of the requirements for the degree of

MASTER OF SCIENCE IN ELECTRICAL ENGINEERING

from the

ABSTRACT

The performance of a phased array antenna depends upon the phase and amplitude distribution across the aperture. A continuous linear phase distribution is required for an efficient focussed beam, but practical phase shifters are digital devices and can only provide an approximation to a linear phase distribution. Consequently some type of roundoff criteria must be established. The method of roundoff affects the radiation pattern characteristics such as beam location and sidelobe level. Accurate target tracking requires that a radar have a small beam pointing error. Low sidelobes are also desirable to prevent jamming and the illumination of clutter. Therefore the goal was to select a roundoff criterion that provides a phase distribution across the aperture to minimize both the beam shift and the sidelobe levels, while simultaneously maximizing the gain. The methods examined are referred to regular roundoff, weighted random roundoff, running sum roundoff and symmetric running sum roundoff. The first two are in common use, but the third and fourth are new methods examined in this paper. It was demonstrated that the latter two have the minimum beam shift of the four roundoff methods, without significantly degrading the other pattern properties.

TABLE OF CONTENTS

LIST OF TABLES

LIST OF FIGURES

I. INTRODUCTION

Early radar and communication systems used antenna arrays consisting of a combination of separate radiating elements. These systems date back to the turn of the century [Ref. 1: p. 11-2]. The antenna radiation characteristics are determined by the position of the radiating elements and the amplitude and phase excitation relationships. As the operating frequency of radar systems increased (decreased wavelength), array antenna radars where replaced by simpler parabolic antennas. With the advent of printed circuit technology, electronically controlled phase shifters have become more compact and low cost. Consequently attention has been directed to array antennas again. The aperture excitation may now be modulated by controlling the individual elements to give beams that are scanned electronically [Ref. 1: p. 11-2]. An electronically steered array antenna can track a large number of targets, illuminate targets with RF energy to guide missiles toward targets, perform a complete hemispherical search with automatic target selection, and perform multiple functions in communication systems [Ref. 1: p. 11-2].

The performance of a phased array antenna depends upon the phase and amplitude distribution across the aperture. A continuous linear phase distribution is required for an

efficient focussed beam, but practical phase shifters are digital devices and can only provide an approximation to a linear phase distribution. Consequently some type of roundoff criteria must be established. However the method of roundoff affects the radiation pattern characteristics such as beam location and sidelobe level. Accurate target tracking requires that a radar have a small beam pointing error. Low sidelobes are also desirable to prevent jamming and the illumination of clutter. Therefore the goal is to select a roundoff criterion that provides a phase distribution across the aperture to minimize both the beam shift and the sidelobe levels, while simultaneously maximizing the gain.

This paper examines the performance degradation of a linear array due to the quantization of phase, which is present in all practical electronically scanned arrays. Analysis was restricted to linear arrays so that the simulations were computationally fast. The same techniques can be extended to two and three dimensional arrays. The performance of a monopulse antenna were simulated on the computer for a linear array using the Bayliss distribution. A Bayliss distribution is a low sidelobe difference beam distribution commonly used in radar. An ideal difference beam has a perfect null at the scan angle for a continuous linear phase distribution. When phase and amplitude errors are present, a perfect null is not possible. In practice a good null is about 35 dB below the sum beam peak [Ref. 1: p. 21-22].

The size of the arrays studied was be limited to 26, 50, and 76 radiating elements using 3, 4, and 5 bit phase shifters. A phase bit is a measure of how accurately a phase shifter can represent a linear phase by a step approximation; the more bits, the closer the phase steps. Although a large number of bits reproduce a linear phase better, they add cost and complexity to the antenna. Thus there is a tradeoff between the bitsize and antenna performance. In addition to the phase bitsize, the method of roundoff also affects the antenna performance. Four different methods of phase roundoff were examined to access their impact on antenna performance. The methods examined are referred to as regular roundoff, weighted random roundoff, running sum roundoff and symmetric running sum roundoff. The first two are in common use, but the third and fourth are new methods examined in this paper. It was demonstrated that the latter two will have the minimum beam shift of the four roundoff methods, without significantly degrading the other pattern properties. The antenna system parameters evaluated include the beam pointing error, maximum sidelobe level, and the null depth of the difference beam.

This paper is divided into the following sections: basic antenna array theory, phase shifters, phase quantization algorithms, and analysis of the data.

II. PHASE SHIFTERS: AN OVERVIEW

The evolution of sophisticated phased array antennas is due to two factors: the development of electronically controlled phase shifters and the integration of computers into the system. Electronically controlled phase shifters allow the beam to be redirected in less than a few microseconds and the computer can process a large amount of data. The principle advantage of these two factors is the minimum amount of time spent moving a beam between targets and making decisions about detection and tracking [Ref. 1: p. 11-2]. The performance of a phased array antenna is highly dependent upon its phase shifters. An N bit phase shifter will have a most significant bit of π radians (180 degrees) and a least significant bit of $2\pi/2^N$ radians. For best performance, a large number of bits should be used in the phase shifters, while for minimum cost and complexity, a small number of bits is desired. Since most feed methods require a phase shifter at every element of the array, the performance, size and cost of the antenna system are strongly affected by the phase shifter [Ref. 1: 12-3,4].

Several parameters of phase shifter design impact the performance of the phased array radar. The issues of concern are insertion loss, switching time, drive power, phase error, and physical size. The insertion loss should be as low as possible to reduce the loss of power during transmission and

lower the signal-to-noise ratio at the receiver. A low insertion loss also reduces phase shifter heating due to ohmic losses. If amplifiers are used between the phase shifter and the radiating element, the power capacity and insertion loss become insignificant. The phase shifter switching time should be as short as possible. A long switching time increases the minimum radar range when non-reciprocal phase shifters are used and when a burst of pulses are transmitted in different directions [Ref. 1: p. 12-3,4].

The drive power should be as small as possible. A large amount of drive power generates heat and may require power supplies that are too large for the given system. They also require expensive driver circuit components [Ref. 1: p. 12-3]. The phase error should also be as small as possible. It should not reduce the antenna gain substantially on transmitting or raise sidelobes on receiving. One cause of phase error is the size of the least significant bit of digital phase shifters. Others are due to the tolerances in the phase shifters and driver. The maximum acceptable physical size is limited by the element separation (usually $\lambda/2$ by $\lambda/2$) in order to be packaged behind each radiating element [Ref. 1: p. 12-3,4].

Today there are two types of phase shifters used in radar systems: ferrite and diode. Ferrite phase shifters are analog devices, although in practice they are digitally controlled. The first ferrite phase shifter employed in an operational phased array was the Reggia-Spencer phase shifter. The

development of a latching toroidal ferrite phase shifter, which employs a transverse magnetizing field, made significant improvements. The driving power was reduced and the driver circuitry was simplified. Also, the switching time was reduced from about a millisecond to a few microseconds. Ferrite phase shifters are impractical in radar systems operating at L-band (1 to 2 Ghz) frequencies and below since the magnetizing field is operating below resonance. This is due to available materials, which have a lower limit of saturation moment of approximately 200 gauss. At L band, a large saturation moment produces peak power limiting at a low power level, in a reasonably compact phase shifter. In addition, a low moment material is very temperature sensitive [Ref. 1: p. 12-4,5].

Diode phase shifters were developed with the recognition of the importance of the pn diode in radar systems. As fabrication techniques improved the diode breakdown voltage, cutoff frequencies, and reliability increased. Diode phase shifters are temperature insensitive over a wide range and do not require air or water cooling, as do the ferrite phase shifters. Use of diode phase shifters in radar systems is practical at all operating frequencies. At lower frequencies (below L band) diode phase shifters perform better since the semiconductor loss decreases as frequency decreases. This decrease can be traded for high peak power performance by adjusting the impedance of the transmission line on which the diodes are mounted [Ref. 1: p. 12-4,5].

At frequencies at or above L band, the selection of the phase shifter type is more difficult, because of high diode phase shifter losses and the difficulty in maintaining manufacturing tolerances. Table 1 summarizes the performance of the phase shifters at these frequencies [Ref. 1: p. 12-5].

TABLE 1: SUMMARY OF PERFORMANCE OF TYPICAL FERRITE AND DIODE PHASE SHIFTERS

	FERRITE(TOROIDAL) PHASE SHIFTER	**DIODE PHASE SHIFTER**
INSERTION LOSS	1.0 dB	1.0-2.0 dB, increases with the number of bits
SWITCHING TIME	2.0-5.0 μsec	50 nsec - 2 μsec
DRIVE POWER	2 W AT 1,000 pps	1.0-2.5 W
TRANSMITTED POWER	75 kW PEAK, 400 W AVERAGE	10 kW PEAK, 200 W AVERAGE

III. ANTENNA ARRAY THEORY

In the following discussion an antenna array refers to a group of similar elements arranged in an arbitrary geometric configuration, and excited with a prescribed phase and amplitude relation to give a desired radiation pattern. The radiation characteristics most commonly examined are the direction and width of the main beam, sidelobe levels, and null depth or main lobe level. In this chapter the fundamental theory and characteristics of linear arrays will be examined.

The total radiation pattern is the sum of the contributions from the individual elements. For a linear array having N radiators, with element n excited by amplitude, a_n, and phase, ψ_n, and inter-element spacing s, the radiation pattern is

$$E(\theta) = \sum_{n=0}^{N-1} a_n e^{j\left(\frac{2\pi}{\lambda} ns(\sin(\theta)+\psi_n)\right)} f(\theta) \qquad \text{(III-1)}$$

where $f(\theta)$ is the radiation pattern of a single element [Ref. 1: p. 11-9]. A typical linear array is shown in Figure 1. The term ψ_n includes the inter-element phase to scan the beam as well as any phase errors that may be present. For convenience, the scanning phase of $2\pi s \sin(\theta_o)/\lambda$ radians per element will be separated out so that ψ_n is entirely due to the phase error [Ref 1. : p. 11-9],

$$E(\theta) = f(\theta)\, e^{-j\frac{2\pi}{\lambda}\frac{[N-1]}{2}s(\sin(\theta)-\sin(\theta_0))} \sum_{n=0}^{N-1} a_n e^{j[\frac{2\pi}{\lambda}ns(\sin(\theta)-\sin(\theta_0)+\psi_n]} \quad . \qquad \textbf{(III-2)}$$

The leading exponential references the phase to the center of the array and will be dropped since it represents a phase shift common to all elements and does not affect the antenna pattern.

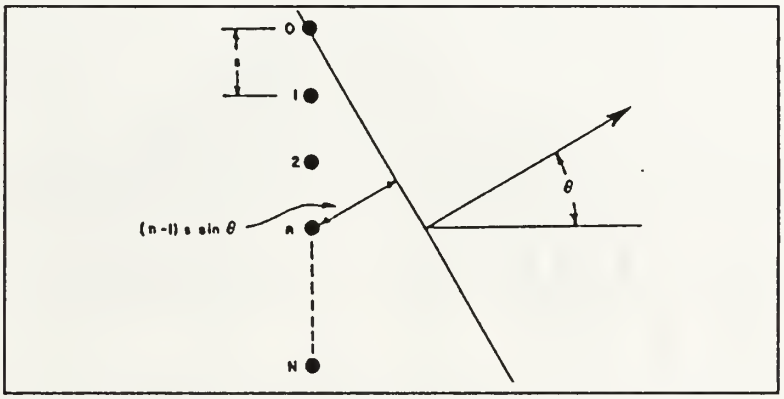

Figure 1. Linear Array with N Radiators Uniformly Spaced by a Distance s

If there are no phase errors and all amplitudes are equal (ψ_n=0 and a_n= 1), then equation III-2 can be reduced to a closed form expression, [Ref 1: p. 11-9]

$$E(\theta) = f(\theta)\, \frac{\sin[N\pi\frac{S}{\lambda}(\sin(\theta)+\sin(\theta_0))]}{N\sin[\pi\frac{S}{\lambda}(\sin(\theta)+\sin(\theta_0))]} \quad . \qquad \textbf{(III-3)}$$

Equations III-2 and III-3 are the fundamental response equations for a scanned array system. As a typical example, Figure 2 shows the radiation pattern calculated from equation

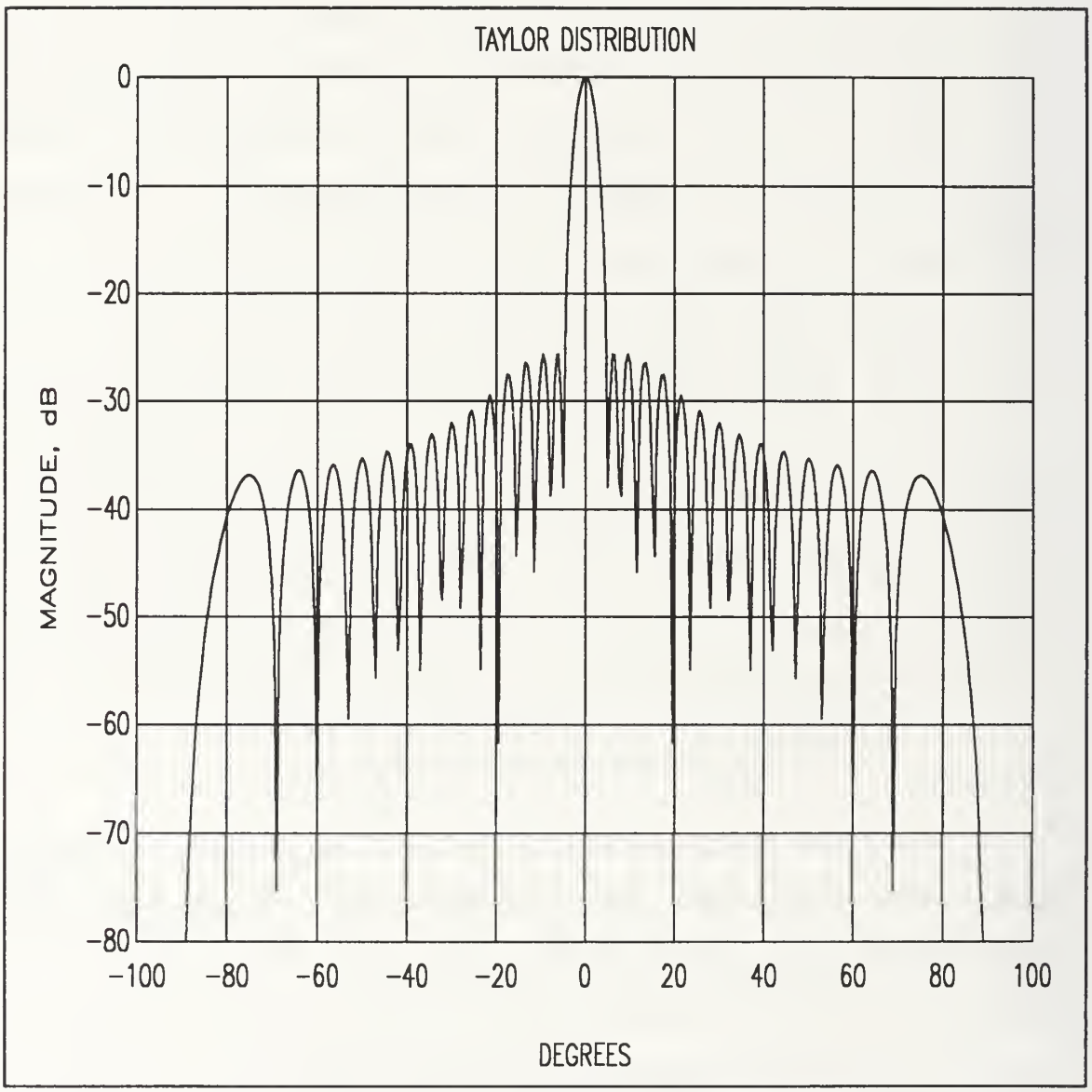

Figure 2. A Continuous Linear Phase Taylor Distribution

III-2 , with 50 elements and s = .3λ . In this case all ψ_n are zero and the a_n are chosen to give a 25 dB Taylor distribution. The radiation pattern will have only one major

lobe and grating lobe maxima will not occur for values of $-\pi/2 < \theta < \pi/2$ as long as [Ref. 1: p. 11-11]

$$\frac{\pi s}{\lambda}(\sin(\theta)-\sin(\theta_o)) < \pm\pi \quad . \qquad \textbf{(III-4)}$$

The beam of an antenna points in the direction normal to the phase front. In phased arrays, the phase front is adjusted by controlling the phase of each radiating element, as shown in Figure 3.

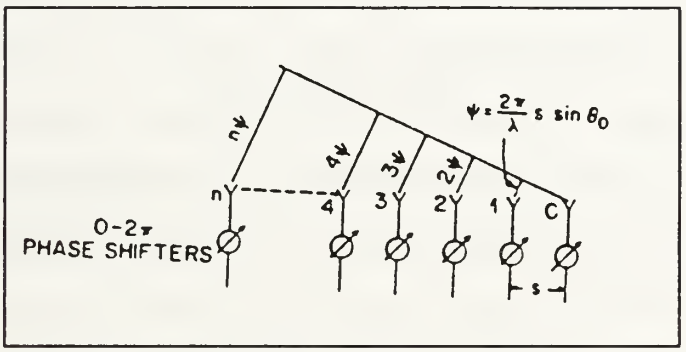

Figure 3. Phased Array

A. RADIATING ELEMENTS

The most common type of radiating elements used in array antennas are slots, dipoles, horns, and more recently conductive patches. Since the size of the radiating element is constrained to fit in the array geometry, the area of the elements are limited to approximately $\lambda^2/4$. The predominate electrical factors in choosing the radiating element in an array environment is the impedance and the pattern of a

radiator. Another factor that influences the type of element is the feeding method. The radiating element should be chosen so that the antenna aperture and feed system can be packaged to satisfy the size and weight requirements of the antenna. For example, if the feed system contains stripline components, a stripline dipole would be the optimal choice. On the other hand, if waveguide feed devices are used, open-ended waveguides or small horn antennas are more convenient [Ref 1: p. 11-5].

Most well matched antenna elements have element patterns that can be approximated by $f(\theta) = \cos(\theta)$, at least for angles near broadside (normal to the antenna aperture). In this analysis only the array factor is considered; the element pattern will be neglected ($f(\theta) = 1$). This simplification will not significantly affect the results because the scan angles of interest are limited to $\theta_o = \pm 60°$, and comparisons are referenced to an error-free array also with $f(\theta) = 1$.

IV. PHASE QUANTIZATION ALGORITHMS

In order to steer a focused beam to a certain direction, a linear phase must be set up across the aperture according to equation III-2. However, most phase shifters are digital devices and the allowable phase values are limited by the bit size. Therefore, in most instances the phase at each element must be quantized. For a n bit phase shifter the bit size is determined by

$$Bit\ Size = \frac{360}{2^n} \quad . \qquad \textbf{(IV-1)}$$

Each allowable phase shifter value is referred to as a phase state. The phase states are given by

$$\phi_i = (i-1) \cdot Bit\ Size \qquad i = 1,2,3,\ldots,2^n \quad . \qquad \textbf{(IV-2)}$$

For example, a 4 bit device has a bit size of $360°/2^4 = 22.5°$ and 16 phase states. The difference between the desired phase and the quantized phase is denoted the quantization error.

In this paper four different methods of phase quantization were used to examine the phased array antenna performance. They are regular roundoff, weighted random roundoff, running sum roundoff and symmetric running sum roundoff. Each of these methods of phase quantization is discussed in detail in the following sections.

To examine the impact of quantization error on the difference beam radiation pattern consider equation III-2:

$$E(\theta) = \sum_{n=0}^{N-1} a_n e^{j(\frac{2\pi}{\lambda} s\, n\, (\sin(\theta) - \sin(\theta_o)) + \psi_n)} \qquad \textbf{(IV-3)}$$

where a_n is the Bayliss coefficient and ψ_n is the quantization error at the nth element. Equation IV-3 assumes a line source and that the only errors present are those due to the phase quantization. Therefore at any scan angle

$$E(\theta_o) = \sum_{n=0}^{N-1} a_n e^{j\psi_n} \quad . \qquad \textbf{(IV-4)}$$

For a difference beam the coefficients a_n will be positive for one half of the elements ($1 \leq n \leq N/2$, N even) and negative for the other half ($N/2 + 1 \leq n \leq N$). Thus, if a null is to occur at θ_o then $|E(\theta_o)| \rightarrow 0$, [Ref. 2: p. 2] and the weighted sum of the quantization errors must be zero.

A. REGULAR ROUNDOFF

Regular roundoff is the most straightforward of the four methods considered. It involves calculating the desired phase at each radiating element and then rounding the phase up or down to the closest allowable state of the phase shifter. This method of phase estimation results in a periodic quantization error, the period of which varies with the bitsize and scan

angle. A typical desired versus quantized phase angle for regular roundoff is shown in Figure 4. This type of phase error causes large sidelobes and potentially large beam pointing errors.

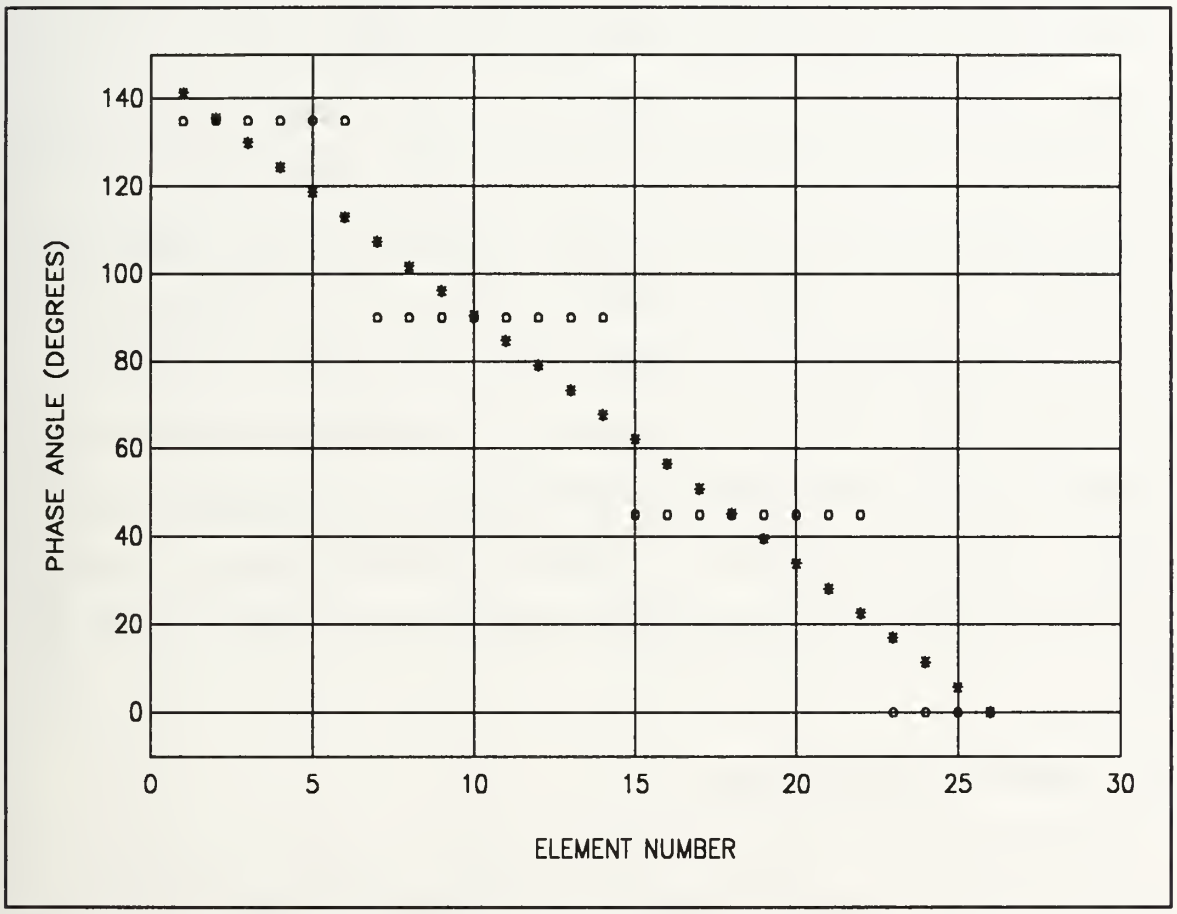

Figure 4. Desired (o) and Regular Roundoff (*) Phase Angle Distribution for a 26 Element Array, 3 Bit Phase Shifter

B. WEIGHTED RANDOM ROUNDOFF

This method rounds up or down randomly such that the expected value of the phase at any element is the desired value. This destroys the periodic quantization error, but also raises the average sidelobe level.

This method is implemented by choosing a random number uniformly distributed between 0 and 1 and assigning it to an element of the array. The algorithm combines the random number and the desired phase to determine the phase state at the given radiating element as follows. At each element the algorithm subtracts the closest phase state from the desired phase (which gives the regular roundoff quantization error) and divides the difference by the bitsize. The algorithm then adds this to the random number chosen for this particular element. If the sum is greater than one, the phase at the radiating element is rounded up, otherwise the phase is rounded down. Using this method, the expected value of the quantization error tend towards zero as the number of the array elements increases. A typical desired versus weighted random roundoff algorithm phase angle, ψ, is shown in Figure 5.

C. RUNNING SUM ROUNDOFF

This method chooses the phase state at the nth radiating element as the one which keeps the magnitude of the cumulative sum of the quantization errors the smallest. This minimizes the cumulative quantization error at any point along the array. For instance, at element n the algorithm compares the cumulative quantization error that results from either rounding up or down at the element. The algorithm then chooses the phase state that minimizes this total quantization error.

This condition will give $|E(\theta_o)| \rightarrow 0$ as the number of elements is increased. A typical desired versus running sum roundoff algorithm phase angle, ψ, is shown in Figure 6.

D. SYMMETRIC RUNNING SUM ROUNDOFF

This method is related to the running sum roundoff just

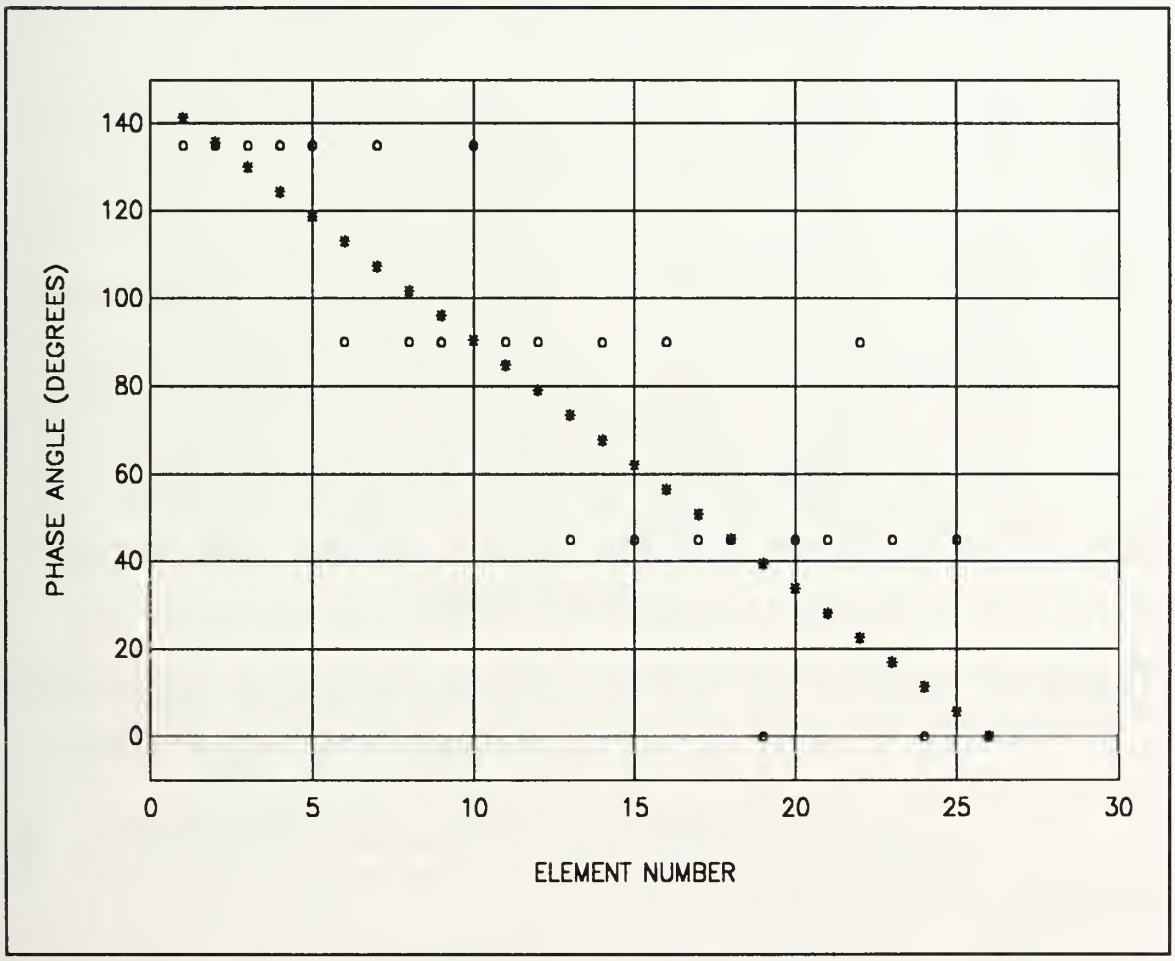

Figure 5. Desired (o) and Weighted Random Roundoff (*) Phase Angle Distribution for a 26 Element Array, 3 Bit Phase Shifter

described, but takes advantage of the phase symmetry across the array. If the phase reference is defined at the center of

the array, then elements located at equal distances from the center will have equal but opposite phase values. For one half

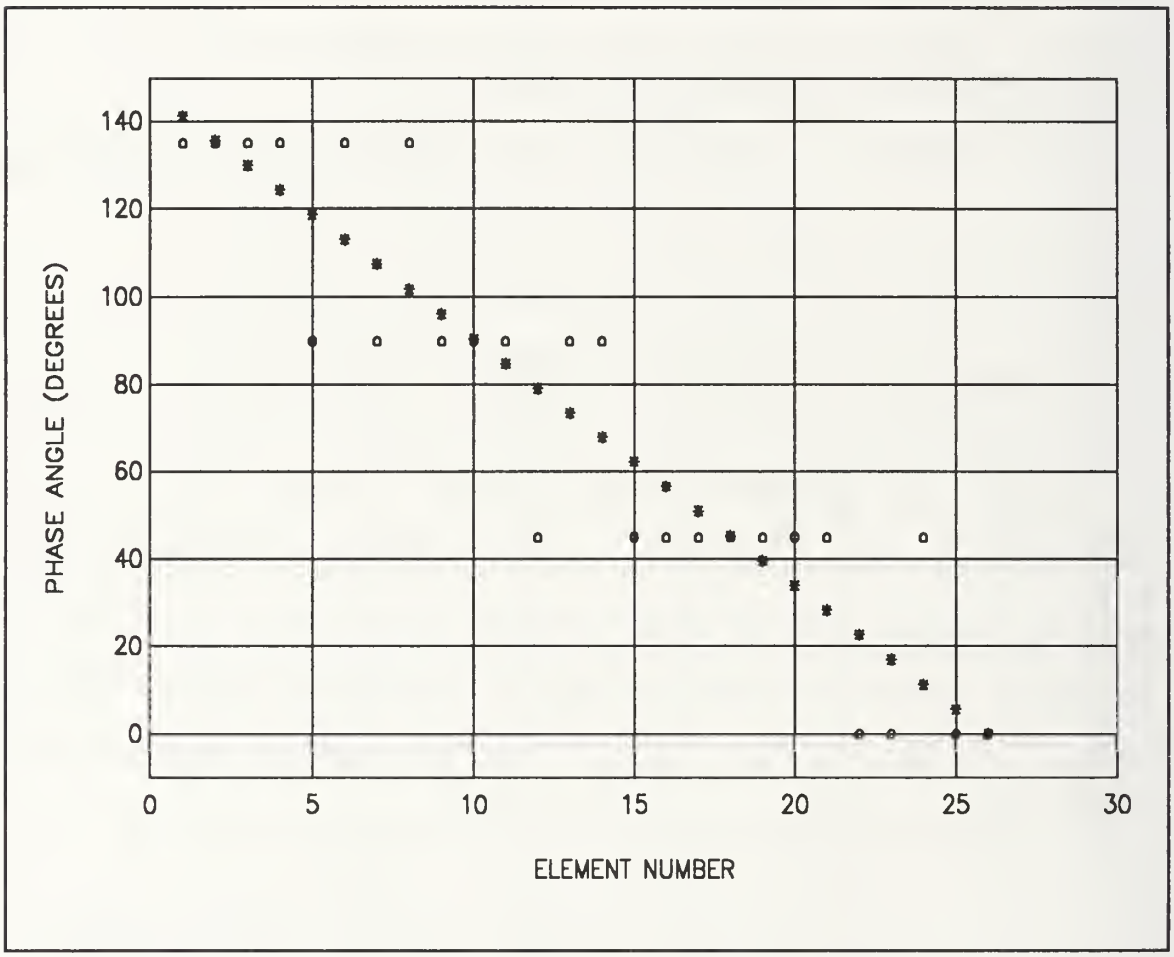

Figure 6. Desired (o) and Running Sum Roundoff Phase Angle Distribution for a 26 Element Array, 3 Bit Phase Shifter

of the array, the running sum roundoff algorithm can be used to determine the quantized phase. The phase state for the corresponding elements on the second half of the array will be set so that the quantization error is equal and opposite.

The rational for this approach is based upon equation IV-4, which for a sum beam with a symmetric amplitude distribution becomes,

$$E(\theta_o) = \sum_{n=1}^{N} a_n e^{j\psi_n}$$
$$= \sum_{n=1}^{\frac{N}{2}} a_n (e^{j\psi_n} + e^{j\psi_{N+1-n}}) \quad . \qquad \text{(IV-5)}$$

For small errors,

$$E(\theta_o) \approx \sum_{n=1}^{\frac{N}{2}} a_n (2 + j\psi_n + j\psi_{N+1-n}) \quad . \qquad \text{(IV-6)}$$

Thus choosing $\psi_{N+1-n} = -\psi_n$ will force the error in each term of the sum to zero. In practice this is not possible because the cosine term from the exponential, which leads to the 2, is significantly in error. Therefore the peak of the beam is somewhat less than $\Sigma\ a_n$. This method is included in the study to determine whether there is a symmetric property that can be exploited. A typical desired versus symmetric running sum roundoff algorithm phase angle, ψ, is shown in Figure 7.

E. QUANTIZATION ERROR AND NULL DEPTH AND LOCATION

In the case of a difference beam, if the roundoff algorithm could set up a linear phase across the aperture at a scan angle, then there would be a perfect null at that angle (i.e. zero pointing error and zero gain). Since the bitsize of the phase shifter is limited, applying a roundoff algorithm to

an array fills the null and introduces a pointing error, as shown in Figure 8. The phase error causes the null to be

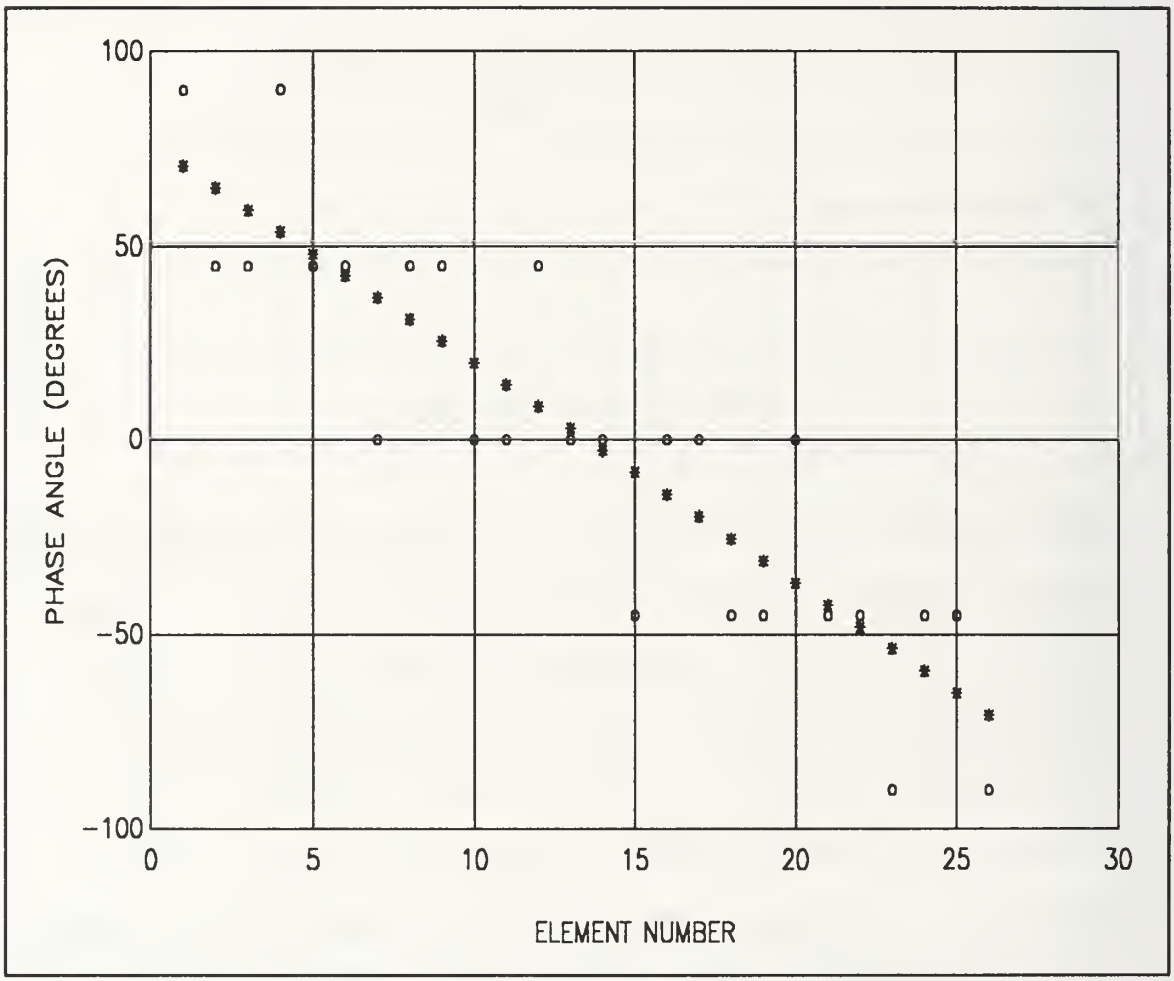

Figure 7. Desired (o) and Symmetric Running Sum Roundoff Phase Angle Distribution for a 26 Element Array, 3 Bit Phase Shifter

rounded instead of a sharp notch, and moves the minimum value away from θ_o. Both the location and depth of the null are important. If a null is sharp but located at the wrong angle, a tracking error will be introduced in a radar system. If the null is too shallow (rounded), then the radar will not be able

to position the minimum on the target, and again a tracking error will be introduced.

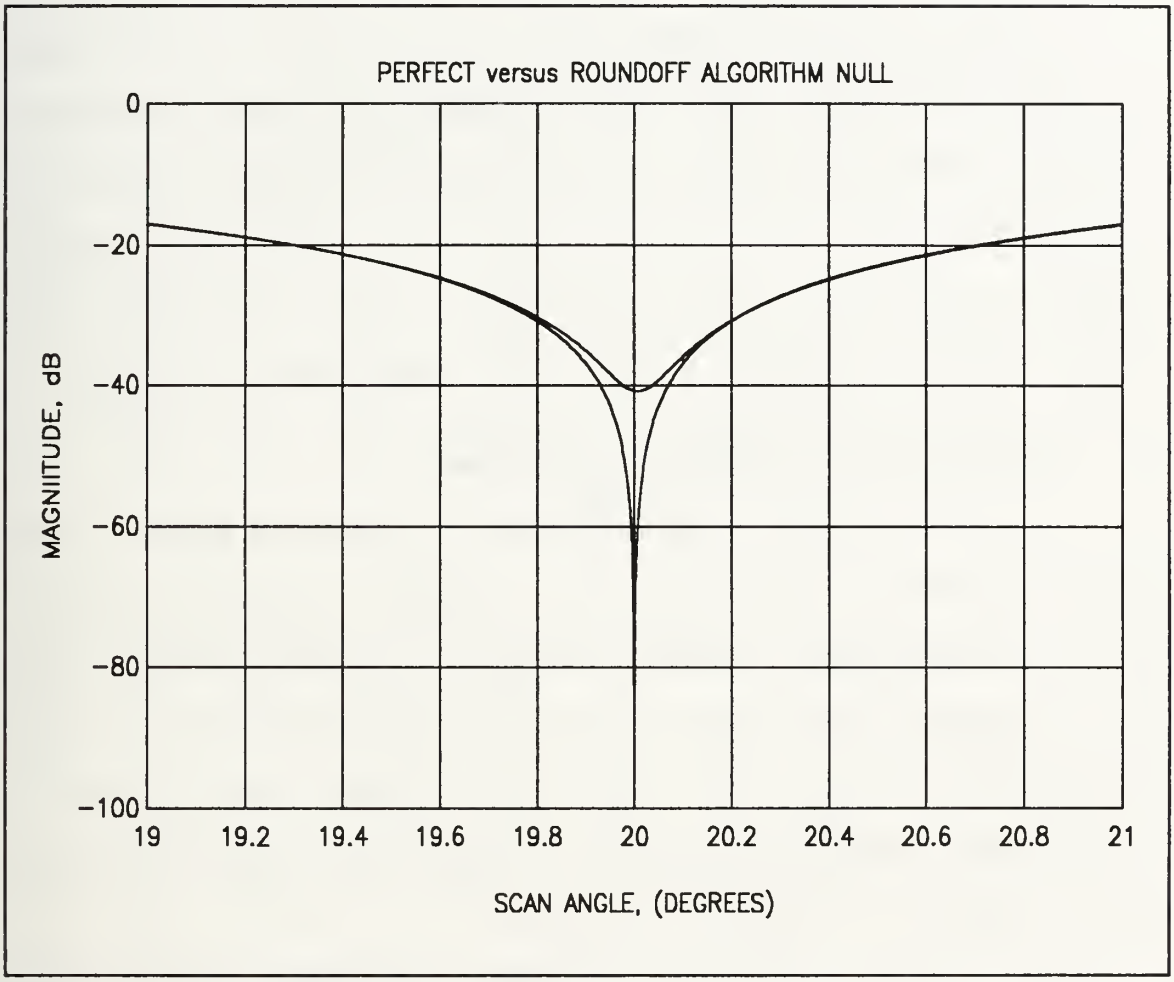

Figure 8. Perfect Bayliss Difference Beam Null versus Roundoff Algorithm Null

V. ANALYSIS OF THE DATA

In this chapter, data from the different phased array antenna configurations will be examined. Comparisons will examine the effects on the null depth, sidelobe levels, and pointing error as a function of the number of elements, roundoff algorithm, and the number of bits. Only one of the these will be changed in any given comparison.

A. COMPARISON BY ROUNDOFF ALGORITHMS

In this section, typical data is presented for an array of 50 elements using the four roundoff algorithms with 3 bit phase shifters. Figures 9 through 12 illustrate the range of sidelobes, null depth and null location that results from quantization errors. The statistics from a large number of calculated patterns at 61 scan angles (0° to 60° in 1° steps) are presented in tables 2 through 7.

The running sum and symmetric running sum roundoff algorithms had the minimum pointing error, in most cases a factor of 10 smaller than the other two algorithms. All four algorithms were comparable as far as sidelobe levels are concerned.

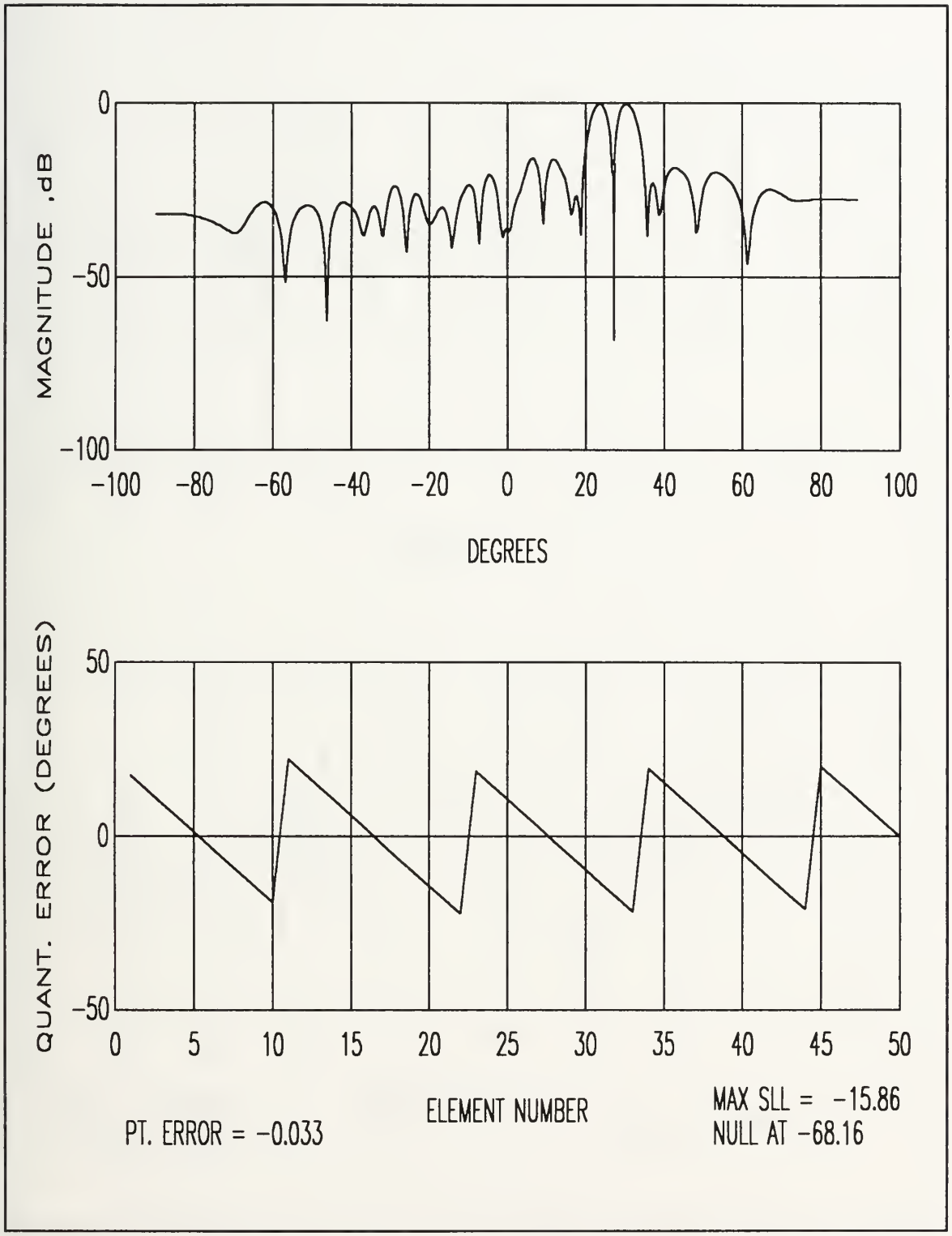

Figure 9. 50 Element Array Bayliss Difference Beam Radiation Pattern for a 3 Bit Phase Shifter using Regular Roundoff

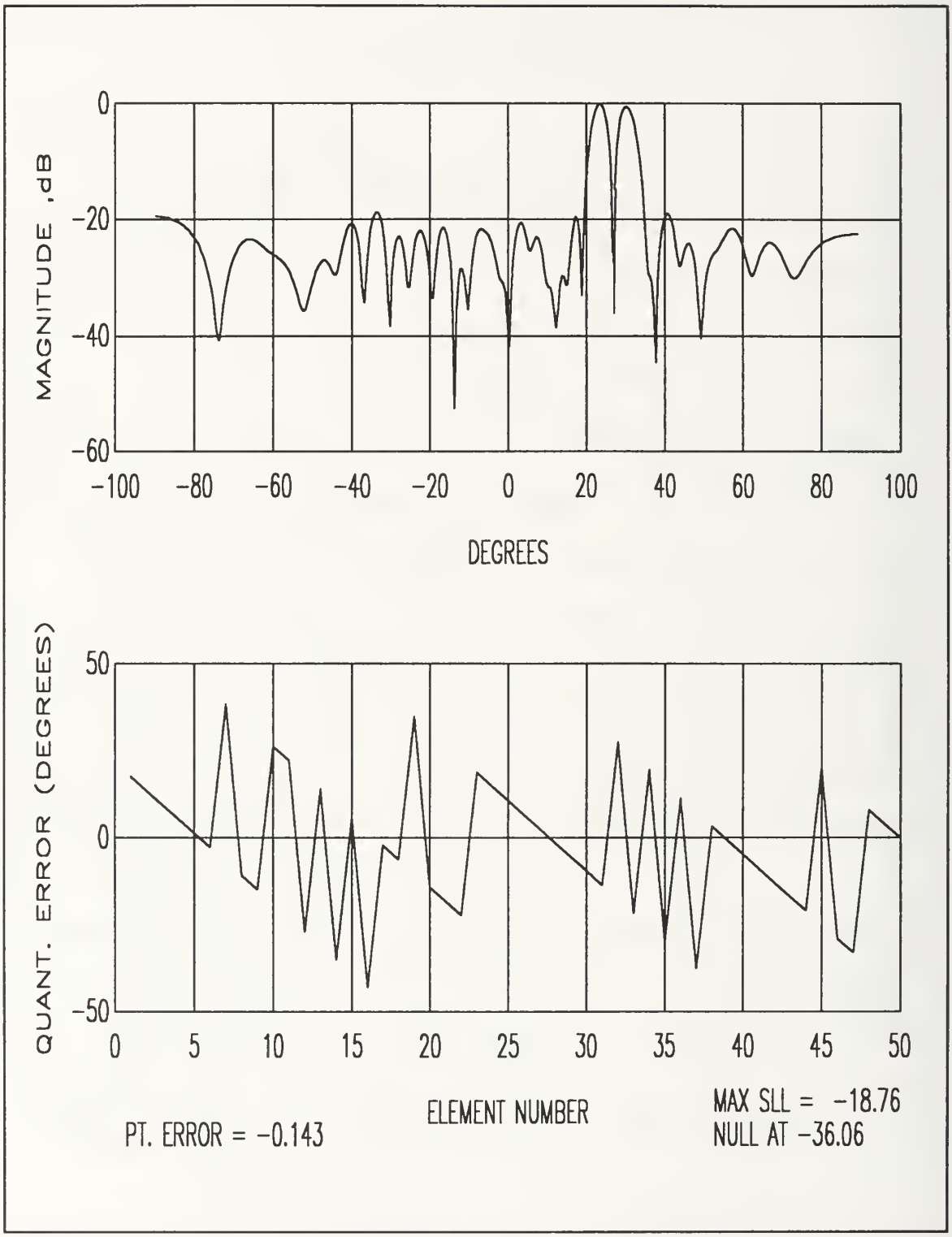

Figure 10. 50 Element Array Bayliss Difference Beam for a 3 Bit Phase Shifter using Weighted Random Roundoff

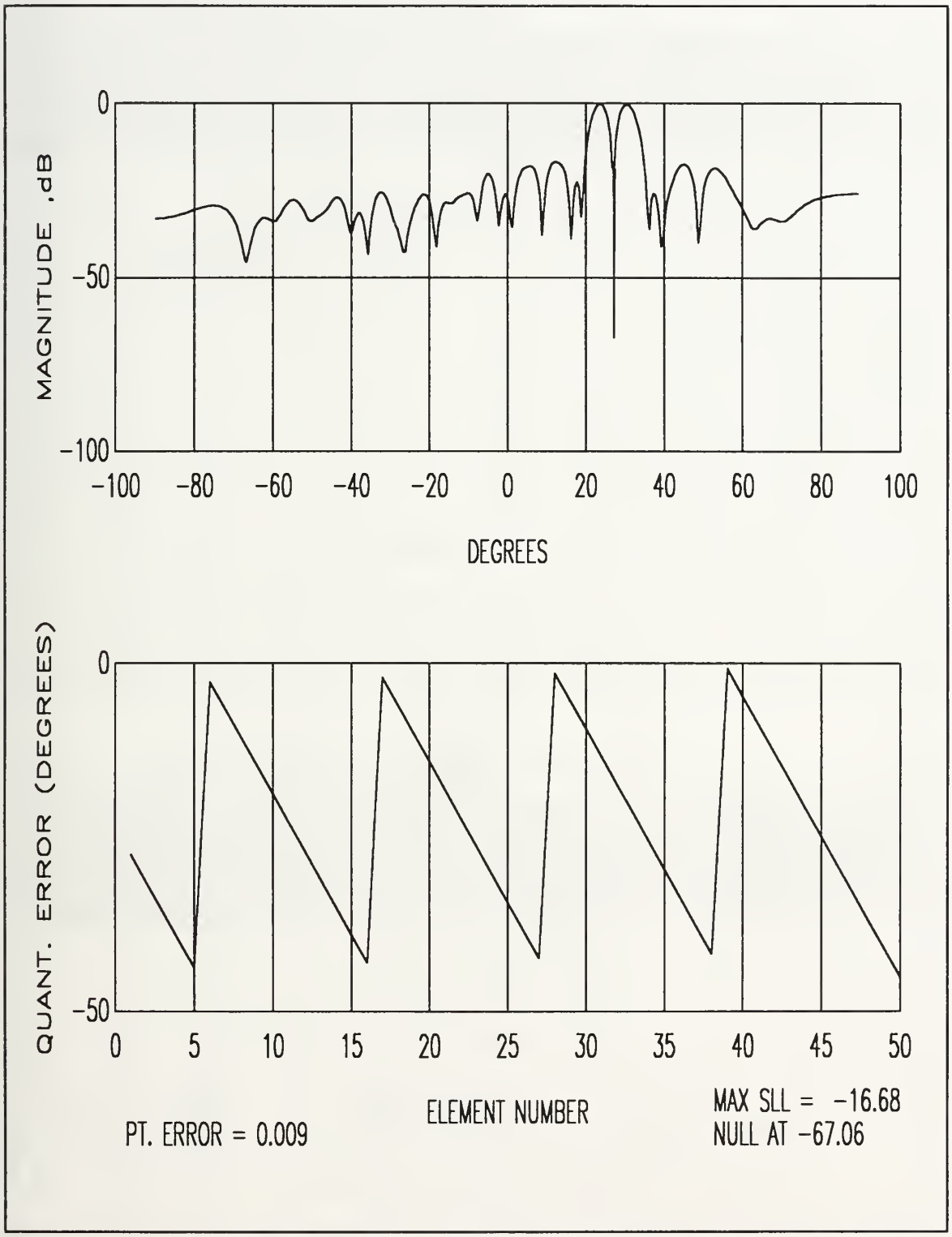

Figure 11. 50 Element Array Bayliss Difference Beam for a 3 Bit Phase Shifter using Running Sum Roundoff

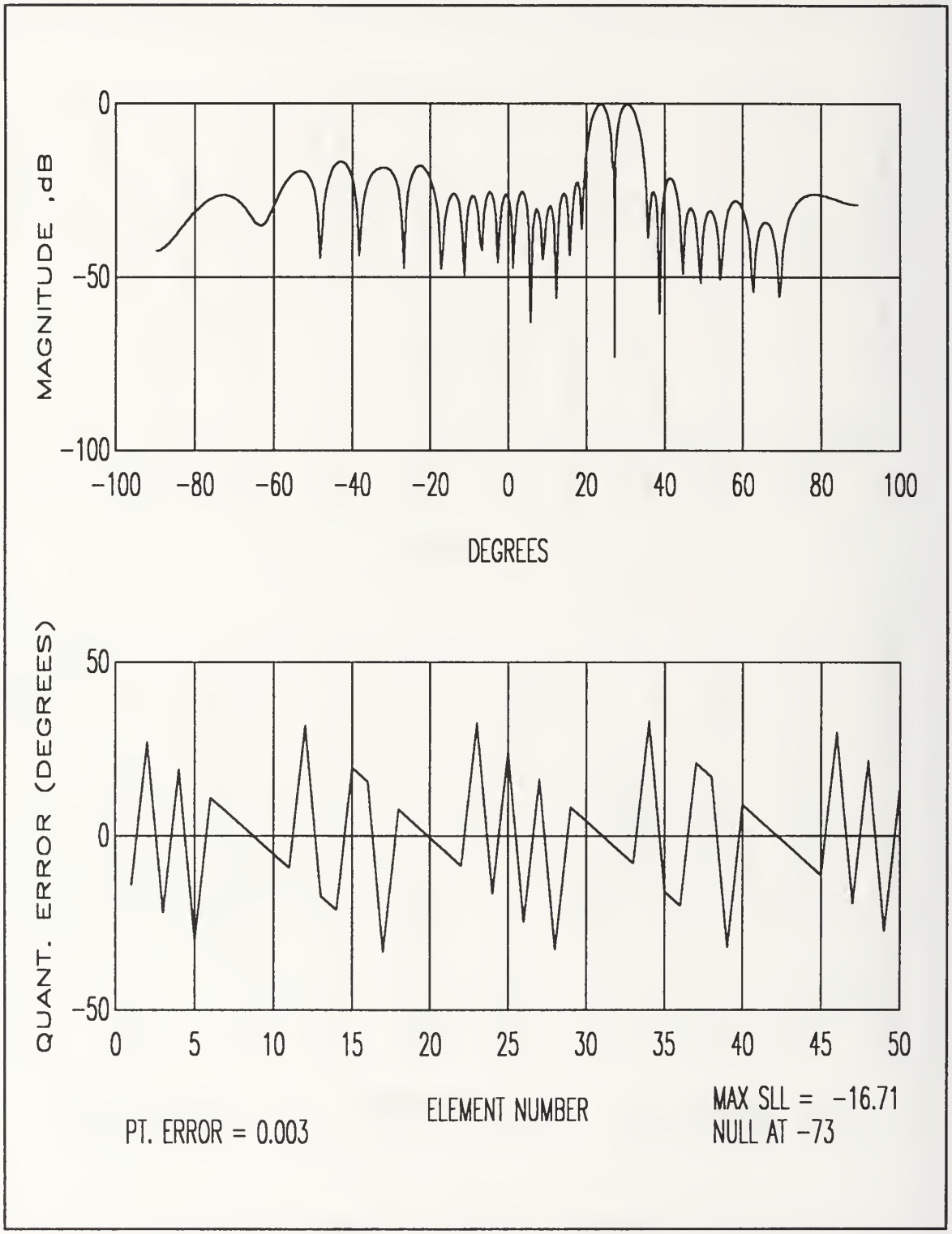

Figure 12. 50 Element Array Bayliss Difference Beam for a 3 Bit Phase Shifter using Symmetric Running Sum Roundoff

TABLE 2. COMPARISON OF 26 ELEMENT ARRAYS WITH 25 dB SIDELOBE LEVEL USING DIFFERENT ALGORITHMS

Number of Elements /Roundoff Algorithm	# of Bits	Pointing Error Mean / Variance (milli Degree)	Null Depth Mean (dB)	Sidelobe Level Mean/ Variance (dB)
26/ REG	3	23.10 / 66.84	-66.39	-17.24 / 7.87
26/ WGT	3	-10.10 / 123.72	-44.03	-16.00 / 3.80
26/ RUN	3	- 4.67 / 3.97	-63.00	-17.66 / 8.69
26/ SYM	3	- 1.64 / 3.83	-88.64	-15.53 / 6.48
26/ REG	4	7.85 / 13.59	-77.49	-21.03 / 3.76
26/ WGT	4	-44.44 / 34.40	-52.75	-20.10 / 2.49
26/ RUN	4	0.90 / 0.91	-75.75	-20.95 / 3.09
26/ SYM	4	- 2.39 / 1.11	-88.27	-19.09 / 4.56
26/ REG	5	- 9.93 / 5.11	-82.72	-23.56 / 1.10
26/ WGT	5	-13.80 / 8.72	-66.90	-22.80 / 1.03
26/ RUN	5	- 0.31 / 0.27	-82.22	-23.20 / 0.80
26/ SYM	5	1.70 / 0.34	-87.02	-22.39 / 2.42

TABLE 3. COMPARISON OF 26 ELEMENT ARRAYS WITH 40 dB SIDELOBE LEVEL USING DIFFERENT ALGORITHMS

Number of Elements /Roundoff Algorithm	# of Bits	Pointing Error Mean / Variance (milli Degree)	Null Depth Mean (dB)	Sidelobe Level Mean / Variance (dB)
26/ REG	4	6.74 / 10.760	-75.94	-20.95 / 5.69
26/ WGT	4	- 8.82 / 26.302	-52.41	-21.52 / 8.25
26/ RUN	4	- 2.16 / 1.525	-62.09	-21.22 / 6.86
26/ SYM	4	- 4.00 / 2.370	-87.43	-20.76 / 5.63
26/ REG	5	-10.80 / 4.981	-83.64	-28.55 / 7.78
26/ WGT	5	- 8.77 / 11.946	-66.50	-26.89 / 3.33
26/ RUN	5	0.64 / 0.376	-66.56	-26.54 / 4.15
26/ SYM	5	3.11 / 0.684	-91.24	-25.79 / 3.42

TABLE 4. COMPARISON OF 50 ELEMENT ARRAYS WITH 25 dB SIDELOBE LEVEL ARRAY USING DIFFERENT ALGORITHMS

Number of Elements /Roundoff Algorithm	# of Bits	Pointing Error Mean / Variance (milli Degree)	Null Depth Mean (dB)	Sidelobe Level Mean / Variance (dB)
50/ REG	3	- 0.31 / 9.337	-68.52	-17.38 / 5.44
50/ WGT	3	-32.85 / 18.455	-48.25	-17.56 / 2.38
50/ RUN	3	- 0.34 / 0.191	-65.69	-17.75 / 6.01
50/ SYM	3	- 2.69 / 0.191	-81.46	-16.18 / 6.48
50/ REG	4	- 5.74 / 5.126	-76.98	-21.99 / 2.69
50/ WGT	4	1.82 / 2.982	-56.64	-21.76 / 1.50
50/ RUN	4	- 0.85 / 0.052	-75.30	-21.88 / 2.53
50/ SYM	4	2.06 / 0.055	-83.68	-21.21 / 2.54
50/ REG	5	- 0.24 / 0.589	-81.49	-24.24 / 0.78
50/ WGT	5	4.50 / 1.616	-68.57	-23.67 / 0.88
50/ RUN	5	1.08 / 0.011	-80.06	-24.20 / 0.40
50/ SYM	5	0.60 / 0.017	-81.18	-24.14 / 1.05

TABLE 5. COMPARISON OF 50 ELEMENT ARRAYS WITH 40 dB SIDELOBE LEVEL ARRAY USING DIFFERENT ALGORITHMS

Number of Elements /Roundoff Algorithm	# of Bits	Pointing Error Mean / Variance (milli Degree)	Null Depth Mean (dB)	Sidelobe Level Mean / Variance (dB)
50/ REG	4	- 4.02 / 4.210	-76.49	-21.01 / 7.77
50/ WGT	4	14.80 / 5.863	-58.41	-21.89 / 5.99
50/ RUN	4	- 0.62 / 0.069	-58.30	-23.09 / 6.23
50/ SYM	4	3.38 / 0.111	-84.18	-22.32 / 6.79
50/ REG	5	0.84 / 0.839	-82.35	-29.17 / 5.21
50/ WGT	5	8.54 / 2.078	-67.45	-28.83 / 1.91
50/ RUN	5	0.67 / 0.014	-78.67	-28.59 / 3.20
50/ SYM	5	0.77 / 0.036	-83.14	-27.19 / 5.12

TABLE 6. COMPARISON OF 76 ELEMENT ARRAYS WITH 25 dB DESIRED SIDELOBE LEVEL USING DIFFERENT ALGORITHMS

Number of Elements /Roundoff Algorithm	# of Bits	Pointing Error Mean / Variance (milli Degree)	Null Depth Mean (dB)	Sidelobe Level Mean / Variance (dB)
76/ REG	3	4.18 / 9.655	-70.19	-17.98 / 4.95
76/ WGT	3	- 5.28 / 4.117	-48.50	-18.66 / 2.50
76/ RUN	3	- 0.30 / 0.042	-68.41	-18.15 / 6.99
76/ SYM	3	- 1.15 / 0.050	-80.79	-16.98 / 6.24
76/ REG	4	- 2.28 / 0.142	-74.74	-22.59 / 3.10
76/ WGT	4	- 0.41 / 1.863	-58.29	-22.46 / 1.05
76/ RUN	4	- 0.06 / 0.007	-74.55	-22.51 / 1.65
76/ SYM	4	- 0.07 / 0.008	-78.31	-22.64 / 2.18
76/ REG	5	- 2.69 / 0.112	-78.05	-24.42 / 0.60
76/ WGT	5	- 4.98 / 0.466	-68.49	-24.04 / 0.86
76/ RUN	5	- 0.05 / 0.002	-78.78	-24.22 / 1.91
76/ SYM	5	0.05 / 0.002	-79.54	-24.61 / 0.57

TABLE 7. COMPARISON OF 76 ELEMENT ARRAYS WITH 40 dB SIDELOBE LEVEL USING DIFFERENT ALGORITHMS

Number of Elements /Roundoff Algorithm	# of Bits	Pointing Error Mean / Variance (milli Degree)	Null Depth Mean (dB)	Sidelobe Level Mean / Variance (dB)
76/ REG	4	- 3.66 / 0.213	-78.14	-24.13 / 4.80
76/ WGT	4	- 1.80 / 1.868	-58.55	-25.31 / 3.36
76/ RUN	4	0.43 / 0.007	-64.40	-24.19 / 4.77
76/ SYM	4	- 0.18 / 0.017	-80.44	-23.66 / 4.39
76/ REG	5	- 2.96 / 0.123	-79.24	-29.68 / 2.42
76/ WGT	5	0.36 / 0.571	-68.22	-30.18 / 2.10
76/ RUN	5	- 0.08 / 0.002	-79.17	-29.82 / 3.74
76/ SYM	5	0.06 / 0.003	-80.02	-28.66 / 3.83

B. COMPARISON BY PHASE SHIFTER BITSIZE

In this section, the phase shifter bit size is varied while all of the other array parameters are held fixed. For all algorithms increasing the number of bits improved the sidelobe level, null depth, and beam pointing error. Therefore the data presented in this section will be limited to the symmetric running sum algorithm because the trends for the other roundoff algorithms are similar. The data is summarized in Table 8. Figures 13, 14, and 15 show the radiation pattern

TABLE 8. COMPARISON OF RADIATION CHARACTERISTICS OF ANTENNA ARRAYS USING SYMMETRIC RUNNING SUM ALGORITHM

# of Elem	# of Bits	Desired SLL (dB)	Pointing Error Mean / Variance (milli Degree)	Null Depth Mean (dB)	Sidelobe Level Mean / Variance (dB)
26	3	25	- 1.64 / 3.83	-88.64	-15.53 / 6.48
26	4	25	- 2.39 / 1.11	-88.27	-19.09 / 4.56
26	5	25	1.70 / 0.34	-87.02	-22.39 / 2.42
26	4	40	- 4.00 / 2.37	-87.43	-20.76 / 5.63
26	5	40	3.11 / 0.685	-91.23	-25.79 / 3.42
50	3	25	- 2.69 / 0.191	-81.46	-16.18 / 6.48
50	4	25	2.06 / 0.055	-83.68	-21.21 / 2.54
50	5	25	0.60 / 0.017	-81.18	-24.14 / 1.05
50	4	40	3.37 / 0.111	-84.18	-22.32 / 6.79
50	5	40	0.77 / 0.036	-83.14	-27.19 / 5.12
76	3	25	- 1.15 / 0.050	-80.79	-16.98 / 6.24
76	4	25	- 0.07 / 0.008	-78.31	-22.64 / 2.18
76	5	25	0.05 / 0.002	-79.54	-24.61 / 0.57
76	4	40	- 0.18 / 0.016	-80.44	-23.66 / 4.39
76	5	40	0.06 / 0.003	-80.02	-28.66 / 3.83

for a 76 element array using 3, 4, and 5 bit phase shifters, respectfully.

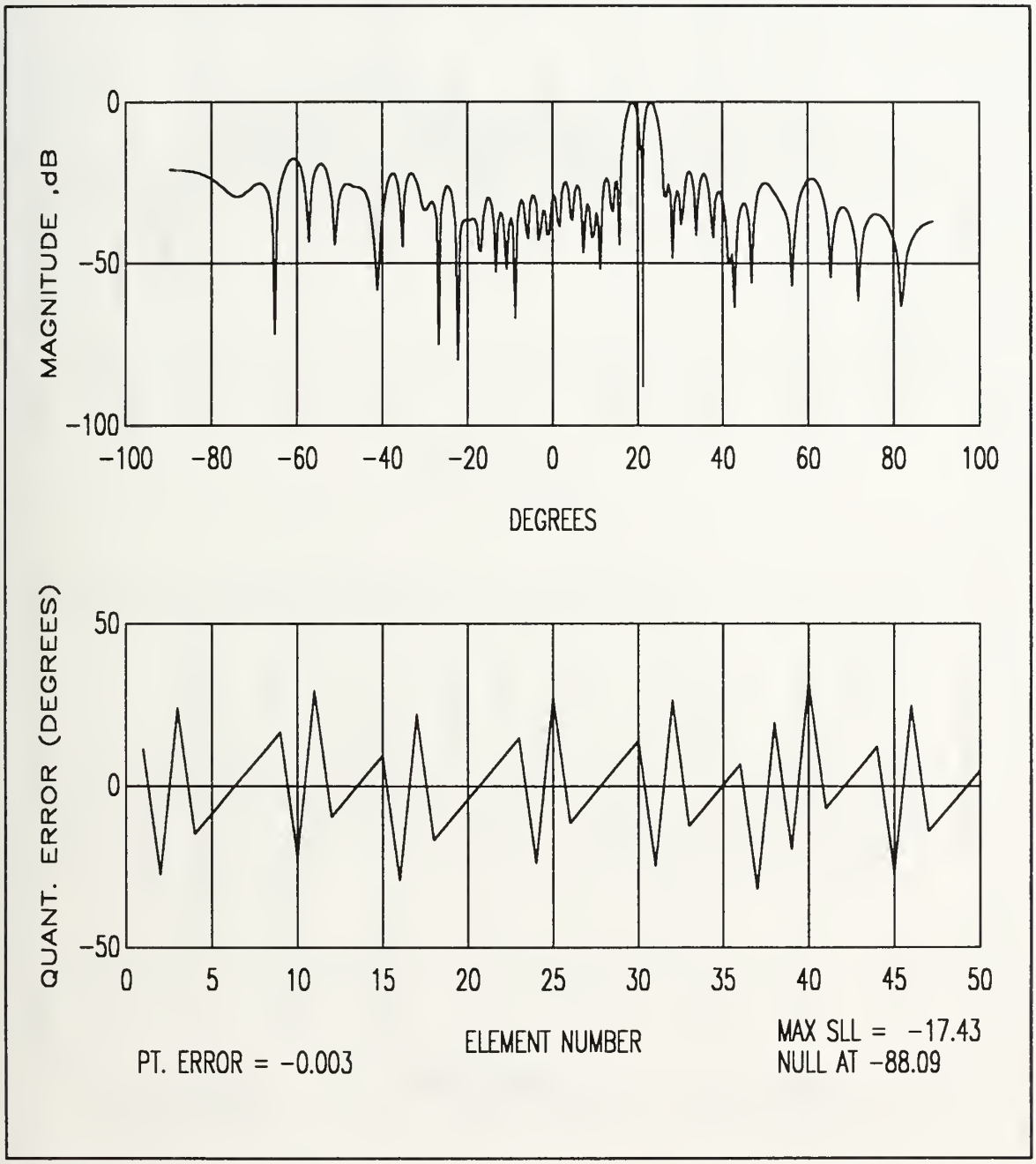

Figure 13. 76 Element Array Bayliss Difference Beam for a 3 Bit Phase Shifter using Symmetric Running Sum Roundoff

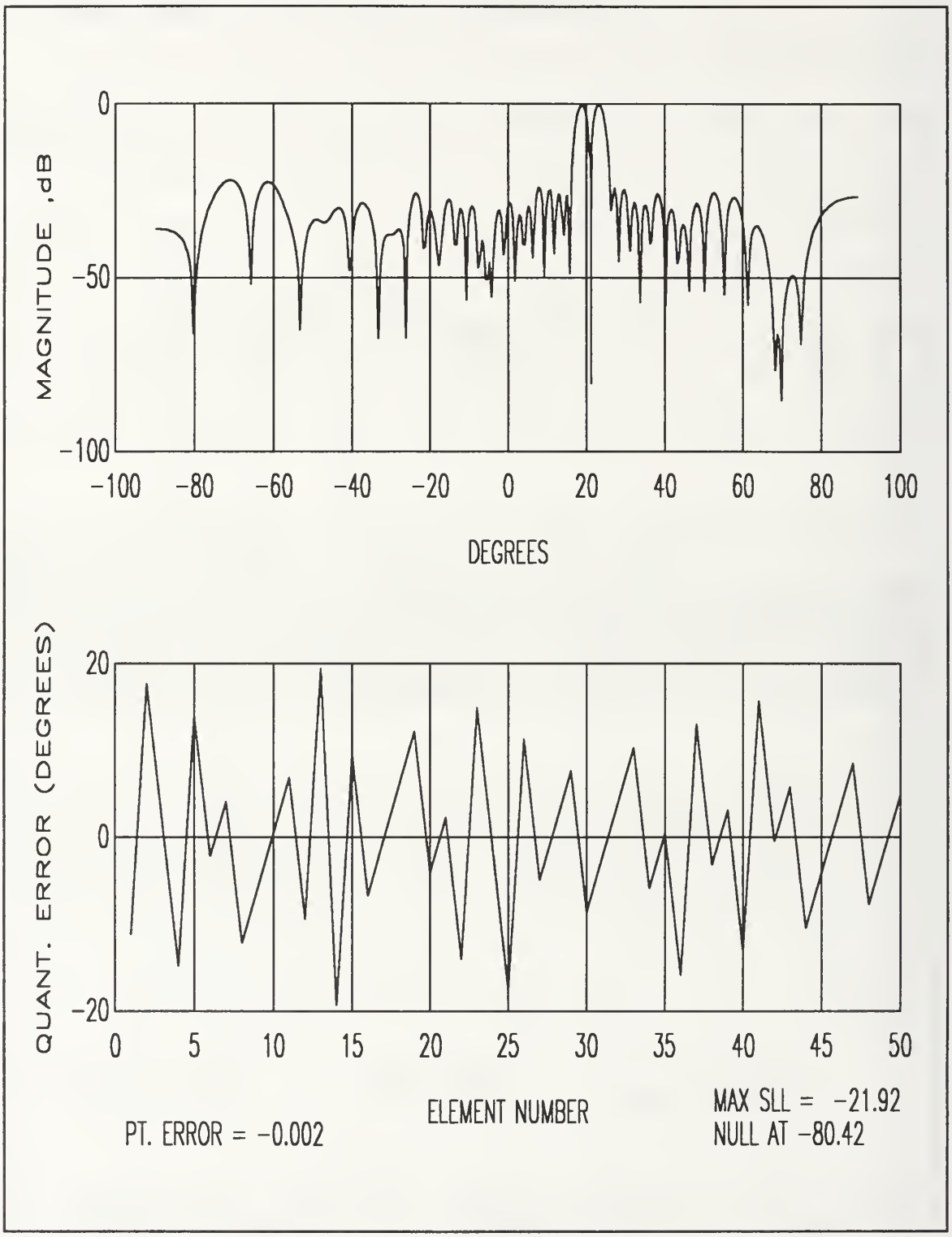

Figure 14. 76 Element Array Bayliss Difference Beam Radiation Pattern for a 4 Bit Phase Shifter using Symmetric Running Sum Roundoff

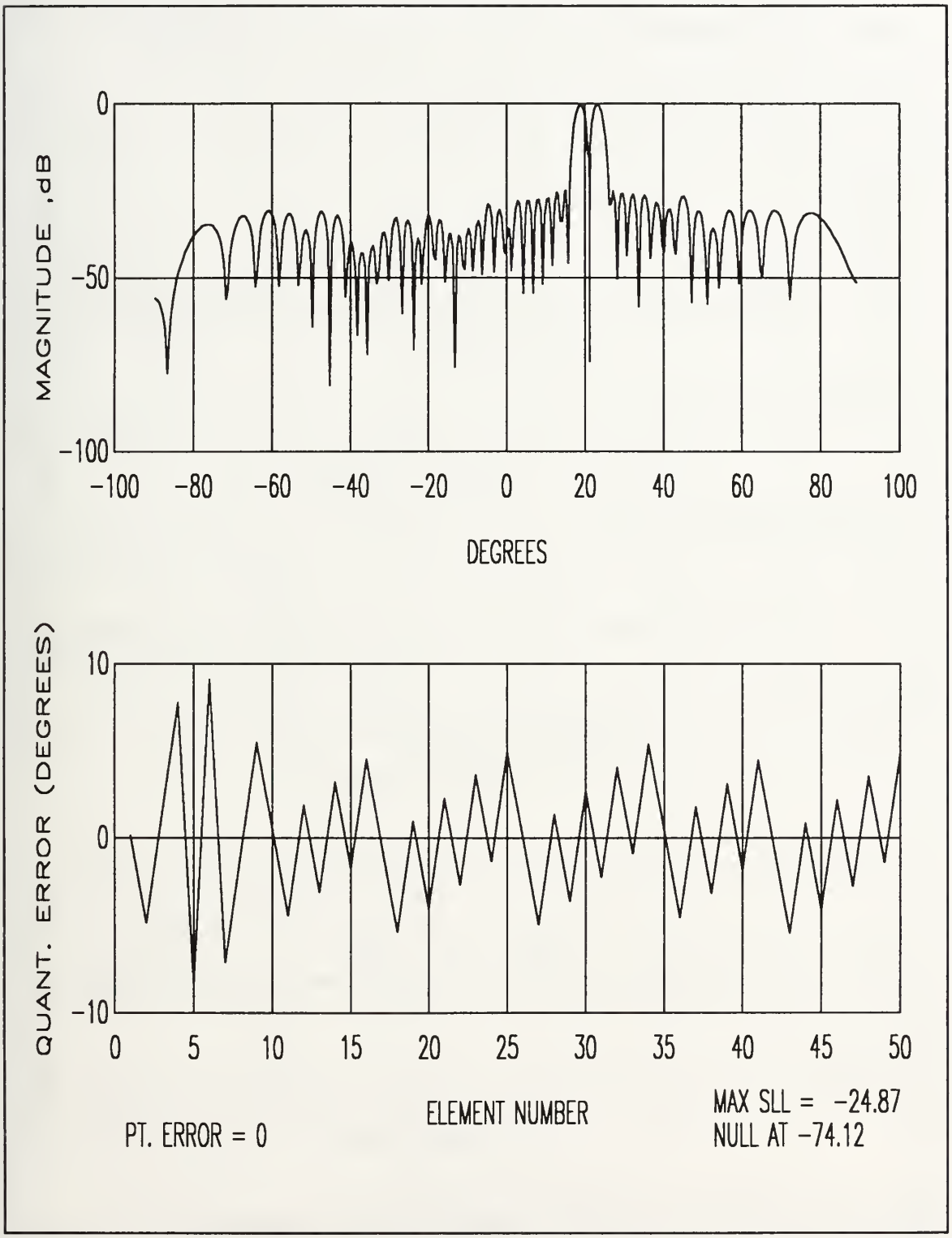

Figure 15. 76 Element Array Difference Beam Radiation Pattern for a 5 Bit Phase Shifter using Symmetric Running Sum Roundoff

Figures 16, 17, and 18 compare the pointing error, null depth, and sidelobe level as a function of bitsize.

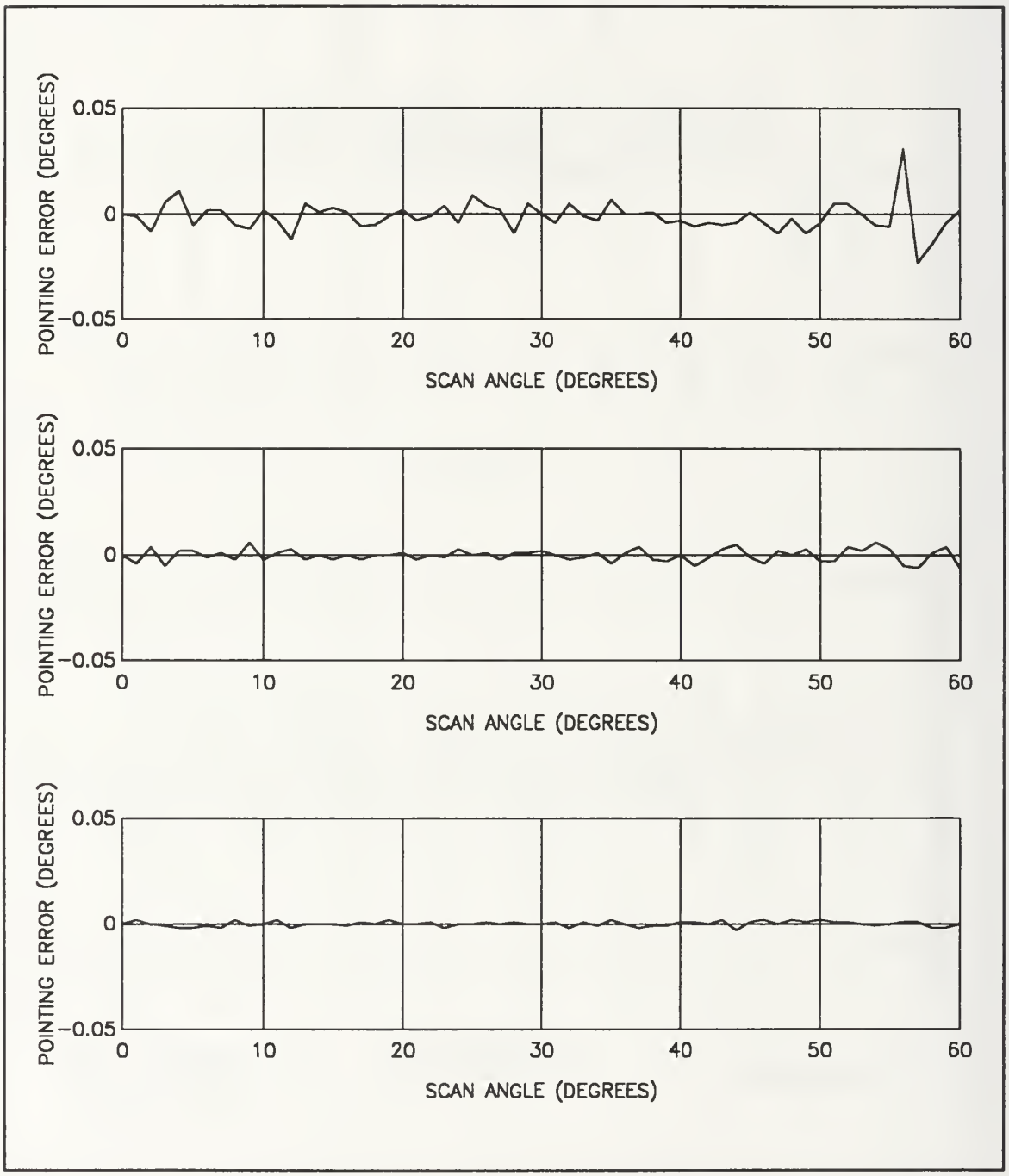

Figure 16. Pointing Error versus Scan Angle for a 76 Element Array with 3, 4, and 5 Bit Phase Shifters using Symmetric Running Sum Roundoff

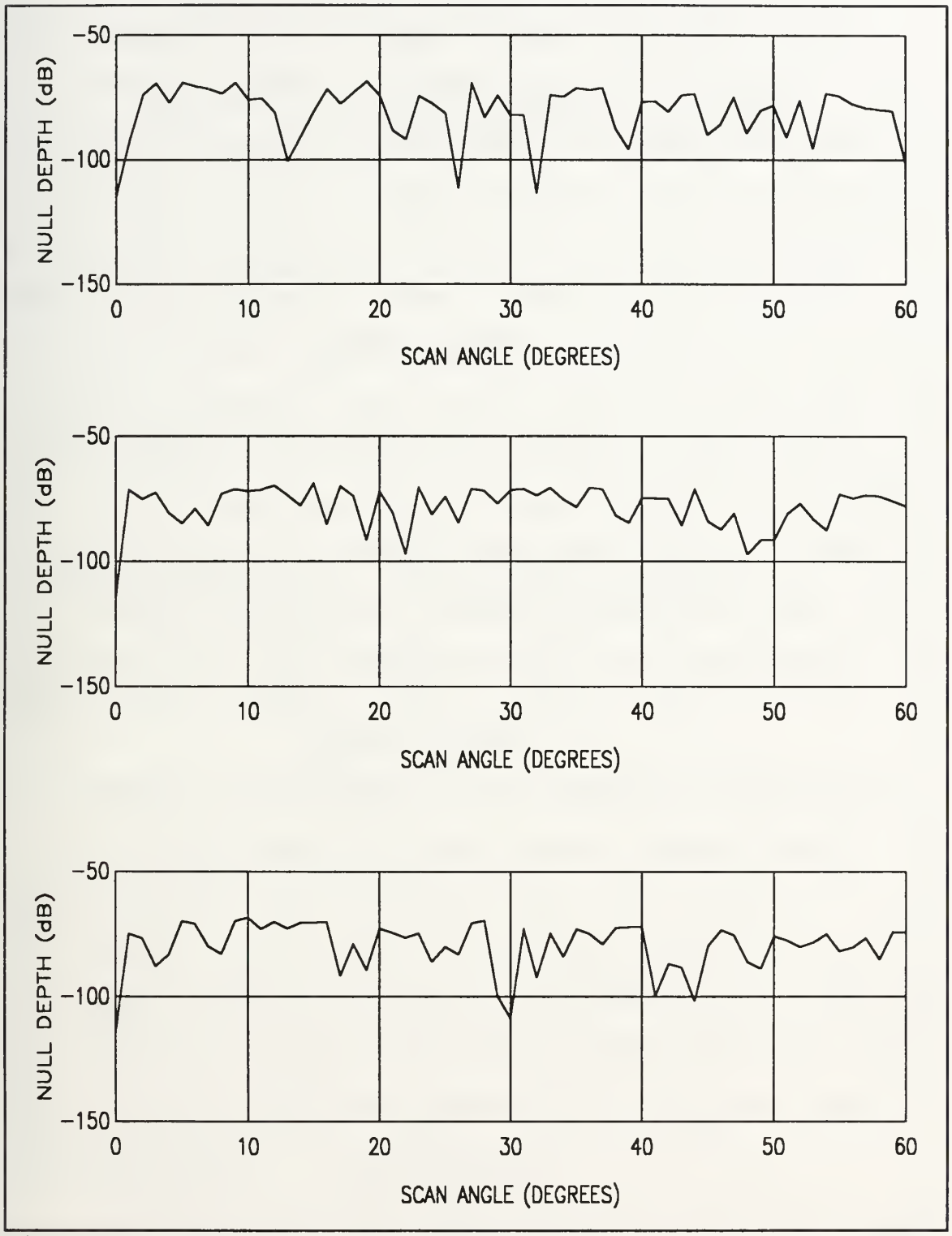

Figure 17. Null Depth versus Scan Angle for a 76 Element Array with 3, 4, and 5 Bit Phase Shifters using Symmetric Running Sum Roundoff

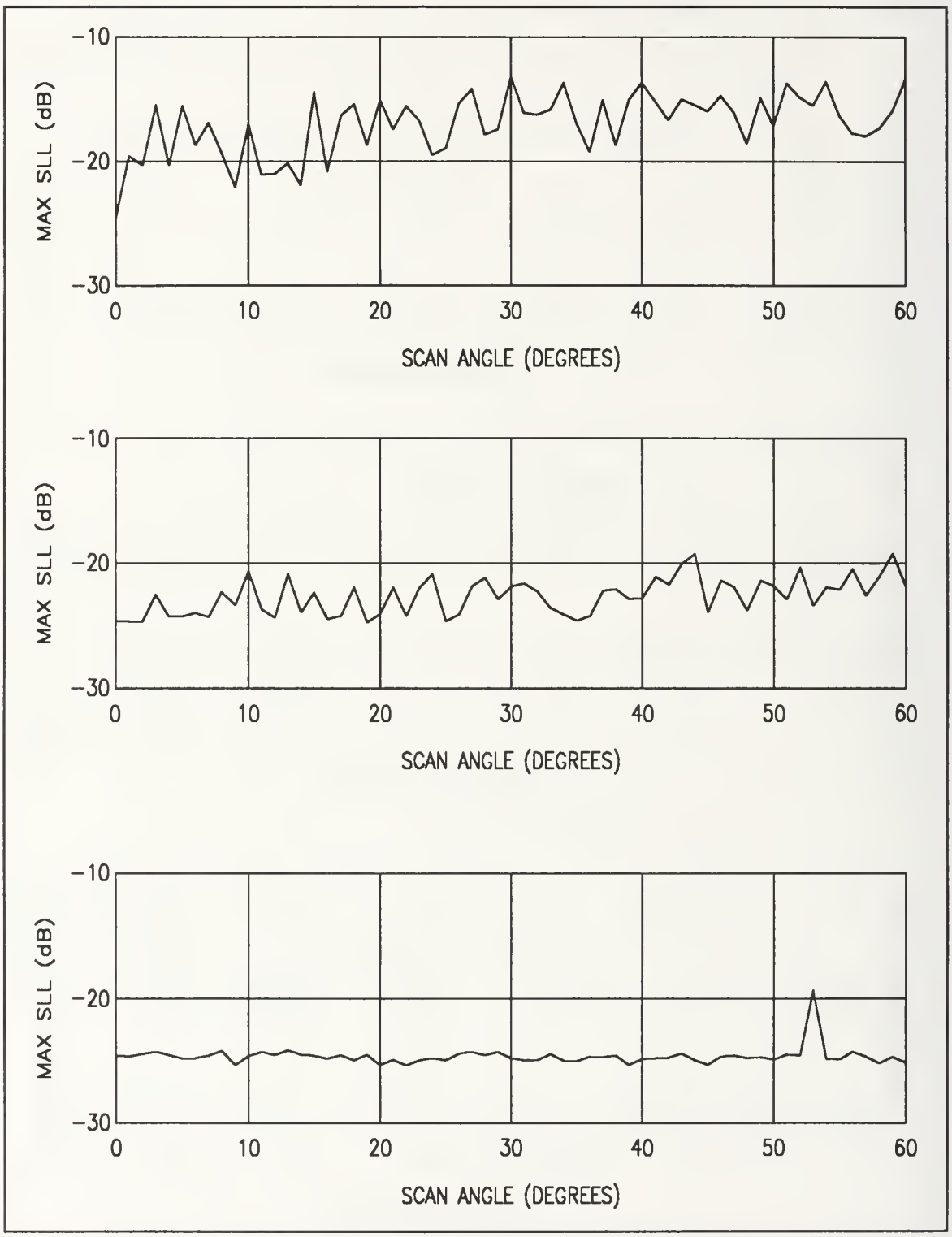

Figure 18. Maximum Sidelobe Level versus Scan Angle for a 76 Element Array with 3, 4, and 5 Bit Phase Shifters using Symmetric Running Sum Roundoff

C. COMPARISON BY THE NUMBER OF ARRAY ELEMENTS

In this section, the number of array elements is varied for each bitsize and roundoff algorithm. Figures 19, 20, and 21 are plots of 26, 50, and 76 element arrays with a 3 bit phase shifter using the running sum roundoff algorithm. The results are similar to those in the previous section. It can be seen in these figures, that as the number of radiating elements increased, the sidelobe level increase above the desired level is smaller, as expected. A larger sampling of the various combinations of the number of radiating elements, bitsize of the phase shifter, and type of roundoff algorithm is included in Appendix A. Appendix B has plots of null depth, pointing error, and sidelobe level as a function of scan angle.

D. FORMULAS FOR EVALUATION OF THE AVERAGE SIDELOBE LEVEL

It has been shown that the maximum sidelobe level of an antenna array is determined by the variance of the quantization error [Ref. 3: p. 2]. By taking the expected value of the radiation pattern, an expression for the mean error level is obtained. This was first done for reflectors by Ruze [Ref. 3]. A similar approach for discrete arrays of elements yields,

$$\overline{P}_{norm} \approx \overline{\Psi}^2 \frac{\cos(\theta)}{N} + P_o \qquad \text{(V-1)}$$

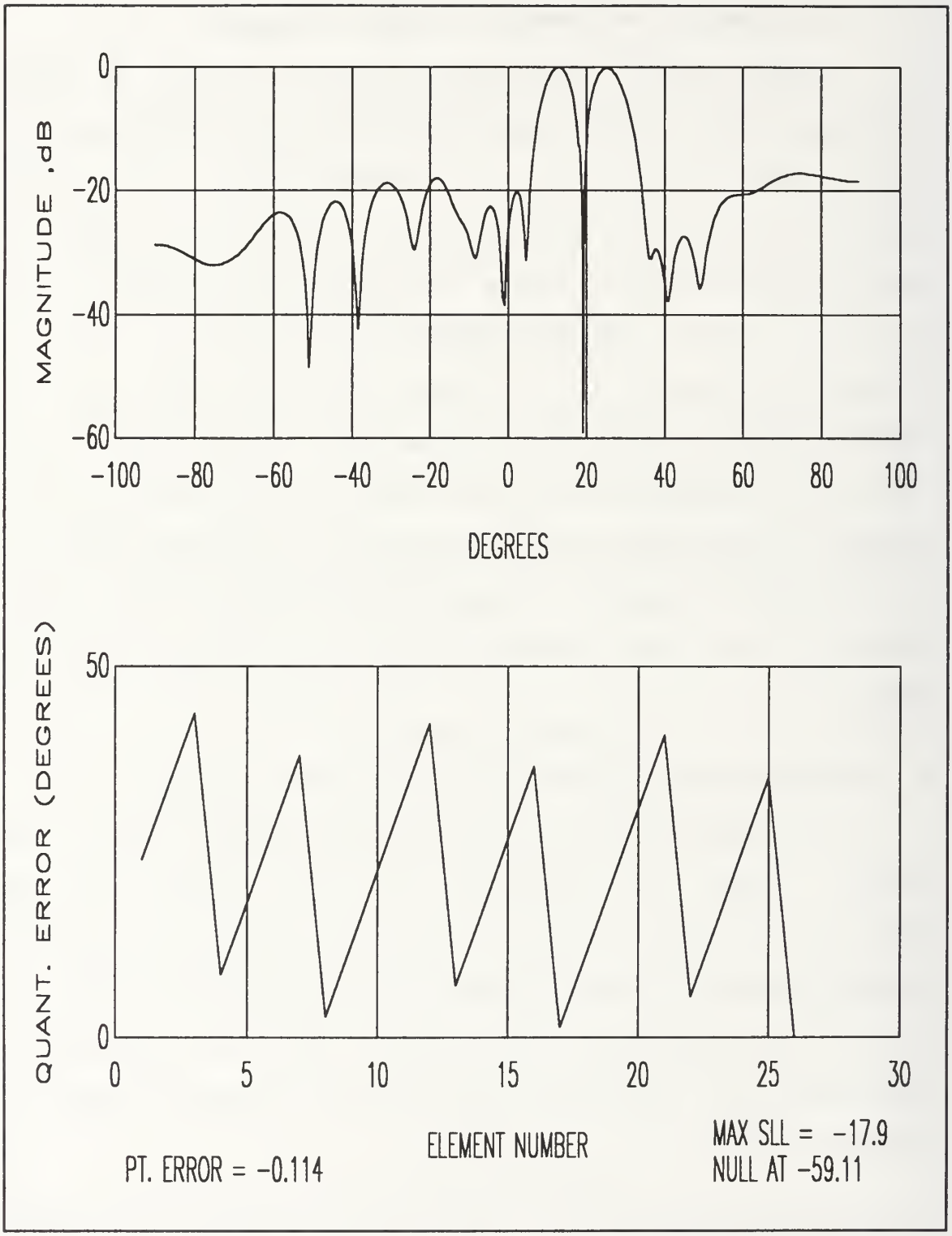

Figure 19. 26 Element Array Difference Beam Radiation Pattern for a 3 Bit Phase Shifter using Running Sum Roundoff

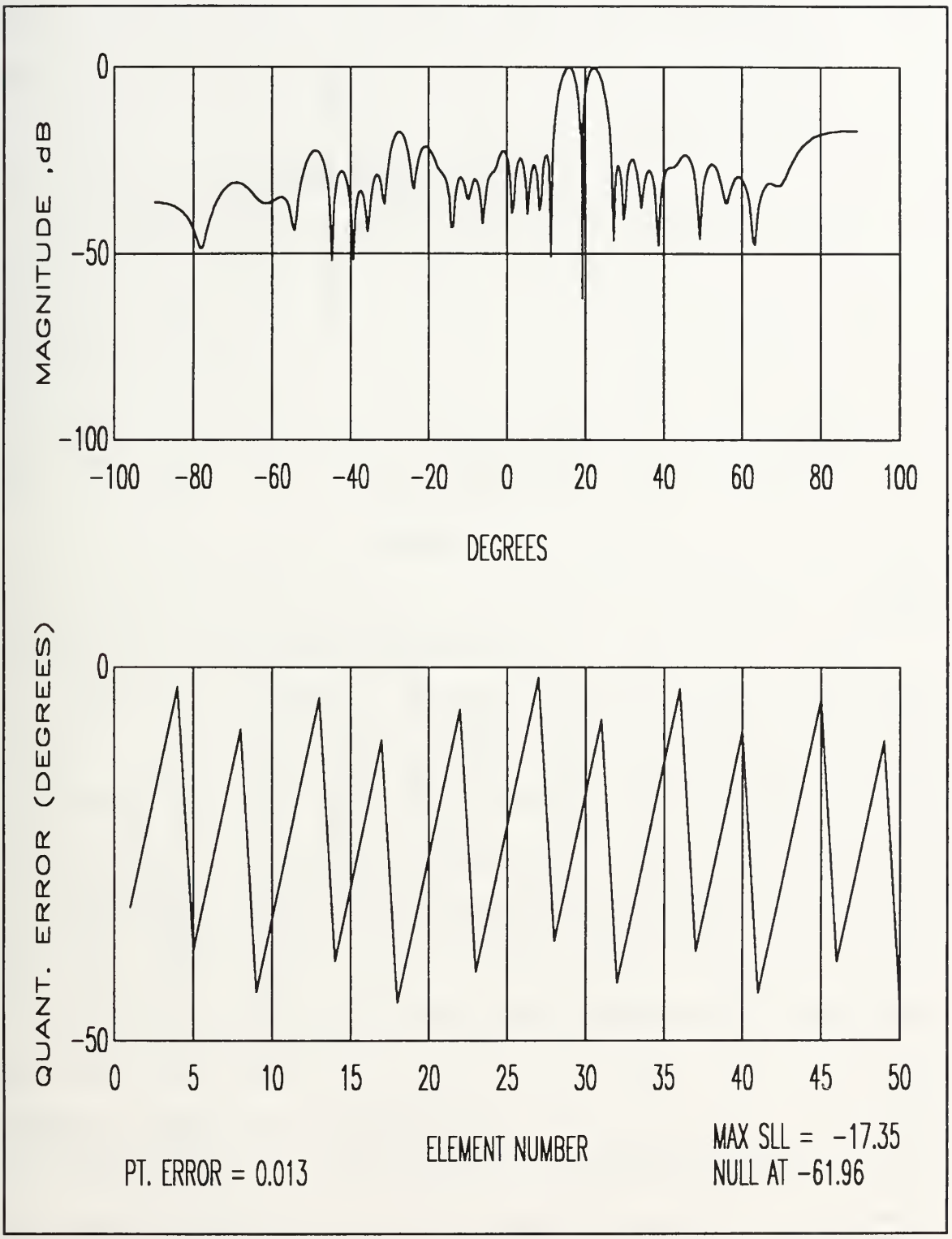

Figure 20. 50 Element Array Difference Beam Radiation Pattern for a 3 Bit Phase Shifter using Running Sum Roundoff

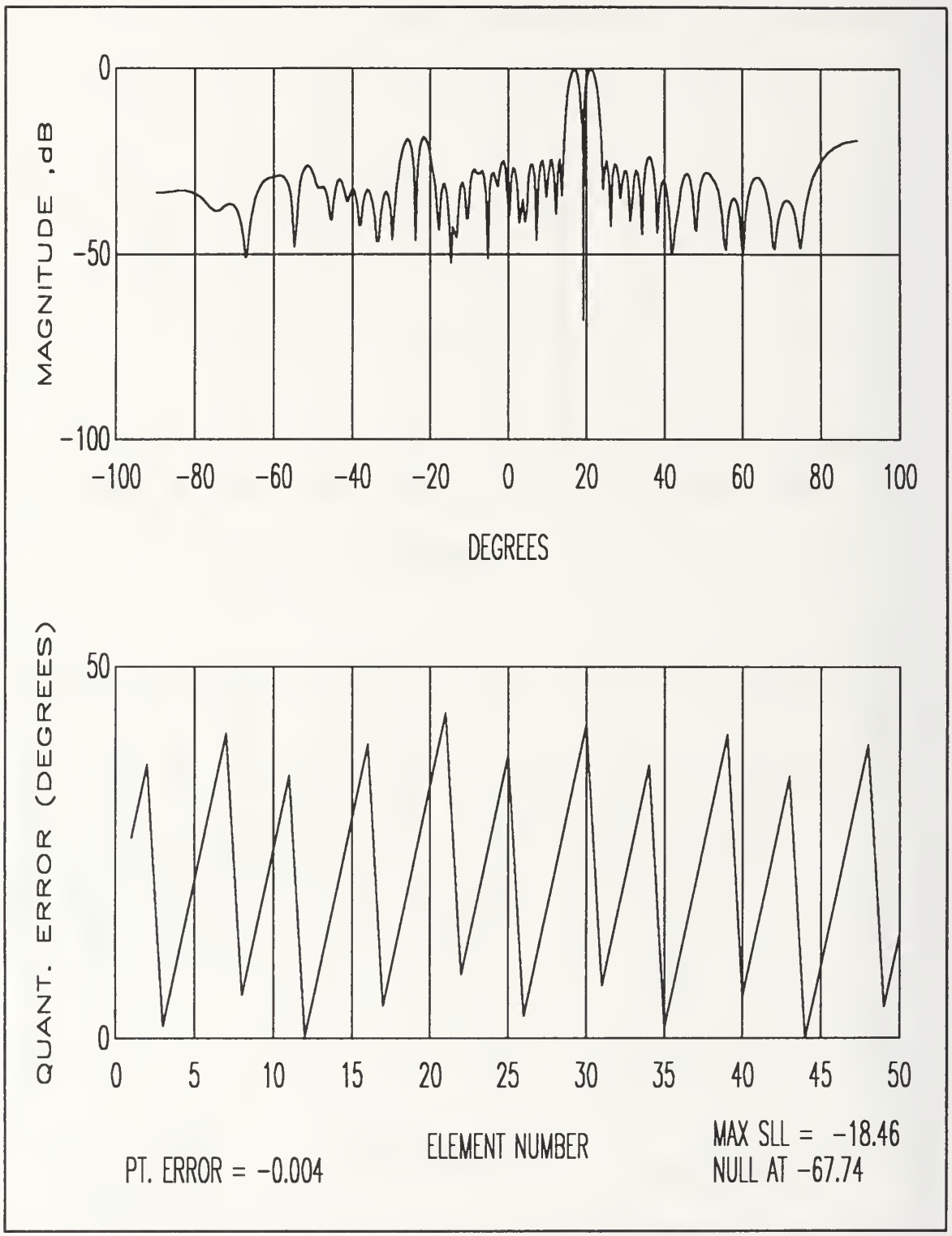

Figure 21. 76 Element Array Difference Beam Radiation Pattern for a 3 Bit Phase Shifter using Running Sum Roundoff

where $\overline{P_{norm}}$ is the expected value of the normalized power pattern (i.e., radiation pattern) and

$\overline{\psi^2}$ is the variance of the quantization error

θ is the pattern angle

N is the number of radiating elements

P_o is the error free power pattern

The quantization error variance is calculated using,

$$\overline{\psi}^2 = \frac{\sum_{n=1}^{N} (\psi_n - \overline{\psi})}{N-1} \qquad \text{(V-2)}$$

where ψ_n is the quantization error at the nth element and $\overline{\psi}$ is the mean of the quantization error.

Equation V-1 gives an estimate of the sidelobe level based on the variance of the quantization error resulting from a roundoff algorithm. Since the statistics of the quantization error for all the roundoff algorithms is determined primarily by the bitsize, the variances associated with each algorithm did not differ by large amounts. Equations V-1 and V-2 explain why the sidelobe levels were essentially independent of roundoff algorithm. Figure 22 is a plot of the average sidelobe level predicted by the first term on the right hand side of V-1 and a power pattern calculated using weighted random roundoff.

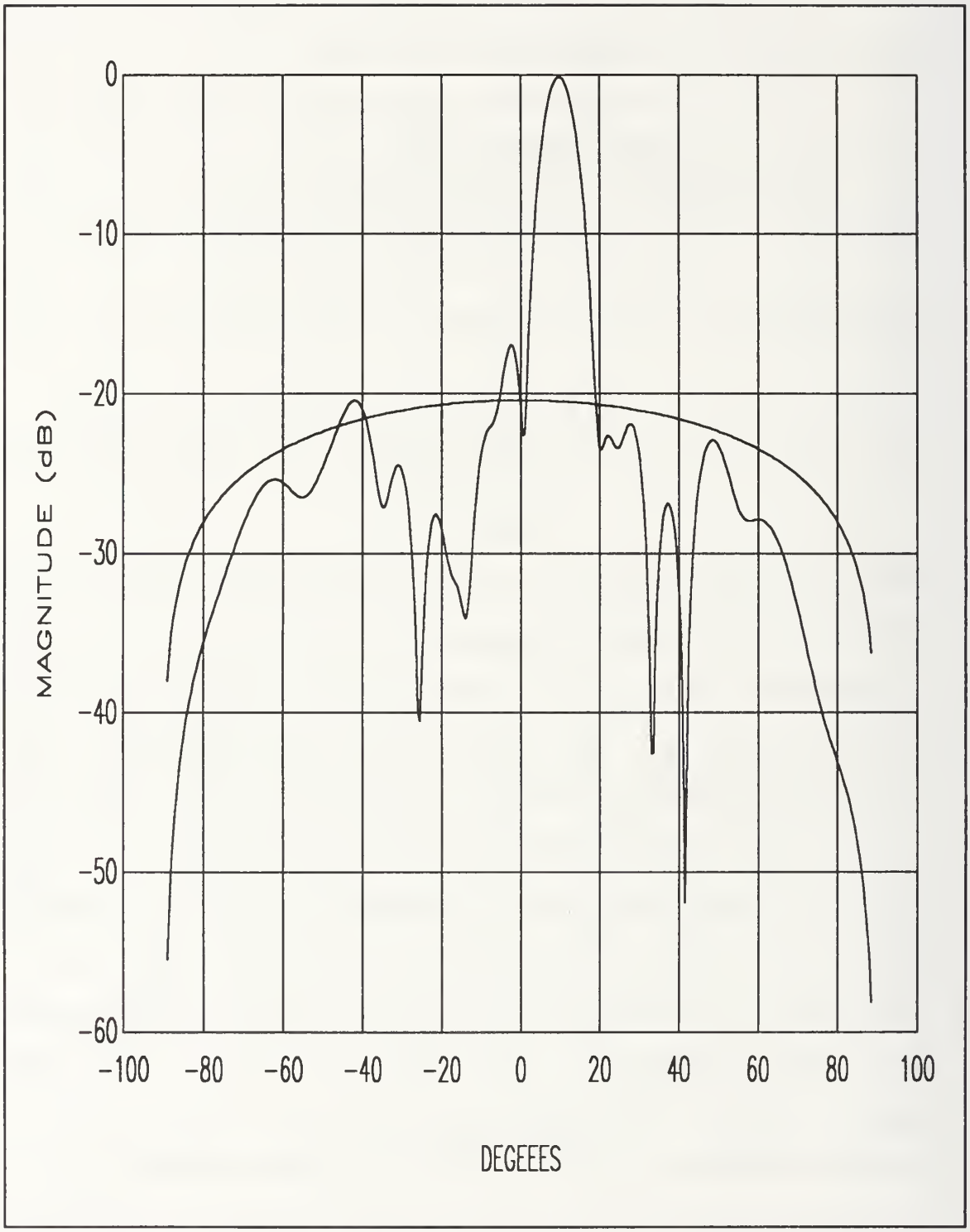

Figure 22. Plot of Predicted Average Sidelobe Level and Actual Power Pattern using Weighted Random Roundoff

E. FORMULAS FOR CALCULATING THE BEAM POINTING ERROR

An accurate determination of target location by a radar is made possible by the difference beam null position. A closed form expression has been derived by Frank and Ruze [Ref. 1:p. 11-37,38] for the beam pointing error when regular roundoff is used. The difference pattern can be written as

$$E(\theta)=2j\left(\sin\left(\frac{\pi s}{\lambda}\sin(\theta)-\psi_1\right)+\sin\left(\frac{3\pi s}{\lambda}\sin(\theta)-\psi_2\right)+\ldots\right.$$
$$\left.+\sin\left(\frac{(N-1)\pi s}{\lambda}\sin(\theta)-\psi_{\frac{N}{2}}\right)\right) \quad . \qquad \textbf{(V-3)}$$

where ψ_n now includes the phase necessary to scan the beam to θ_o, as well as any quantization error. For a difference pattern at θ_o, the beam pointing error, $\delta\theta$ is

$$\delta\theta=\sum_{n=1}^{\frac{N}{2}}\sin\left(\frac{(2n-1)\pi s}{\lambda}\sin(\theta)-\psi_n\right) \quad . \qquad \textbf{(V-4)}$$

If the phases are nearly those required to produce a null at θ_o, the sine can be replaced by its argument, and equation V-4 reduces to,

$$\delta\theta=\sin^{-1}(\theta)\,\frac{2\pi}{2^{bit\ size-1}}\,\frac{4}{\pi\left(\frac{s}{\lambda}\right)N^2}\sum_{n=1}^{\frac{N}{2}}\psi_n \quad . \qquad \textbf{(V-5)}$$

Figure 23 is a plot of the predicted pointing error using equation V-5 versus the calculated pointing errors for regular roundoff.

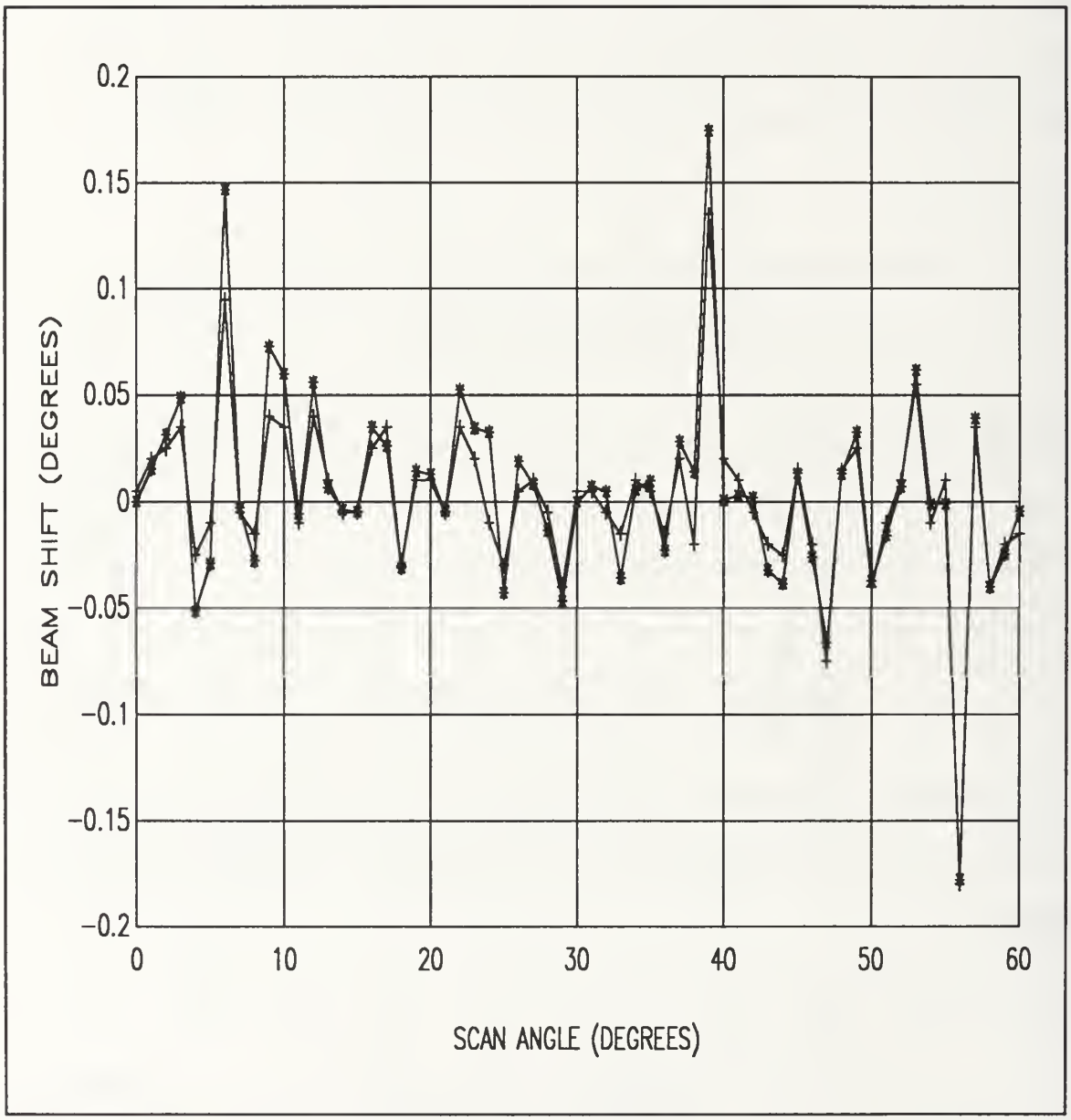

Figure 23. Predicted Pointing Error (*) and Calculated Pointing Error (+) versus Scan Angle for a 50 Element Array with a 4 Bit Phase Shifter using Regular Roundoff

V. CONCLUSIONS

The running sum roundoff algorithms reduce the beam pointing error by a factor of 10 compared to the other roundoff algorithms, without degrading the maximum sidelobe levels or gain performance. The symmetric running sum roundoff algorithm does not seem to offer any significant performance advantage over the running sum algorithm. The only possible advantage the symmetric algorithm may offer is in beam scanning rate. Since the roundoff algorithm is only applied to N/2 elements as opposed to N elements, a faster beam scanning rate may result.

Even though the running sum algorithm yielded essentially zero beam shift and 60 to 80 decibel null depths, these numbers will not be achieved in practice due to manufacturing and assembly errors. Phase shifters are designed to a set of electrical and mechanical tolerances. In a 4 bit phase shifter, for example, the least significant bit may not be exactly 22.5°. It could be slightly more or less depending on how that individual phase shifter's circuits were fabricated and assembled. These errors tend to be random from phase shifter to phase shifter and therefore their effects can be estimated using statistical approaches such as those described in Chapter IV.

APPENDIX A - PLOTS OF RADIATION PATTERNS AND QUANTIZATION ERRORS

This section will allow the reader to examine the detailed effect of the number of elements, bitsize, and the roundoff algorithm on the radiation pattern and quantization error. The radiation patterns were arbitrarily chosen for a scan angle of 5 degrees using 26, 50, and 76 elements with 3, 4, and 5 bit phase shifters using regular, weighted random, and running sum algorithms. The data is contained in figures 24 through 62.

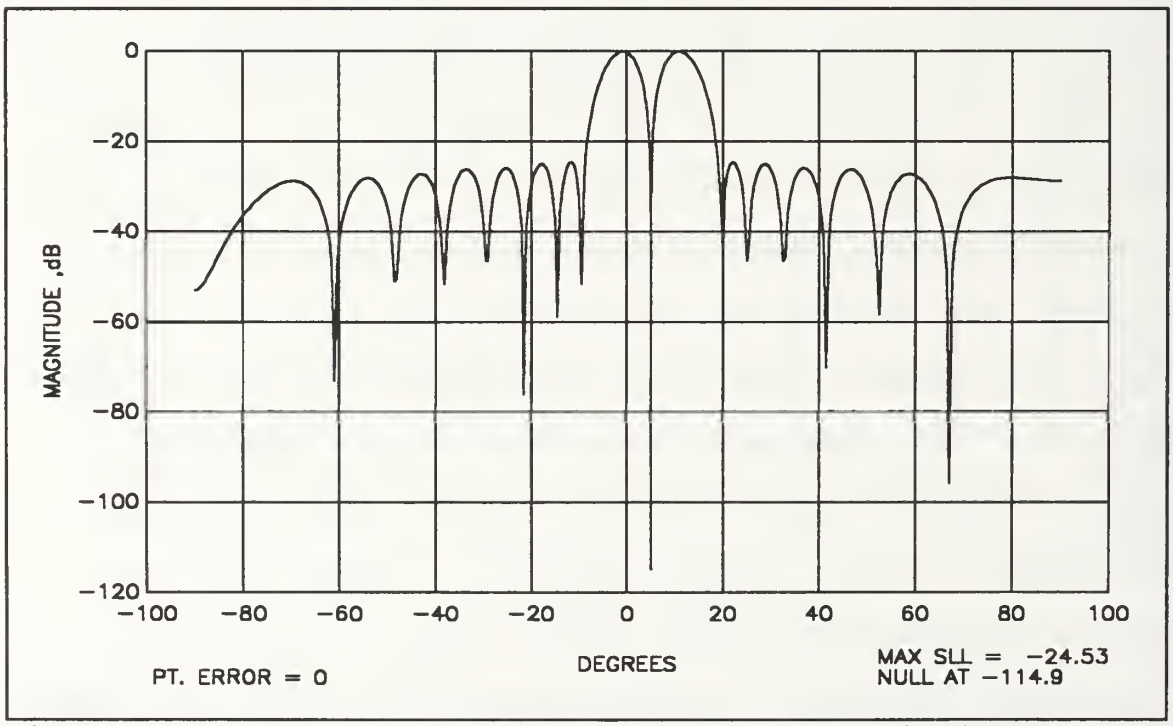

Figure 24. 26 Element Array Difference Beam Radiation Pattern for a 3 Bit Phase Shifter with Perfect Phase

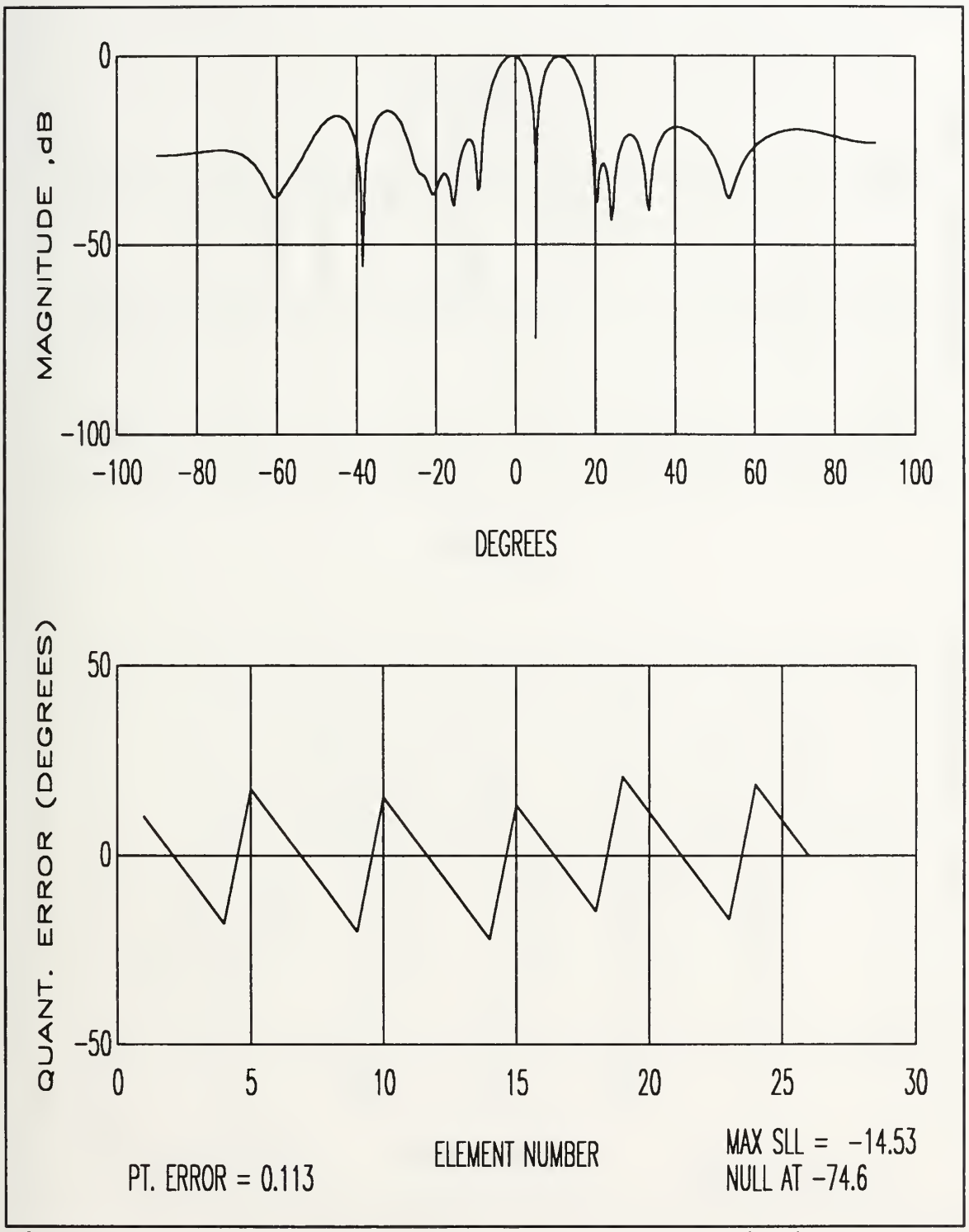

Figure 25. 26 Element Array Difference Beam Radiation Pattern for a 3 Bit Phase Shifter using Regular Roundoff

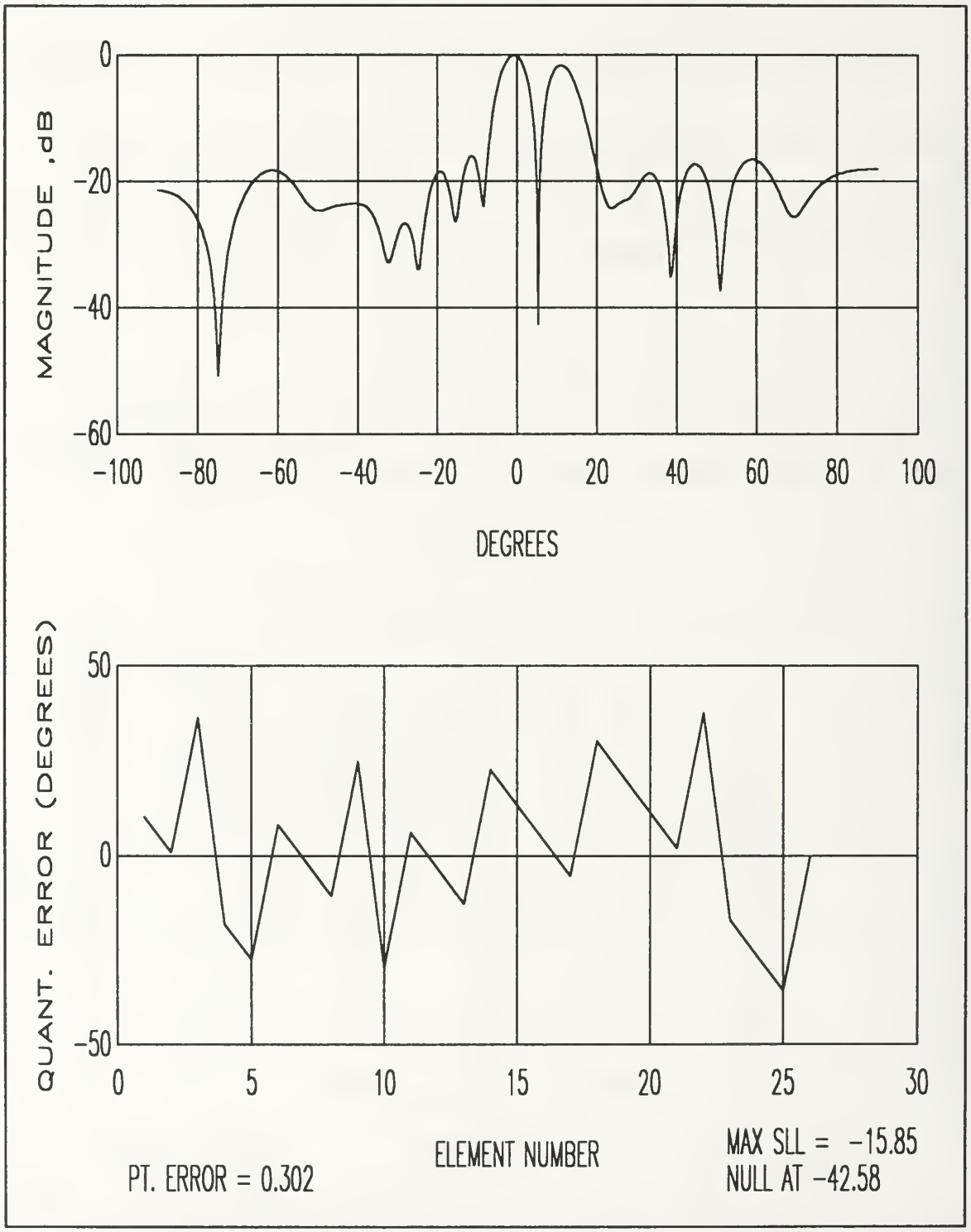

Figure 26. 26 Element Array Difference Beam Radiation Pattern for a 3 Bit Phase Shifter using Weighted Random Roundoff

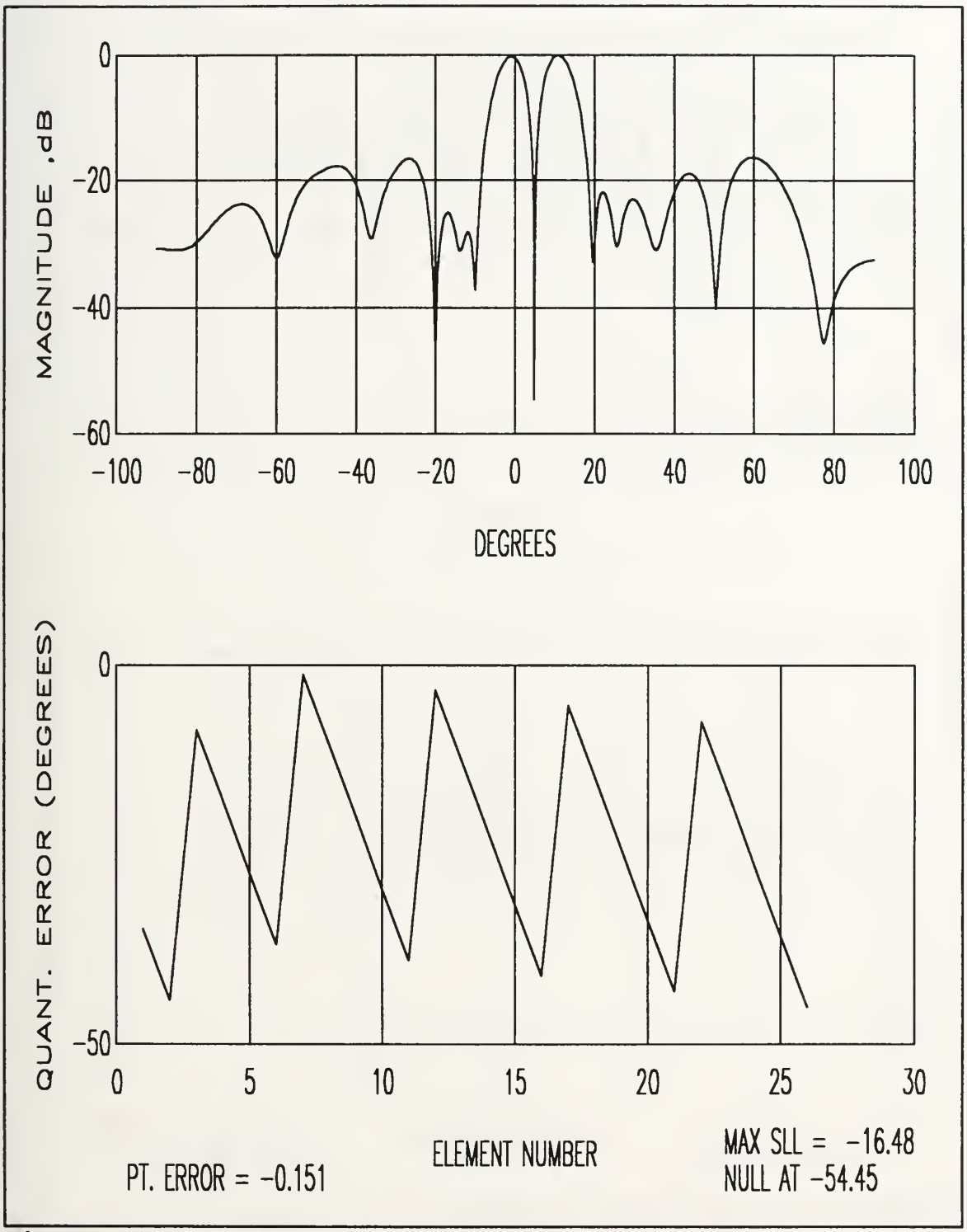

Figure 27. 26 Element Array Difference Beam Radiation Pattern for a 3 Bit Phase Shifter using Running Sum Roundoff

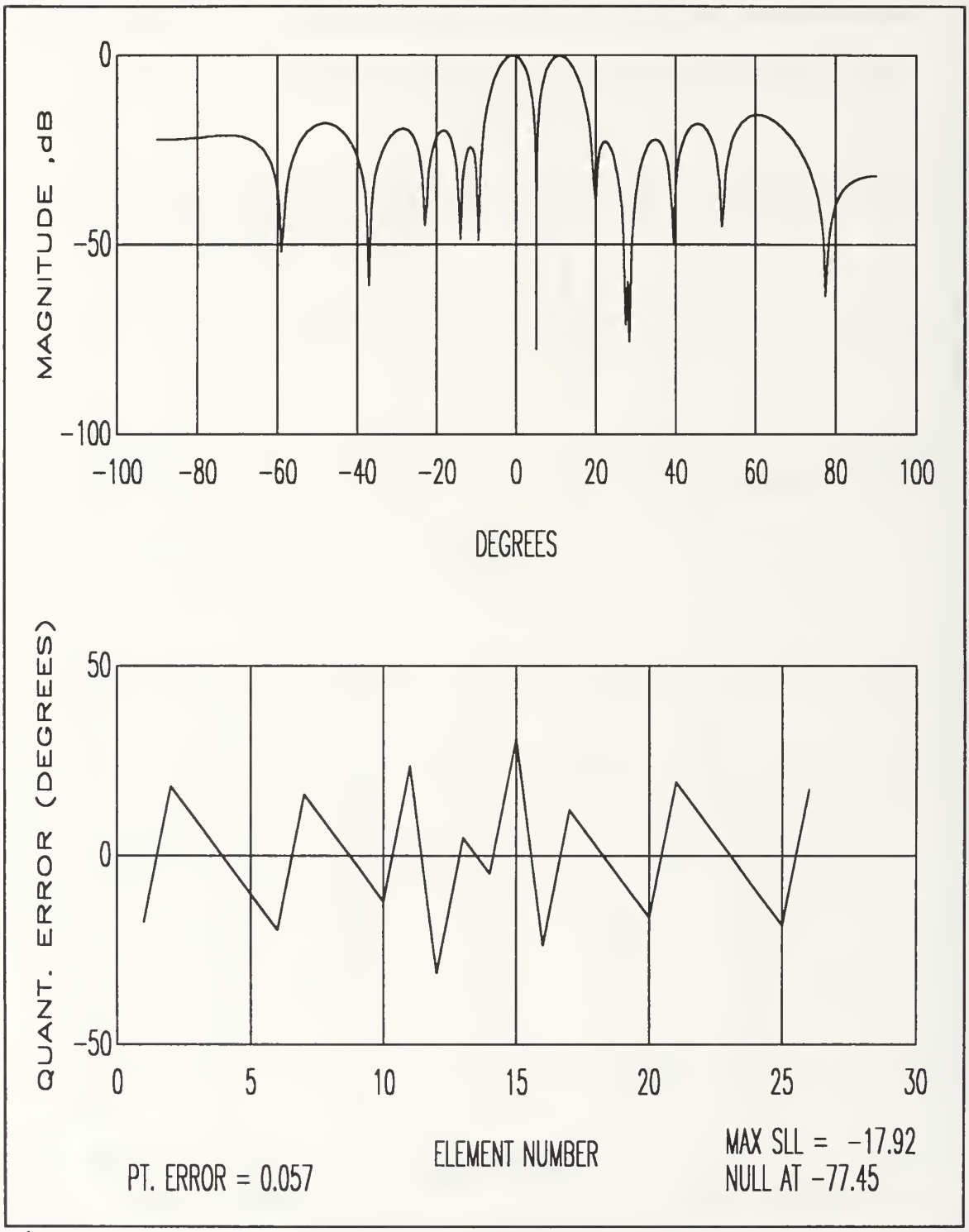

Figure 28. 26 Element Array Difference Beam Radiation Pattern for a 3 Bit Phase Shifter using Symmetrical Running Sum Roundoff

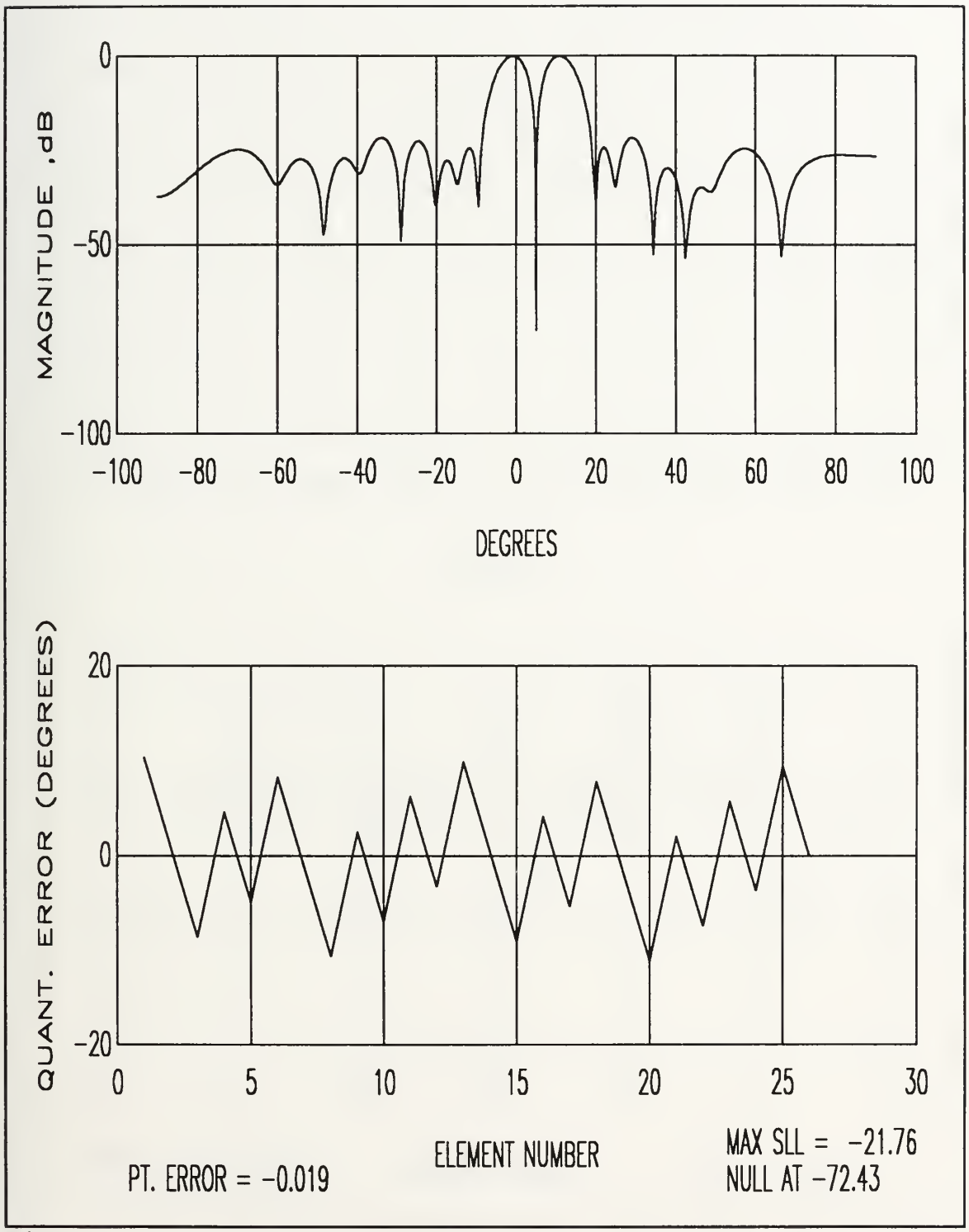

Figure 29. 26 Element Array Difference Beam Radiation Pattern for a 4 Bit Phase Shifter using Regular Roundoff

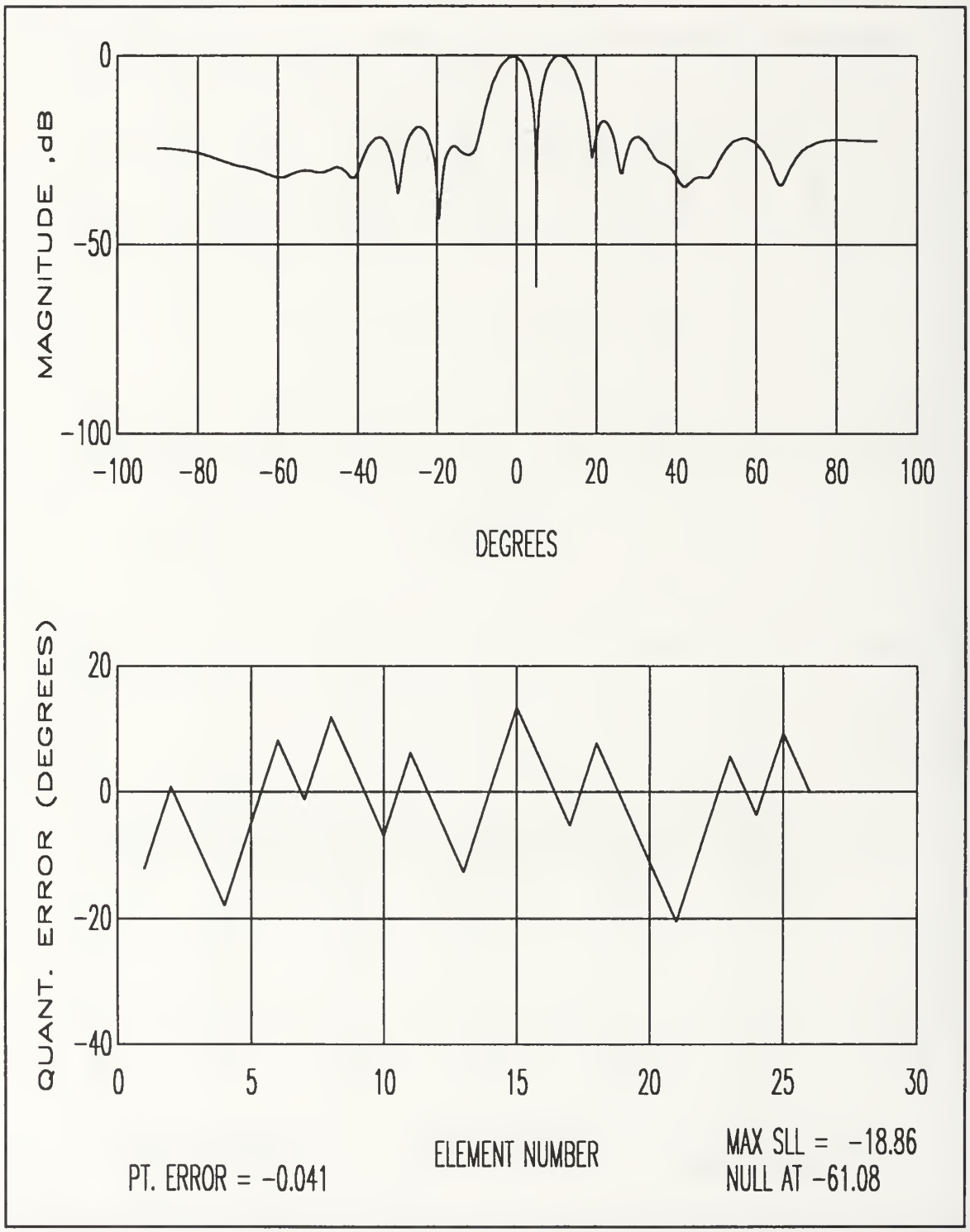

Figure 30. 26 Element Array Difference Beam Radiation Pattern for a 4 Bit Phase Shifter using Weighted Random Roundoff

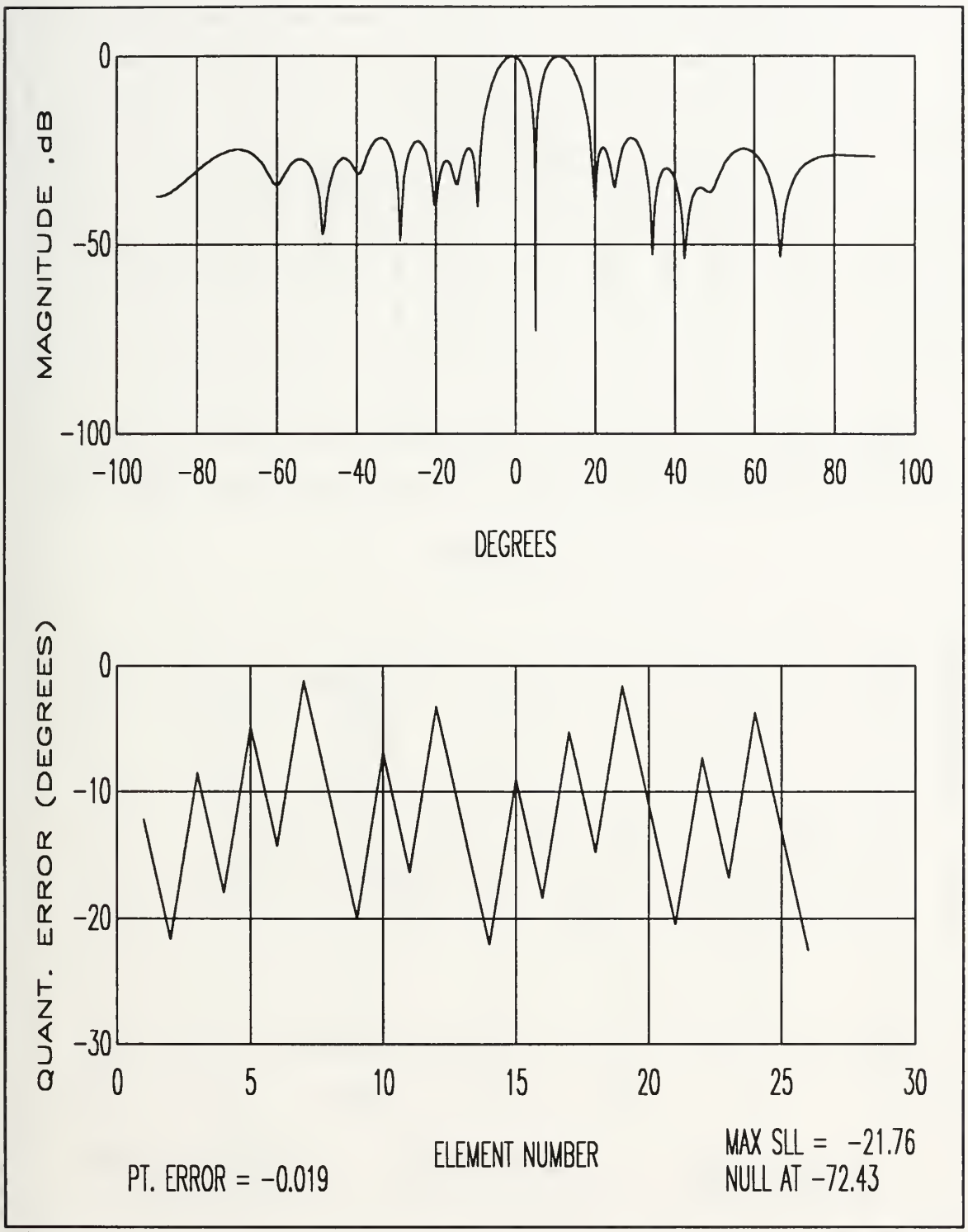

Figure 31. 26 Element Array Difference Beam Radiation Pattern for a 4 Bit Phase Shifter using Running Sum Roundoff

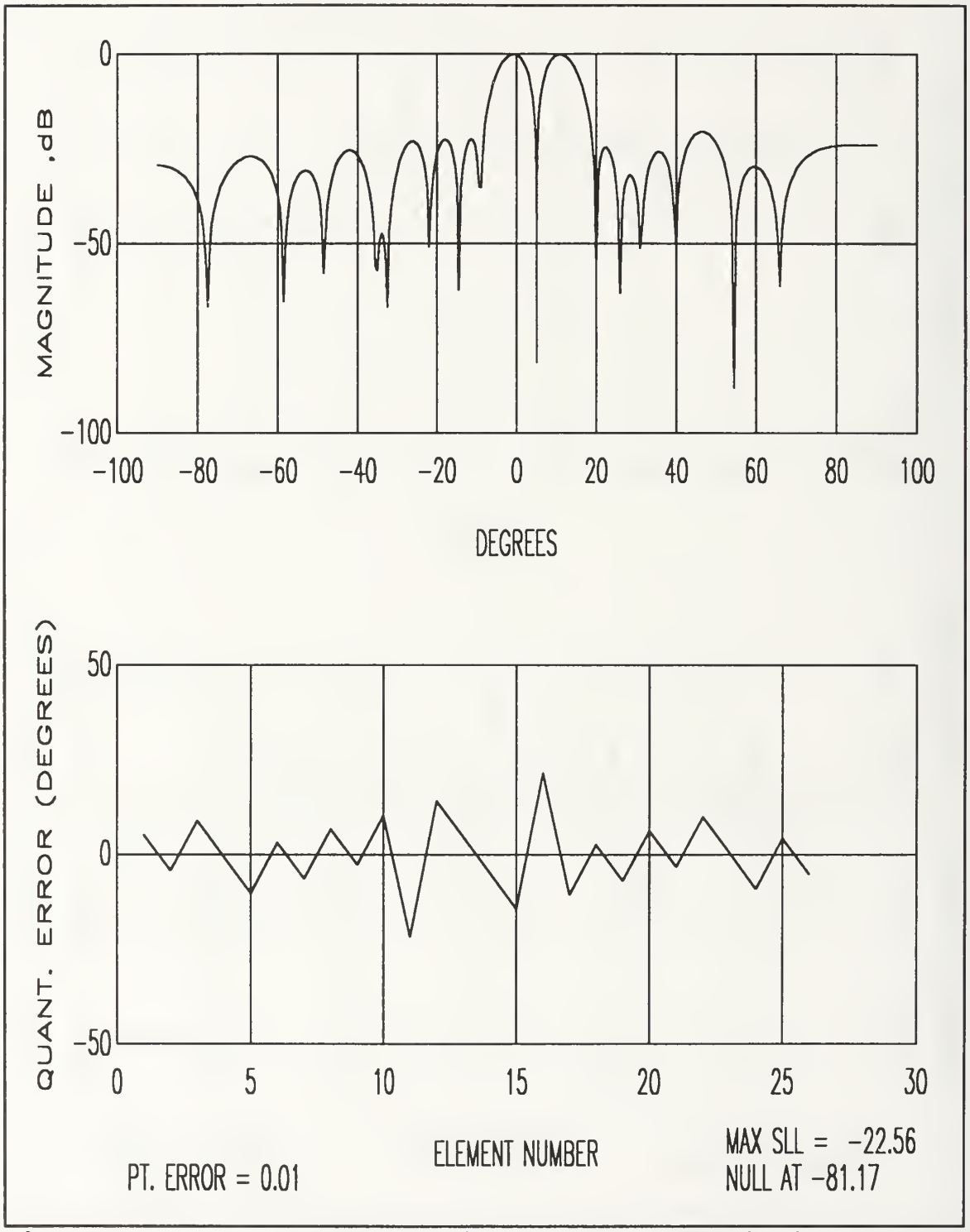

Figure 32. 26 Element Array Difference Beam Radiation Pattern for a 4 Bit Phase Shifter using Symmetric Running Sum Roundoff

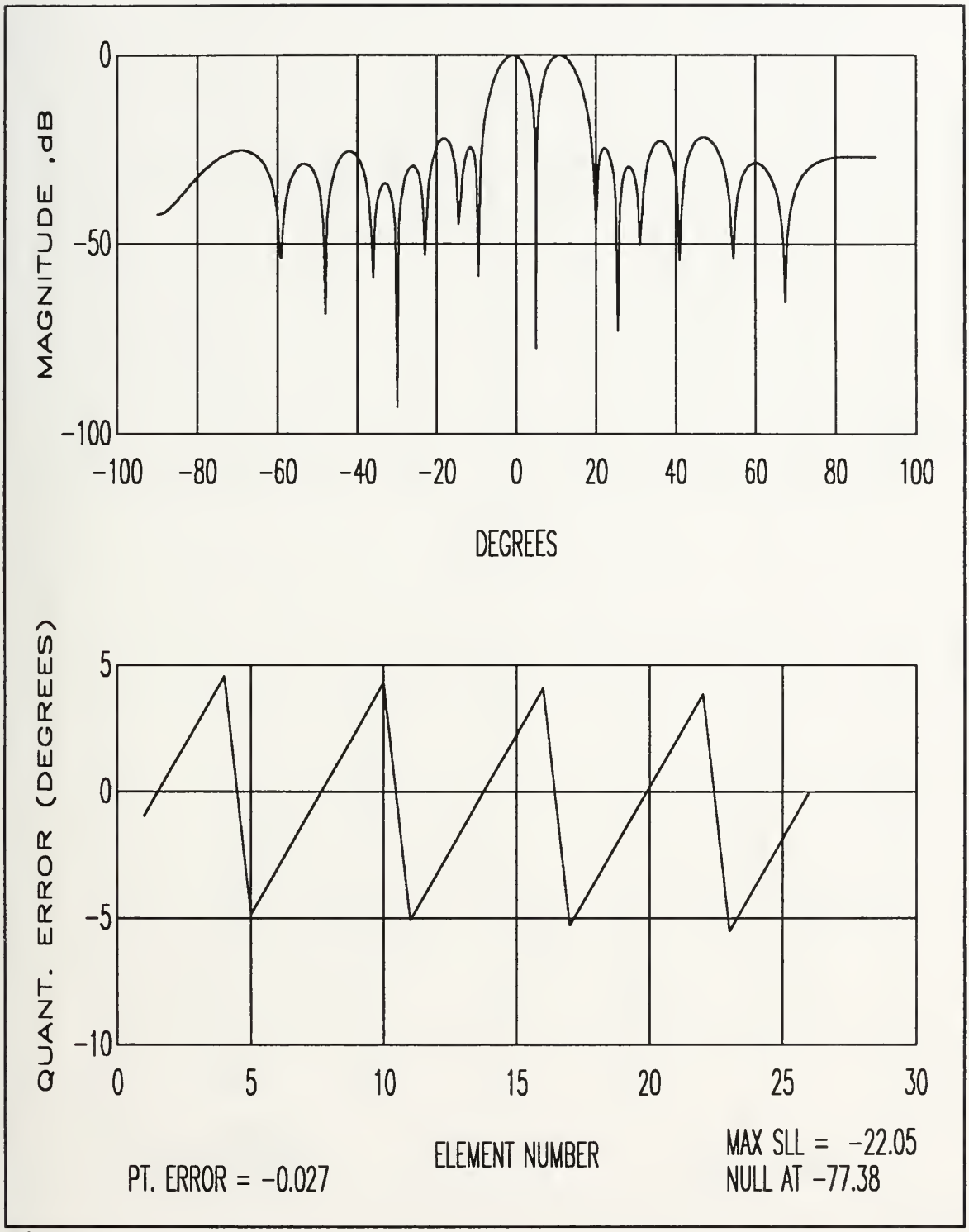

Figure 33. 26 Element Array Difference Beam Radiation Pattern for a 5 Bit Phase Shifter using Regular Roundoff

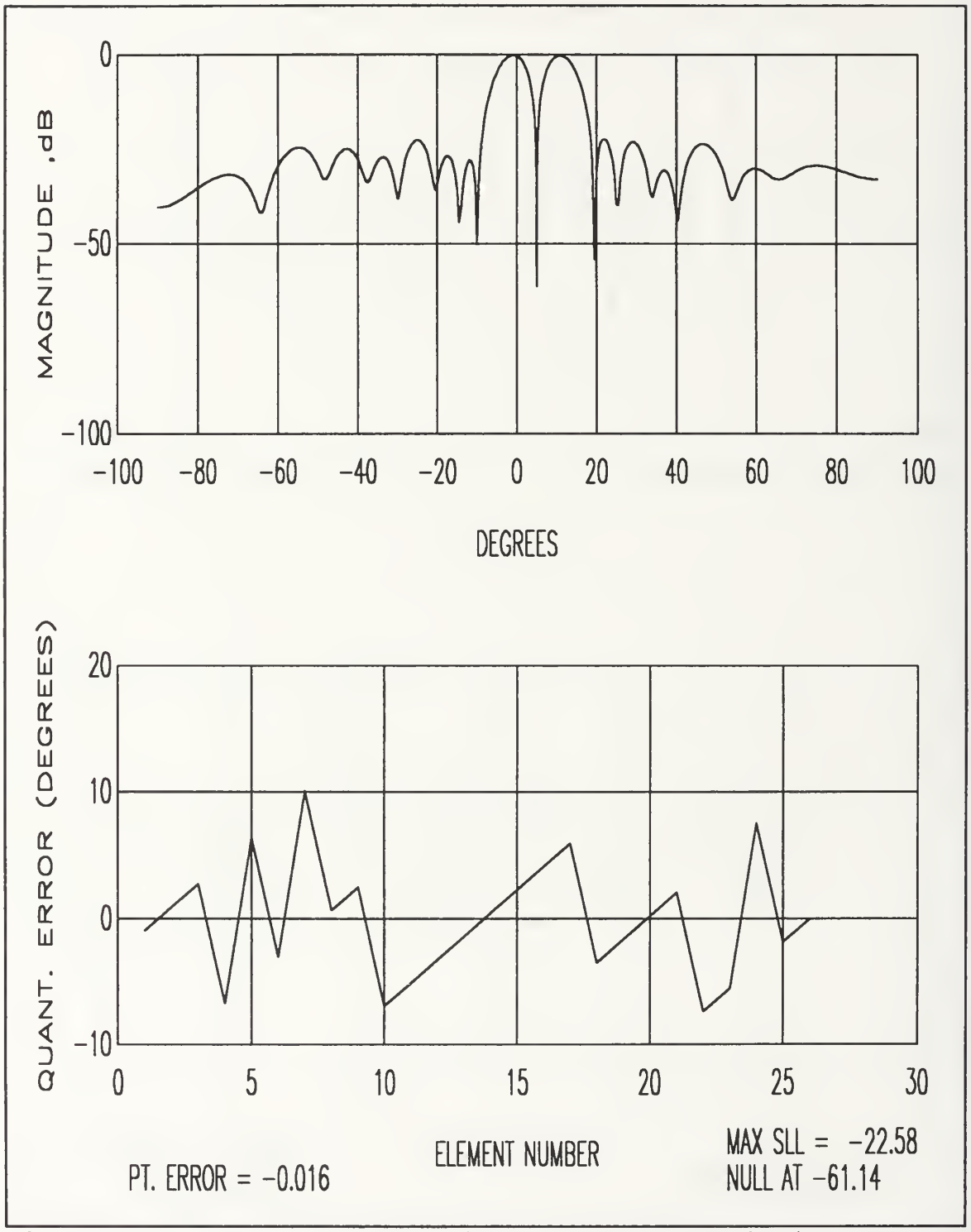

Figure 34. 26 Element Array Difference Beam Radiation Pattern for a 5 Bit Phase Shifter using Weighted Random Roundoff

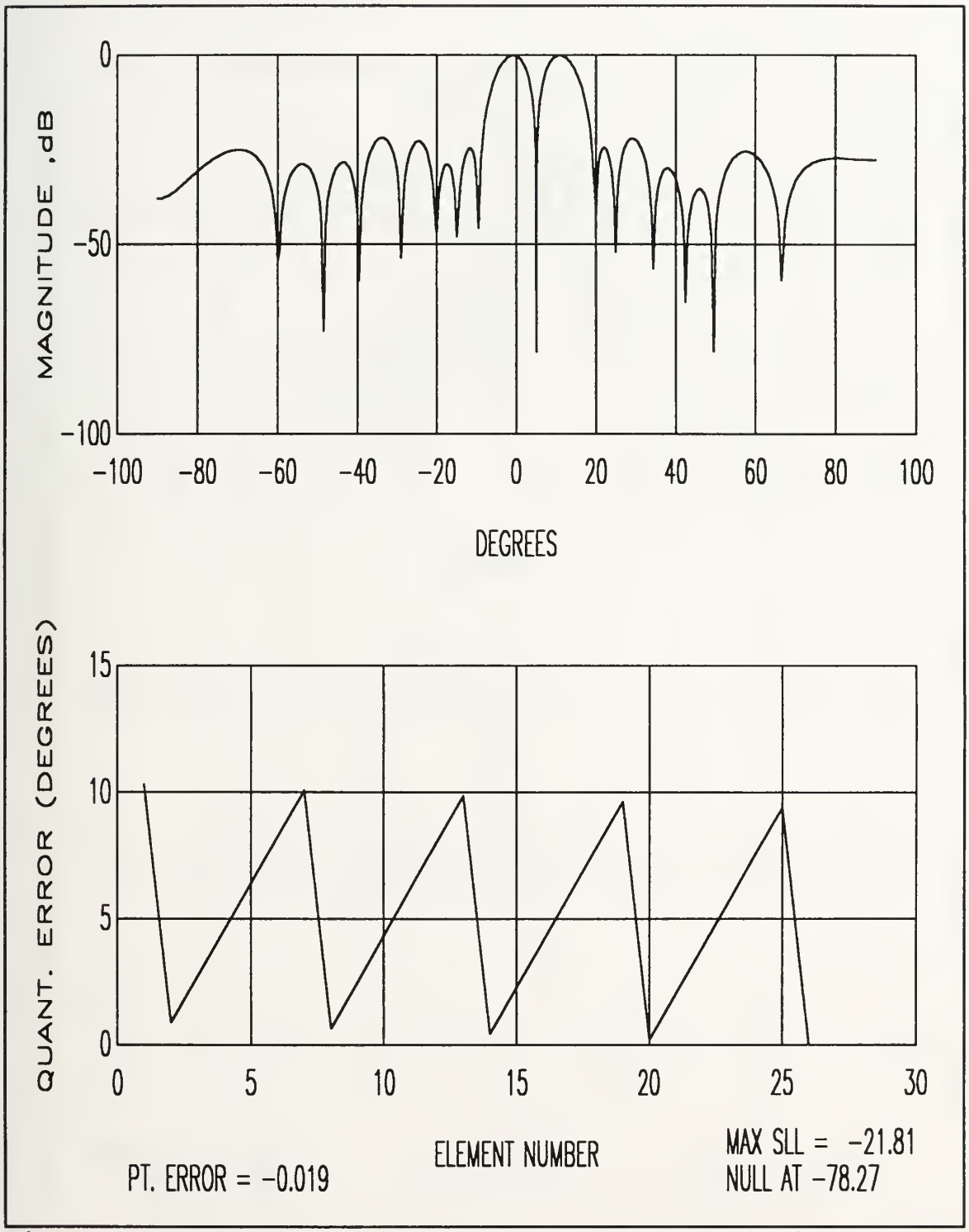

Figure 35. 26 Element Array Difference Beam Radiation Pattern for a 5 Bit Phase Shifter using Running Sum Roundoff

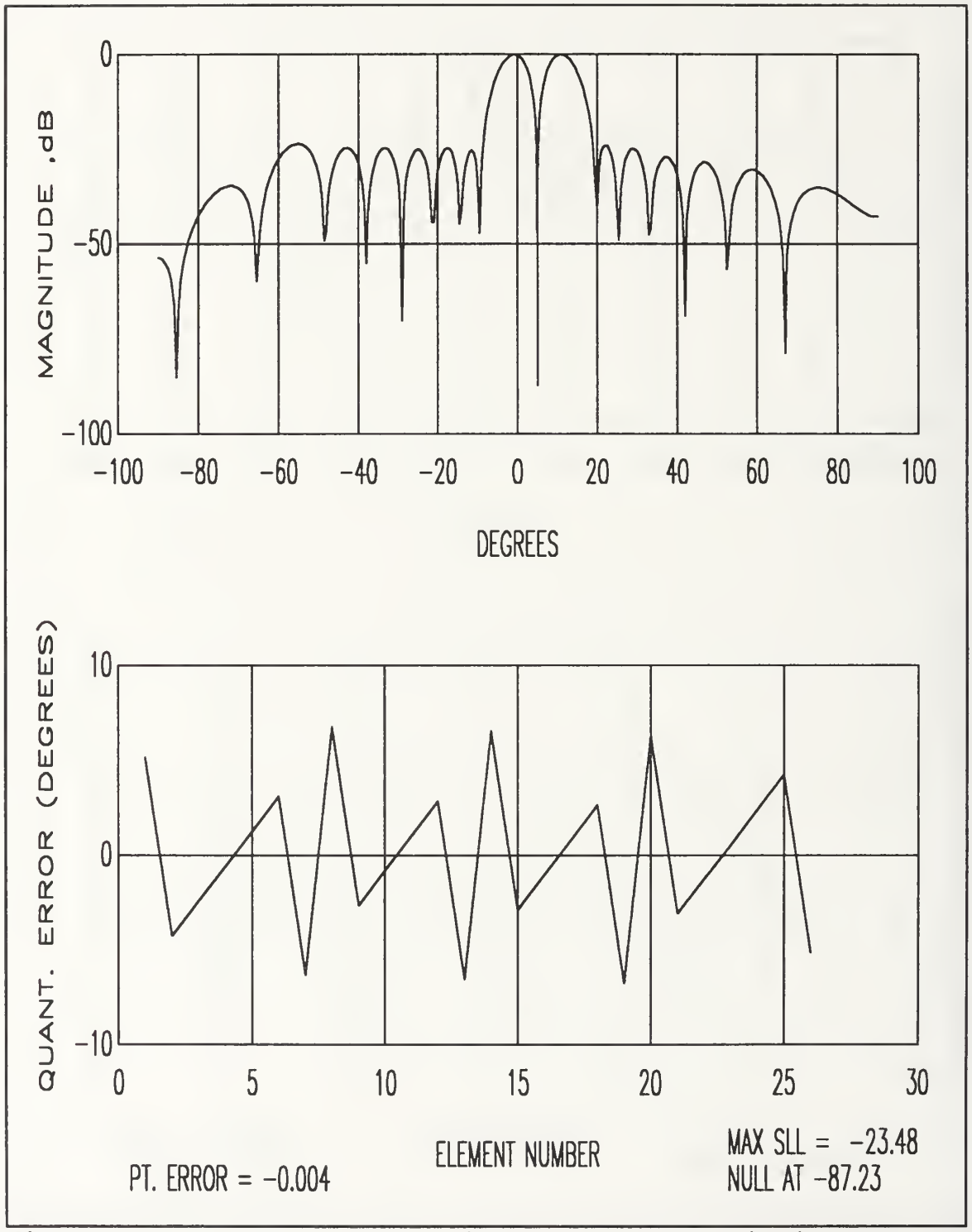

Figure 36. 26 Element Array Difference Beam Radiation Pattern for a 5 Bit Phase Shifter using Symmetric Running Sum Roundoff

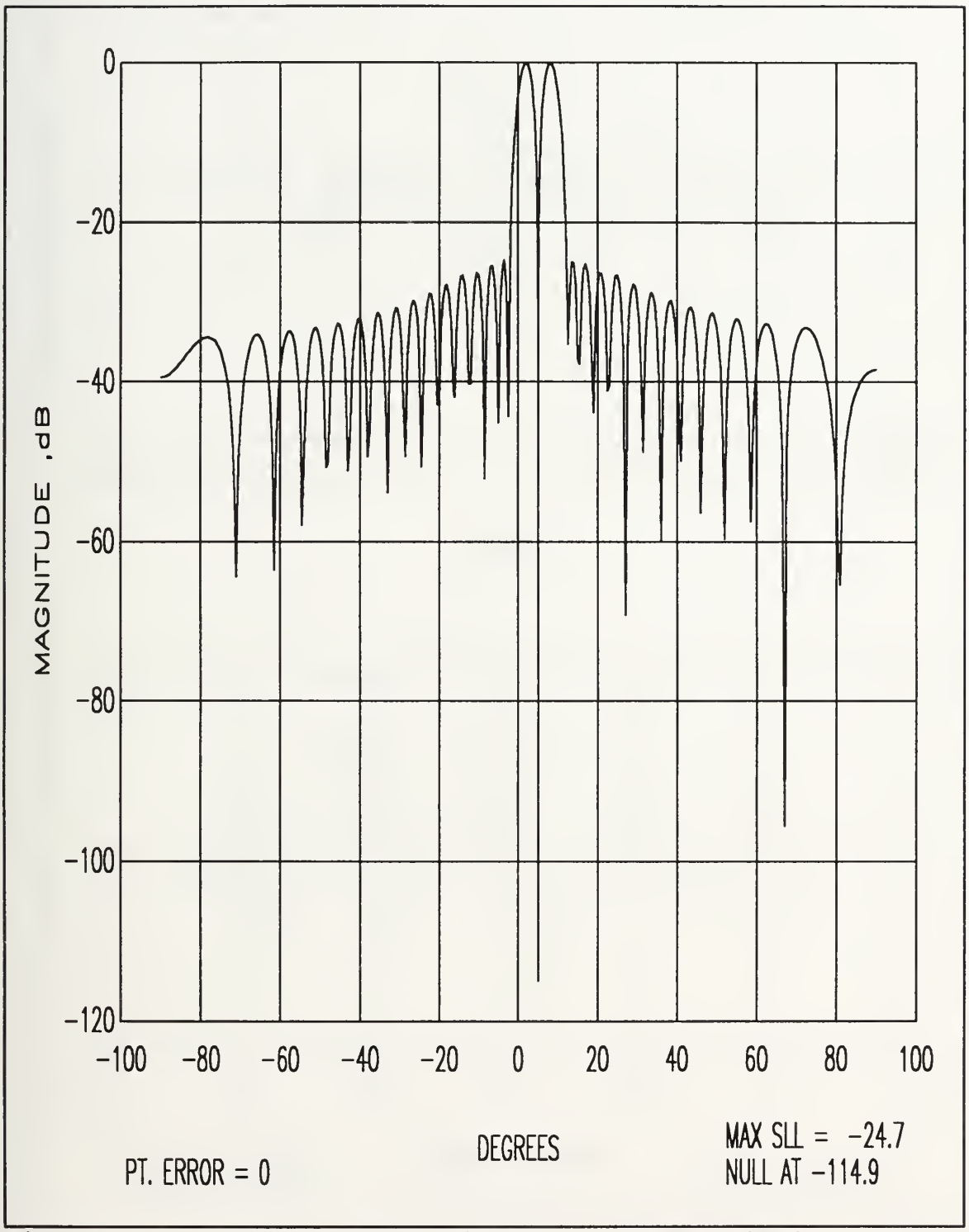

Figure 37. 50 Element Array Difference Beam Radiation Pattern for a 3 Bit Phase Shifter with Perfect Phase

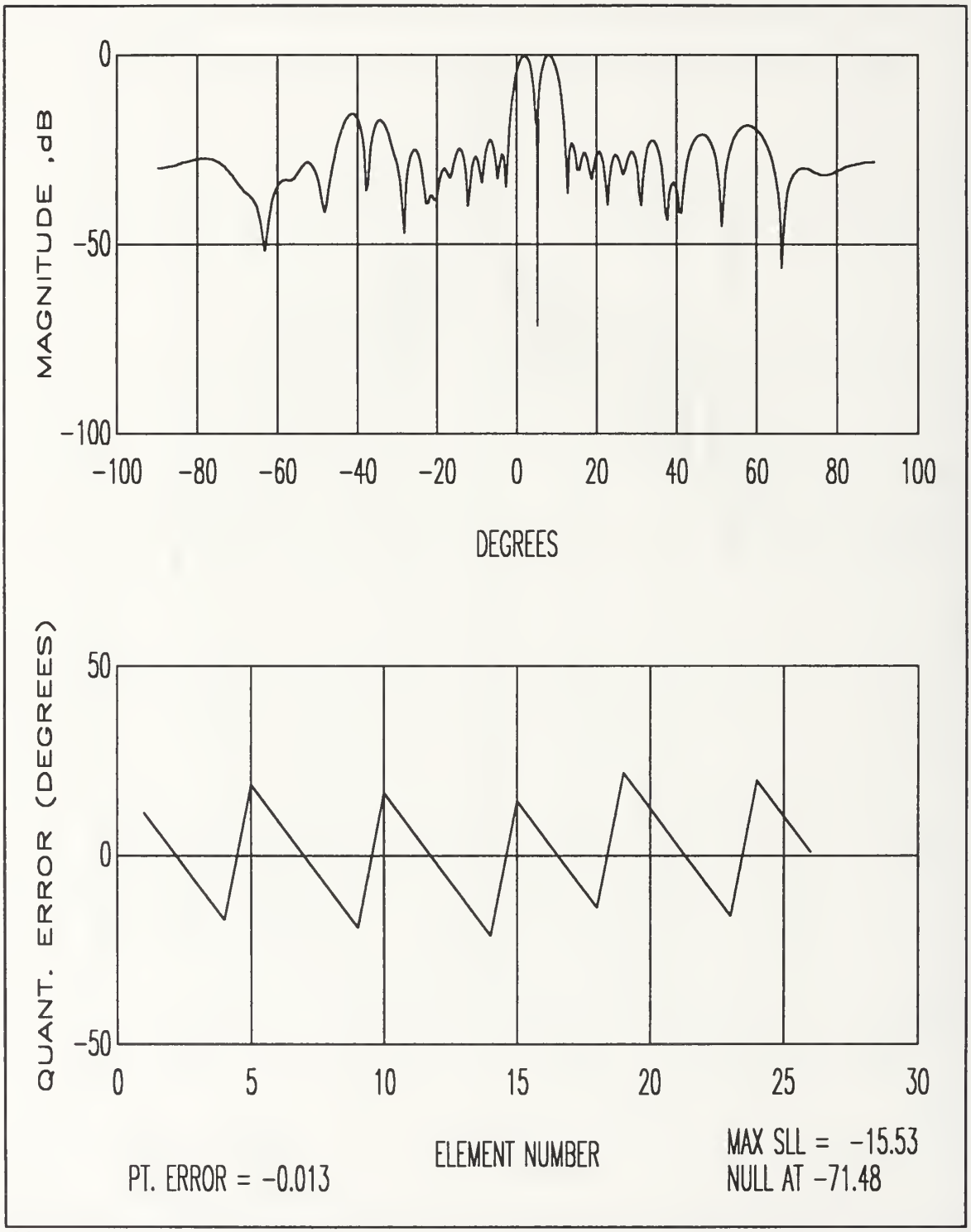

Figure 38. 50 Element Array Difference Beam Radiation Pattern for a 3 Bit Phase Shifter using Regular Roundoff

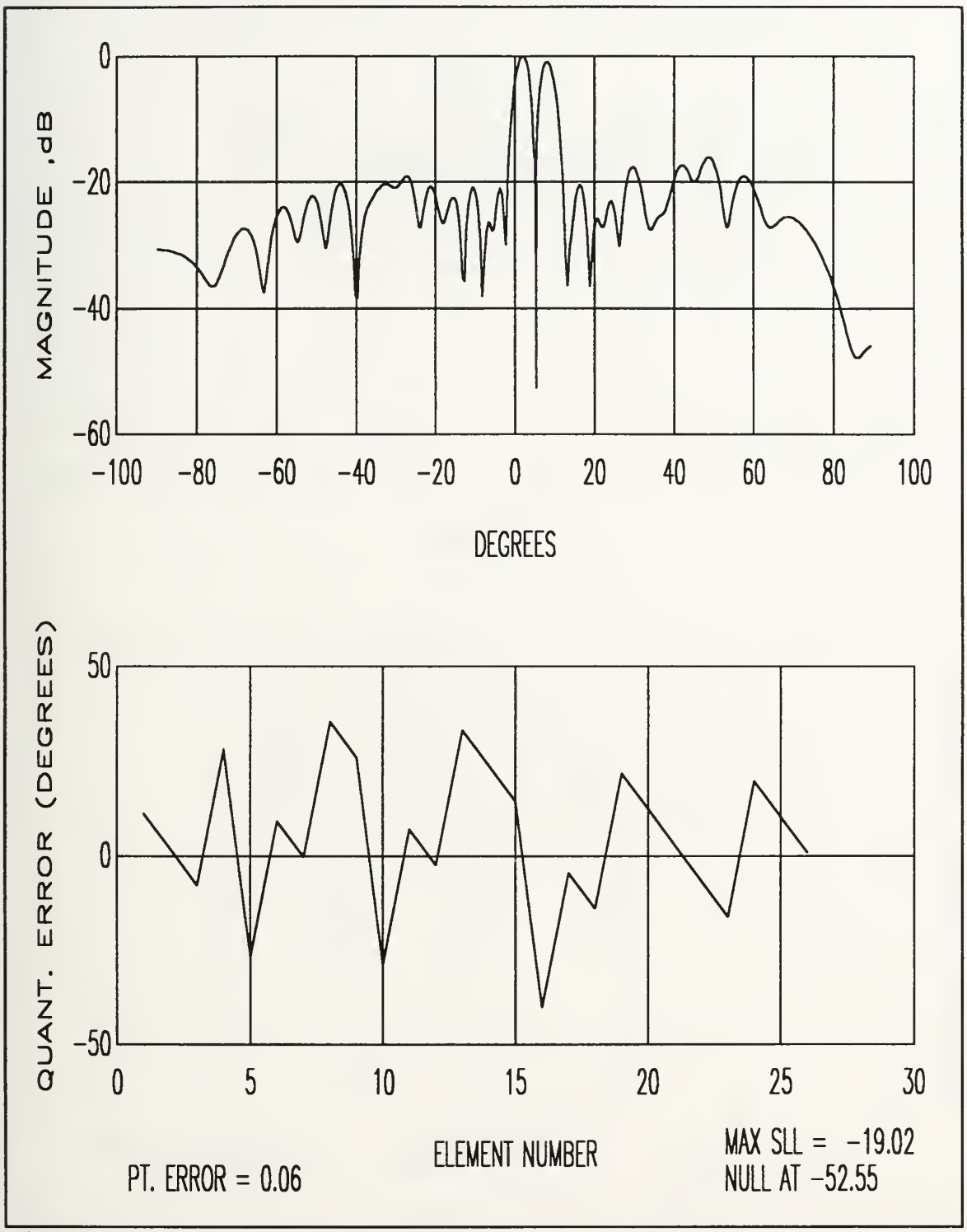

Figure 39. 50 Element Array Difference Beam Radiation Pattern for a 3 Bit Phase Shifter using Weighted Random Roundoff

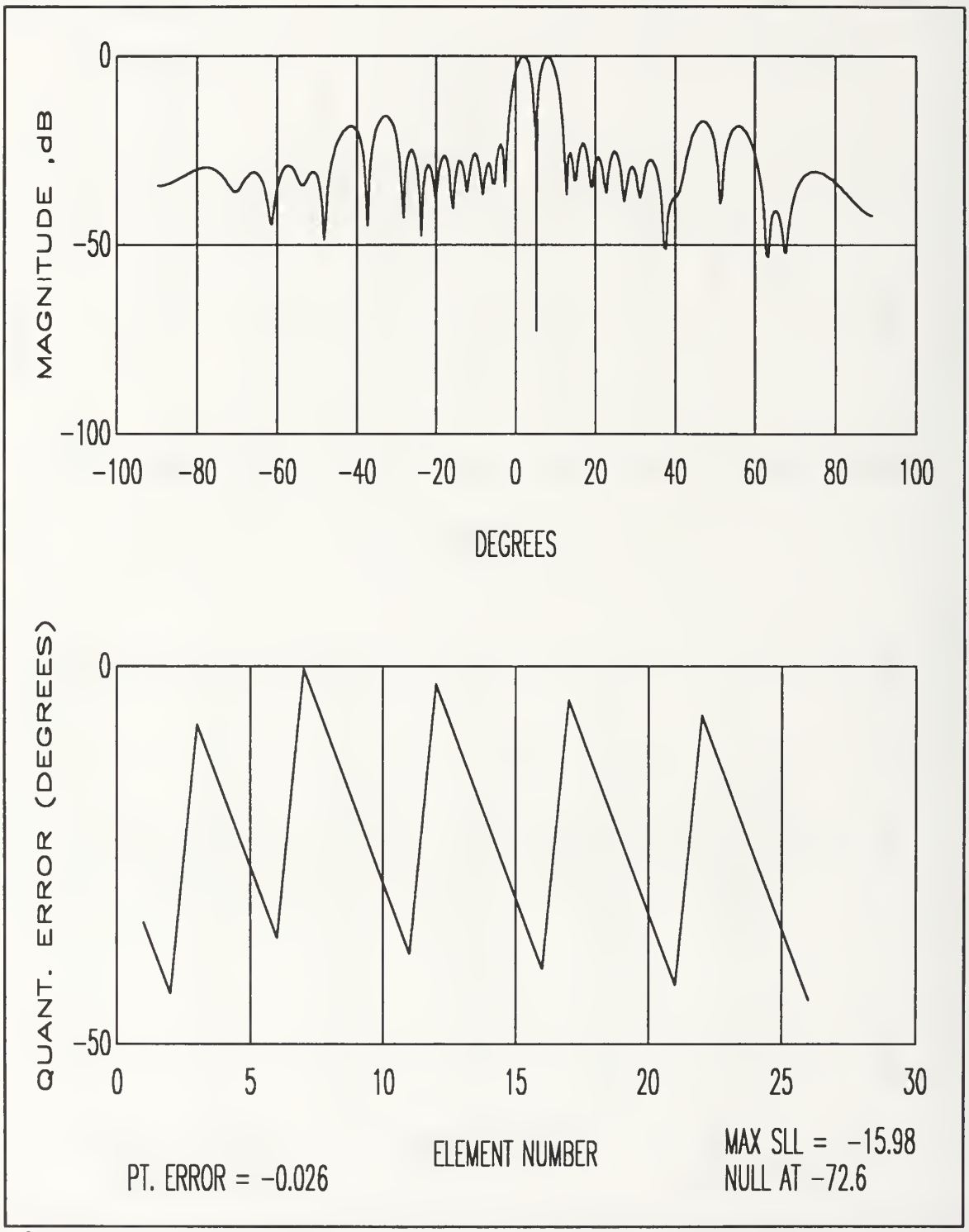

Figure 40. 50 Element Array Difference Beam Radiation Pattern for a 3 Bit Phase Shifter using Running Sum Roundoff

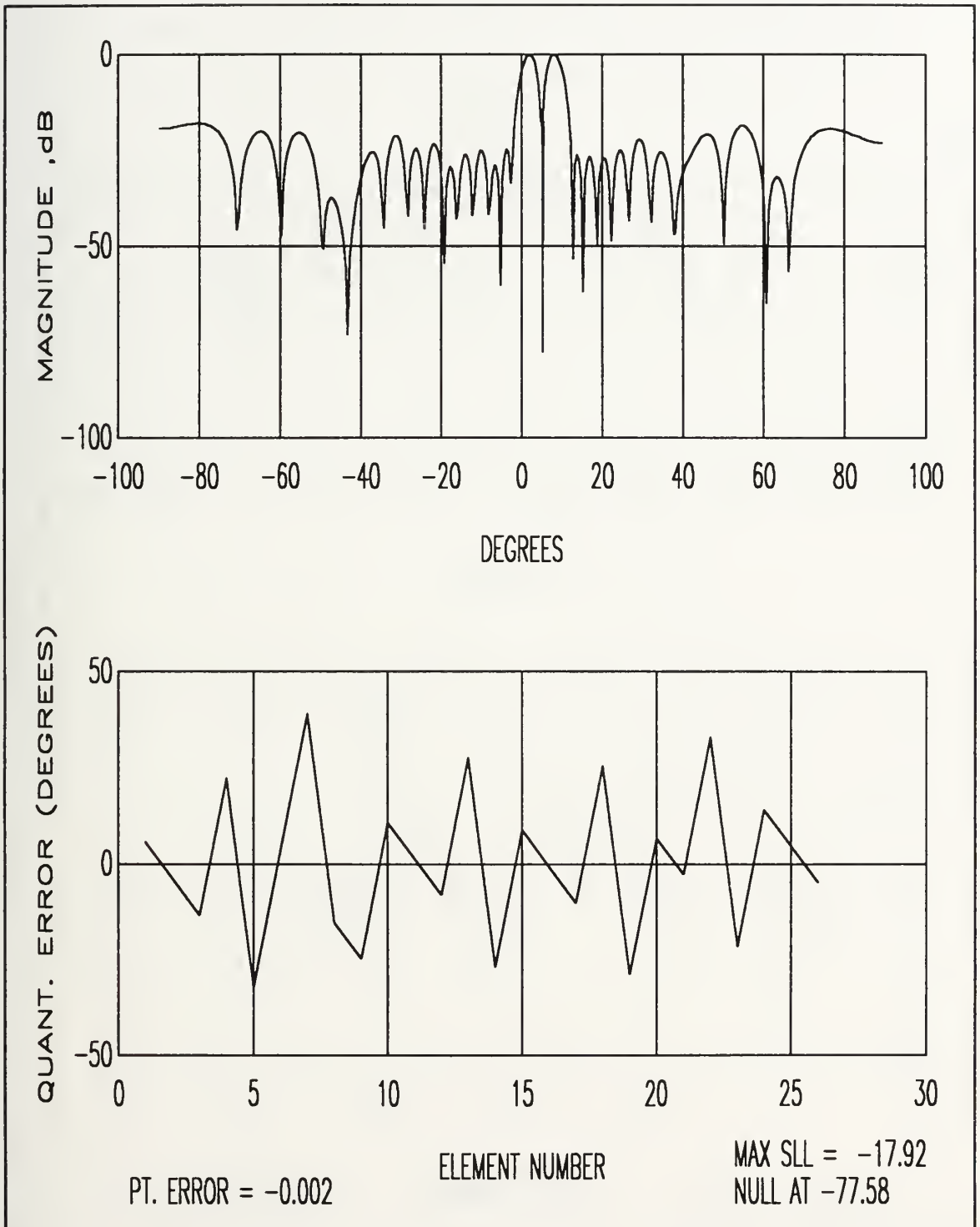

Figure 41. 50 Element Array Difference Beam Radiation Pattern for a 3 Bit Phase Shifter using Symmetrical Running Sum Roundoff

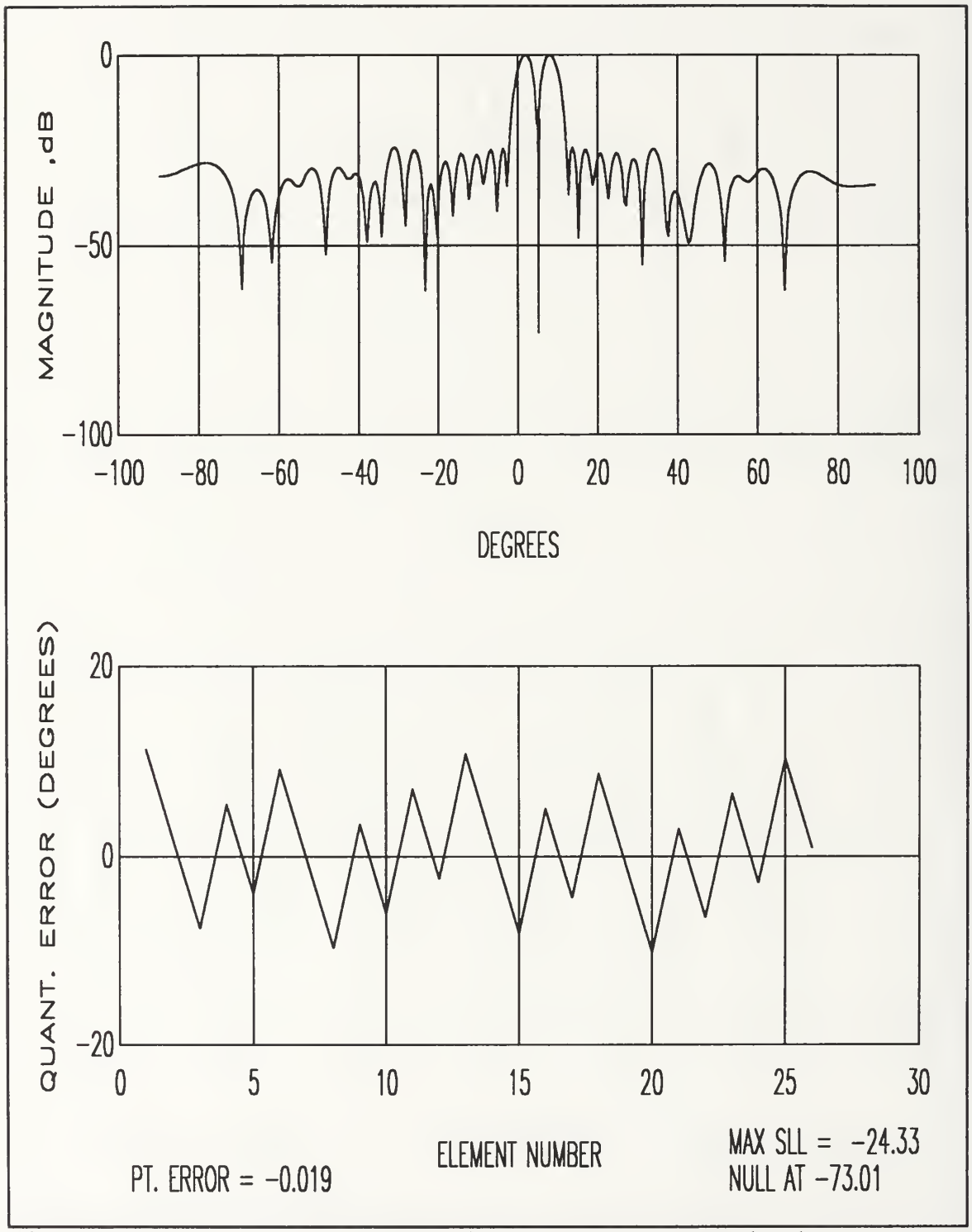

Figure 42. 50 Element Array Difference Beam Radiation Pattern for a 4 Bit Phase Shifter using Regular Roundoff

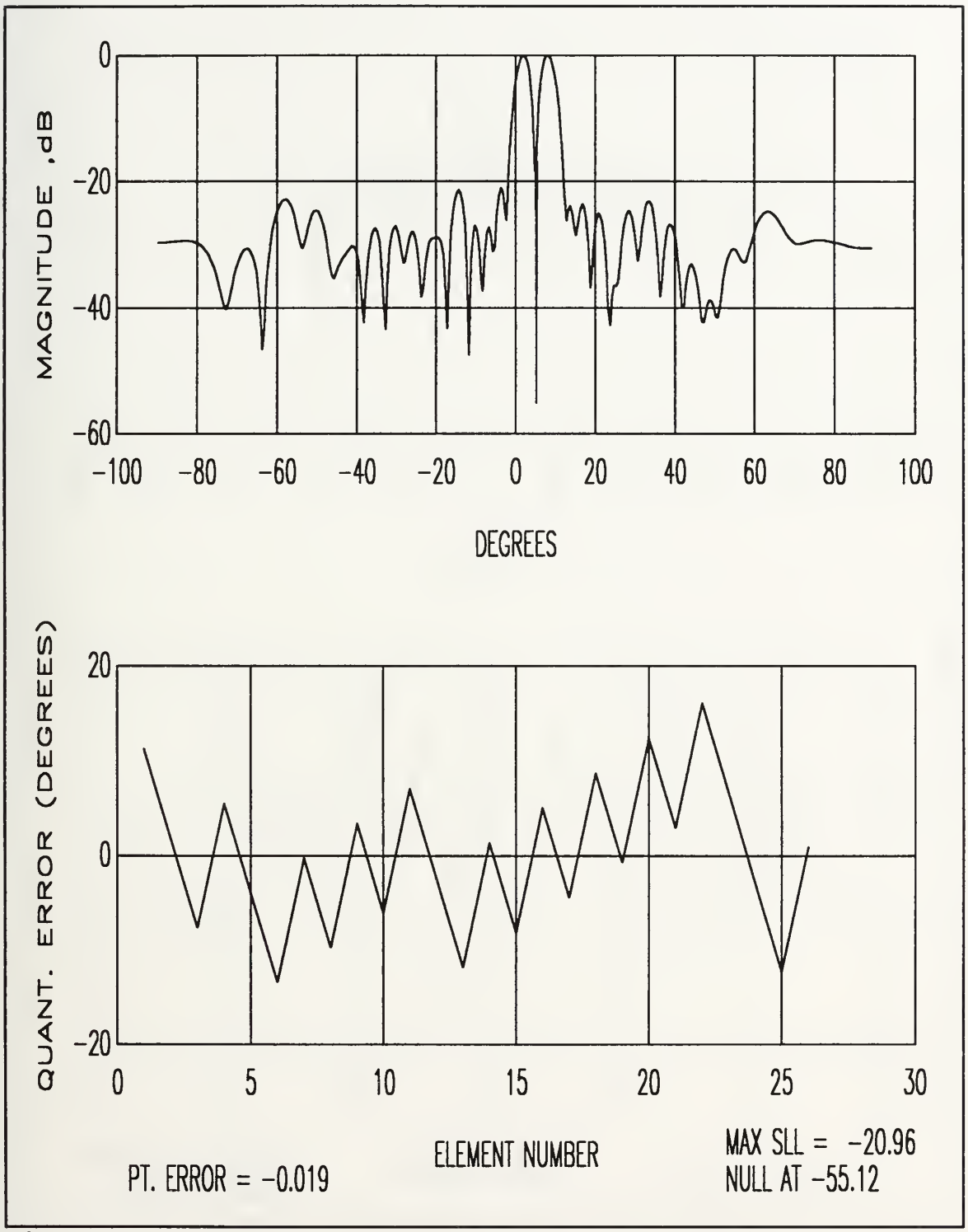

Figure 43. 50 Element Array Difference Beam Radiation Pattern for a 4 Bit Phase Shifter using Weighted Random Roundoff

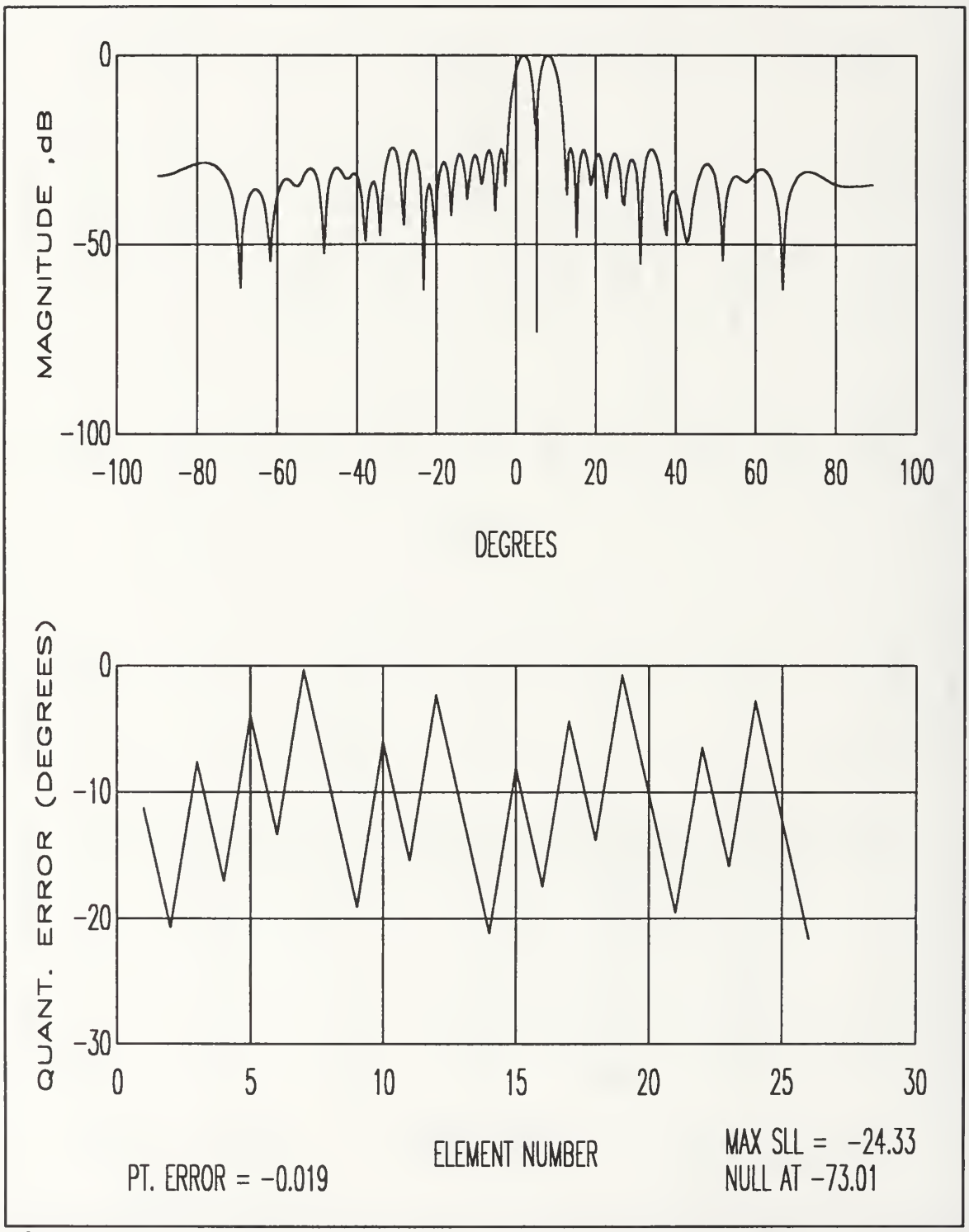

Figure 44. 50 Element Array Difference Beam Radiation Pattern for a 4 Bit Phase Shifter using Running Sum Roundoff

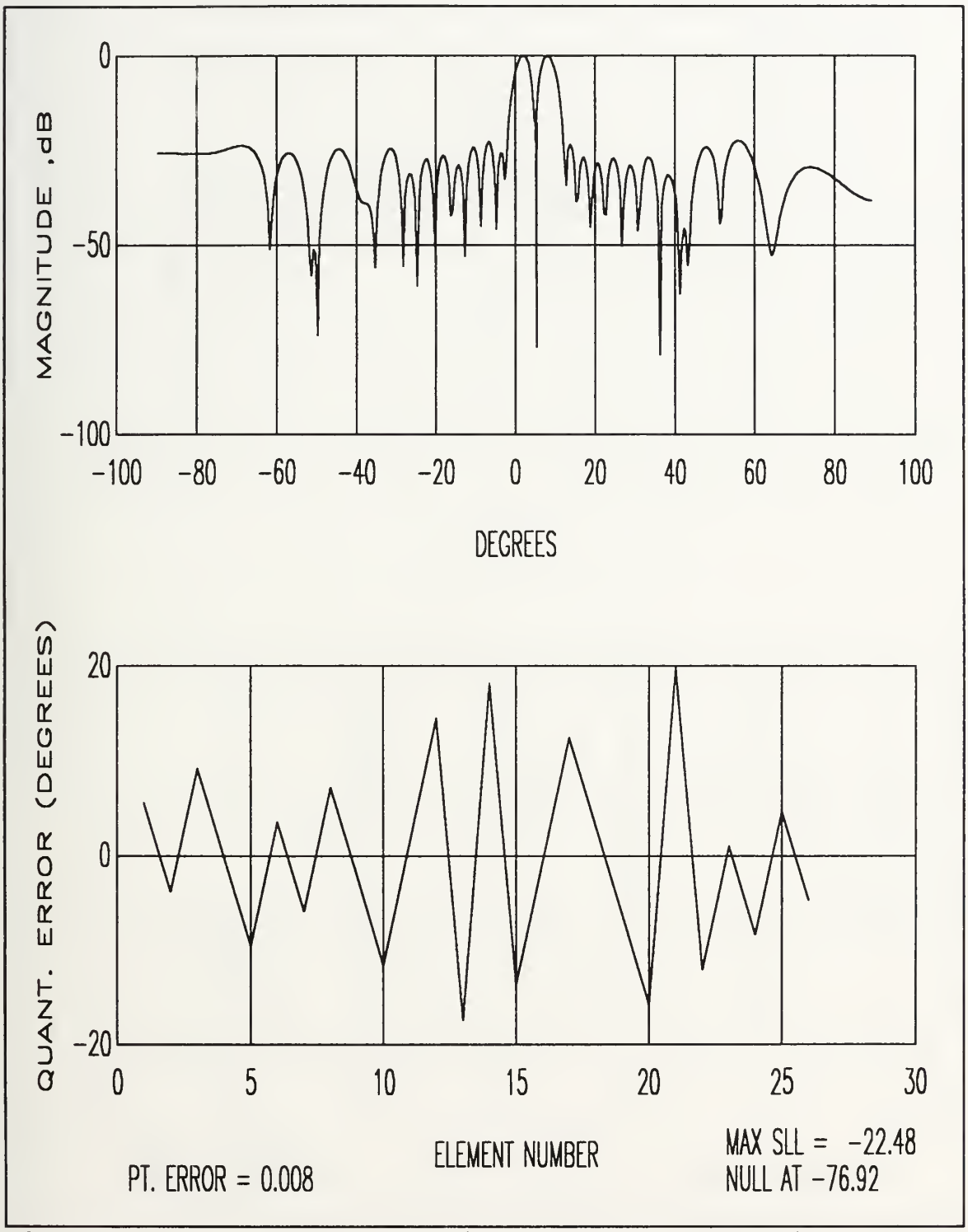

Figure 45. 50 Element Array Difference Beam Radiation Pattern for a 4 Bit Phase Shifter using Symmetric Running Sum Roundoff

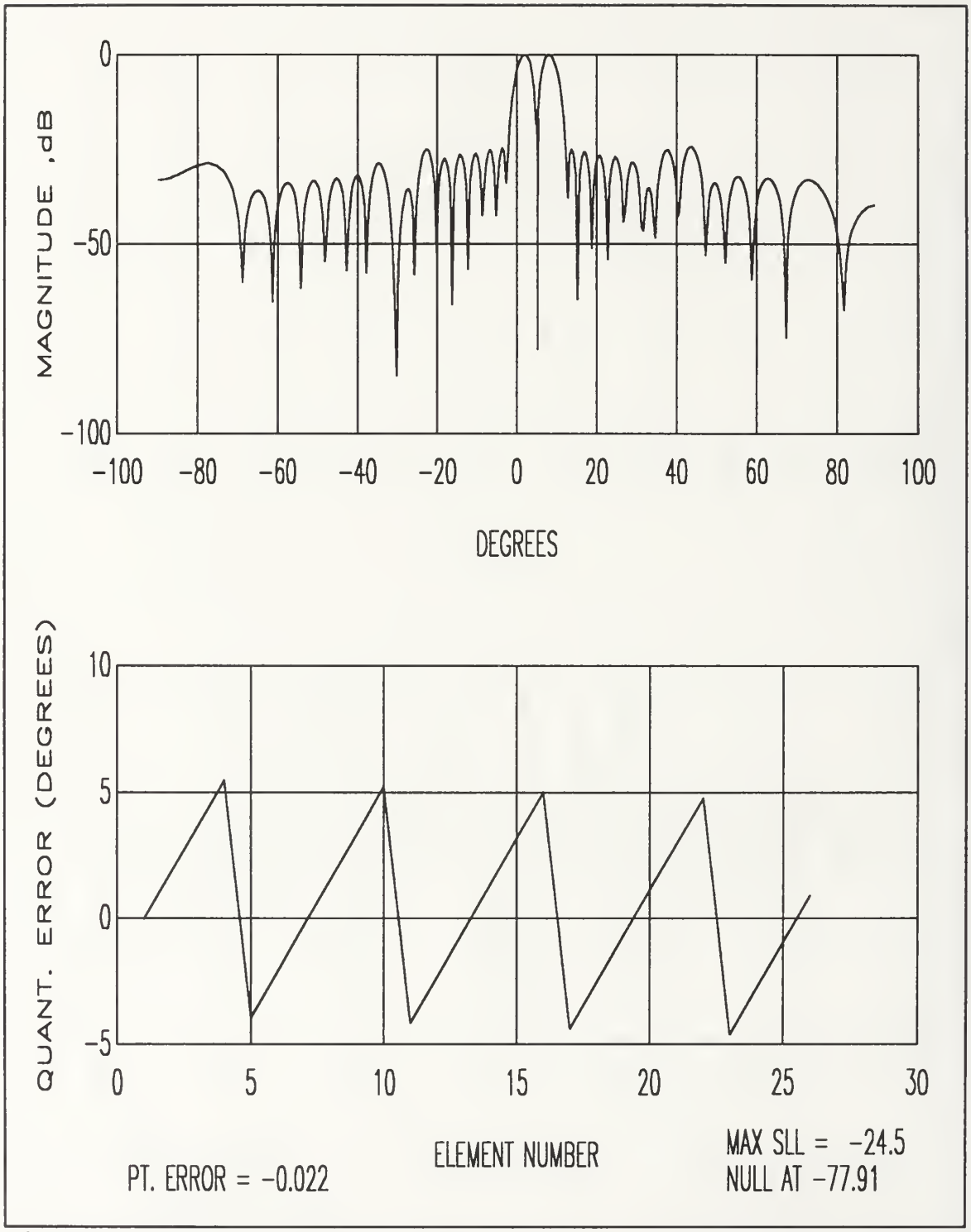

Figure 46. 50 Element Array Difference Beam Radiation Pattern for a 5 Bit Phase Shifter using Regular Roundoff

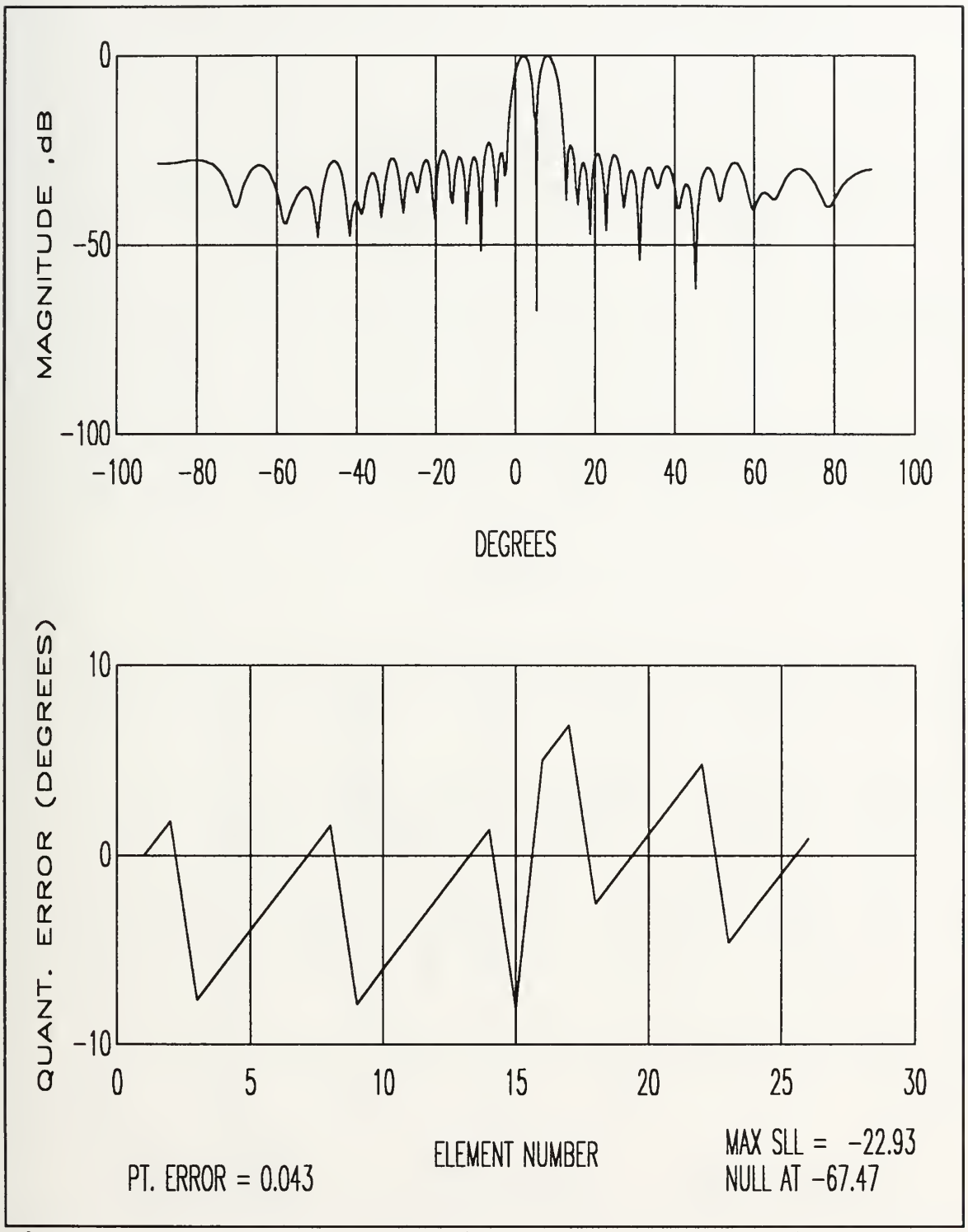

Figure 47. 50 Element Array Difference Beam Radiation Pattern for a 5 Bit Phase Shifter using Weighted Random Roundoff

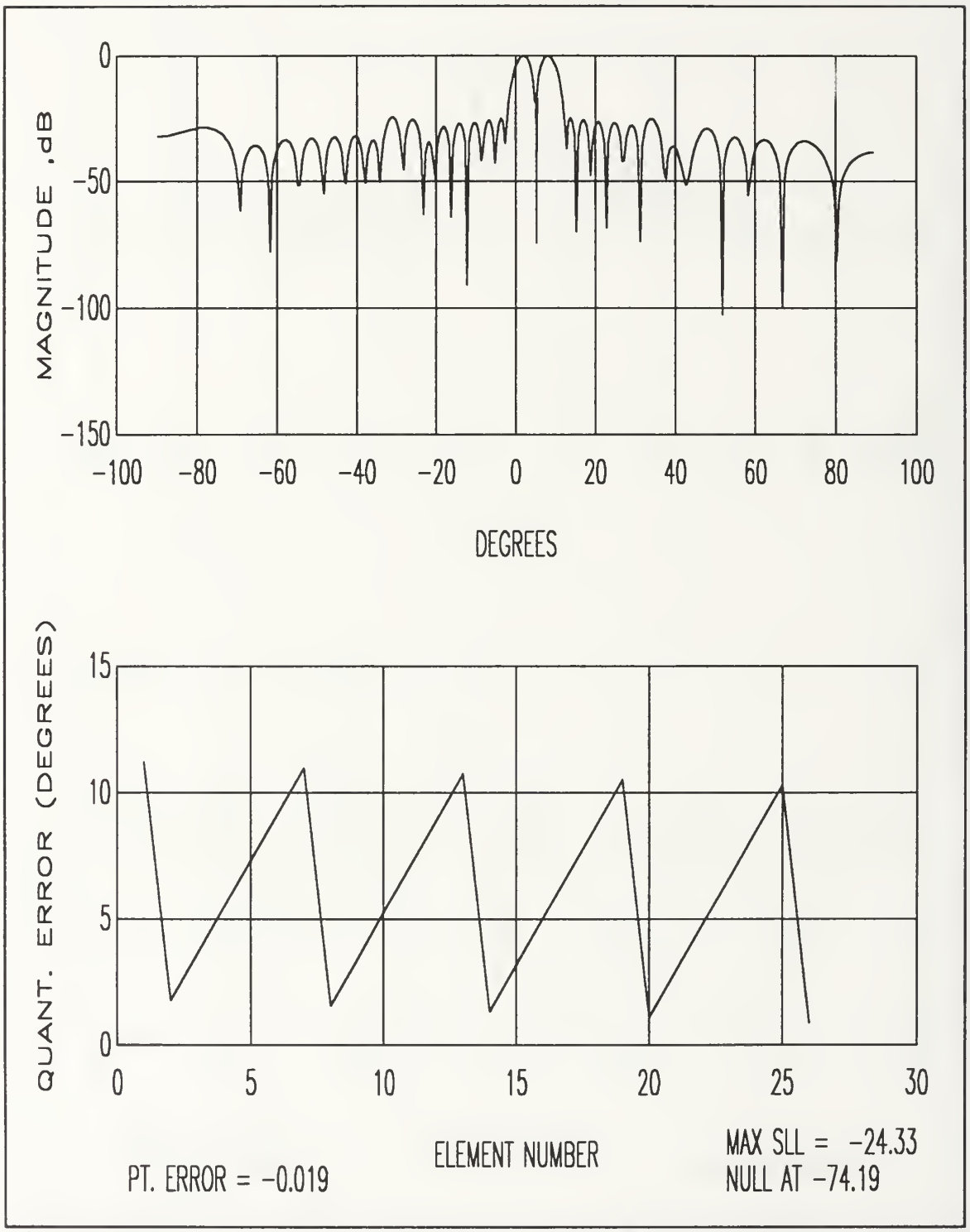

Figure 48. 50 Element Array Difference Beam Radiation Pattern for a 5 Bit Phase Shifter using Running Sum Roundoff

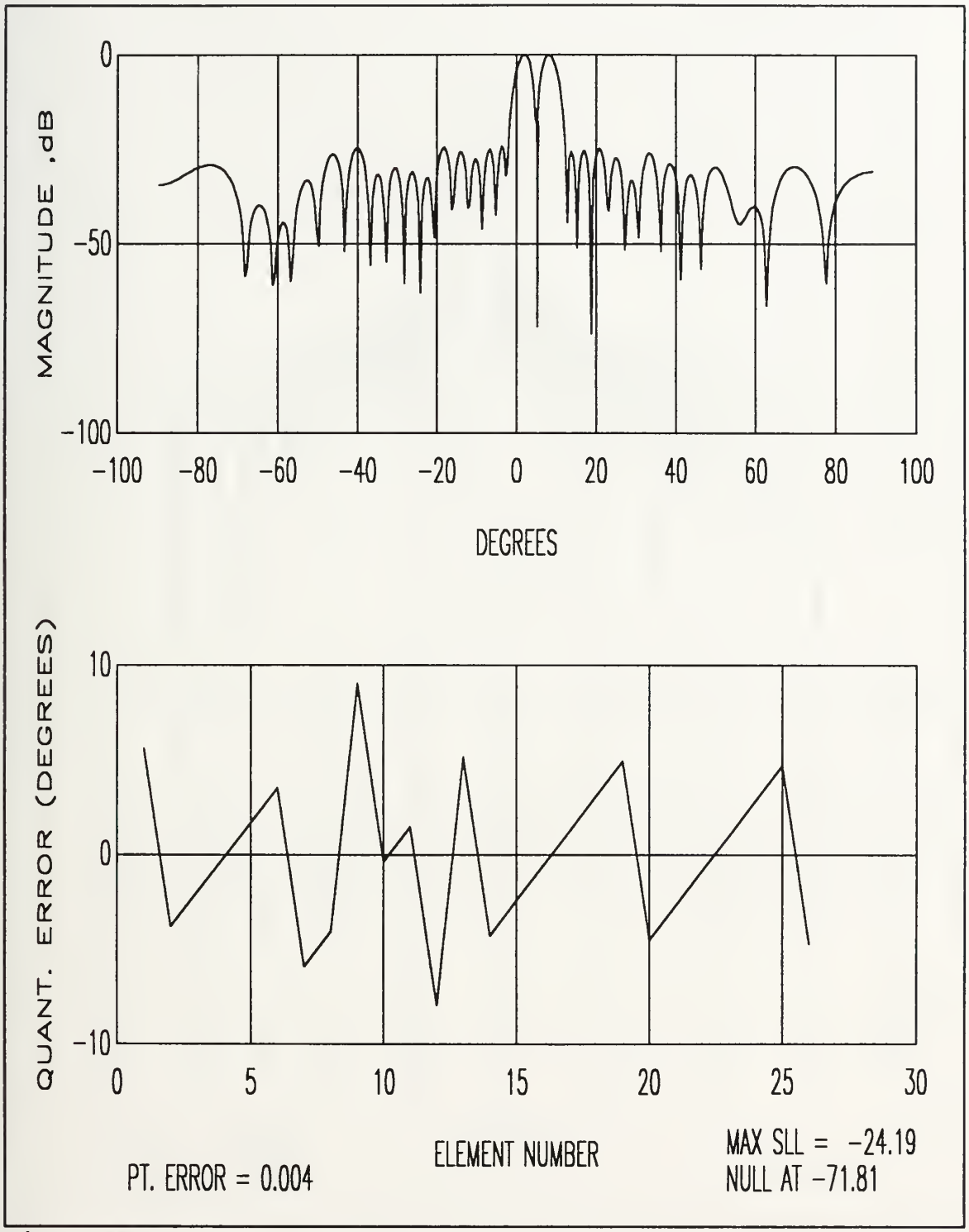

Figure 49. 50 Element Array Difference Beam Radiation Pattern for a 5 Bit Phase Shifter using Symmetric Running Sum Roundoff

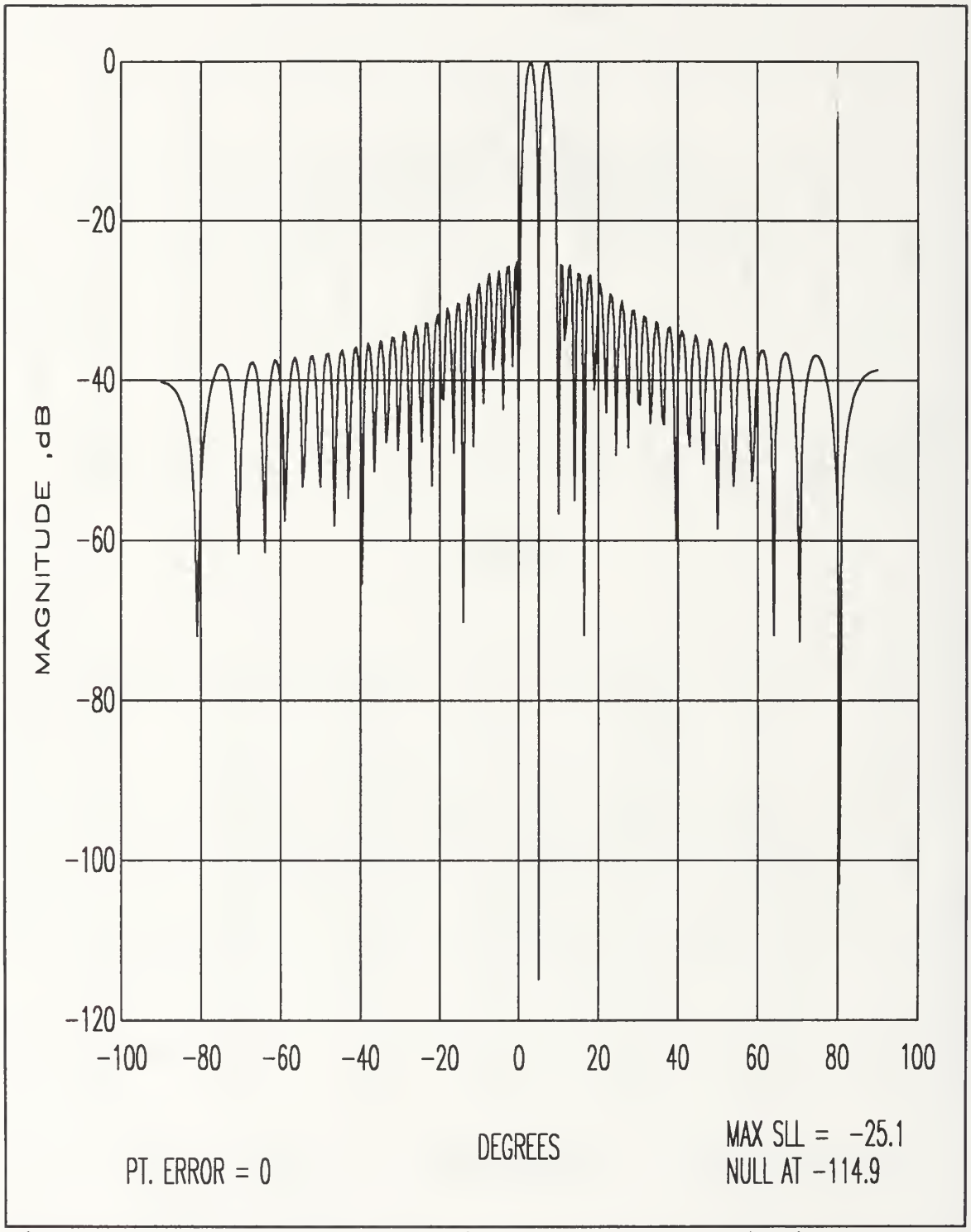

Figure 50. 76 Element Array Difference Beam Radiation Pattern for a 3 Bit Phase Shifter with Perfect Phase

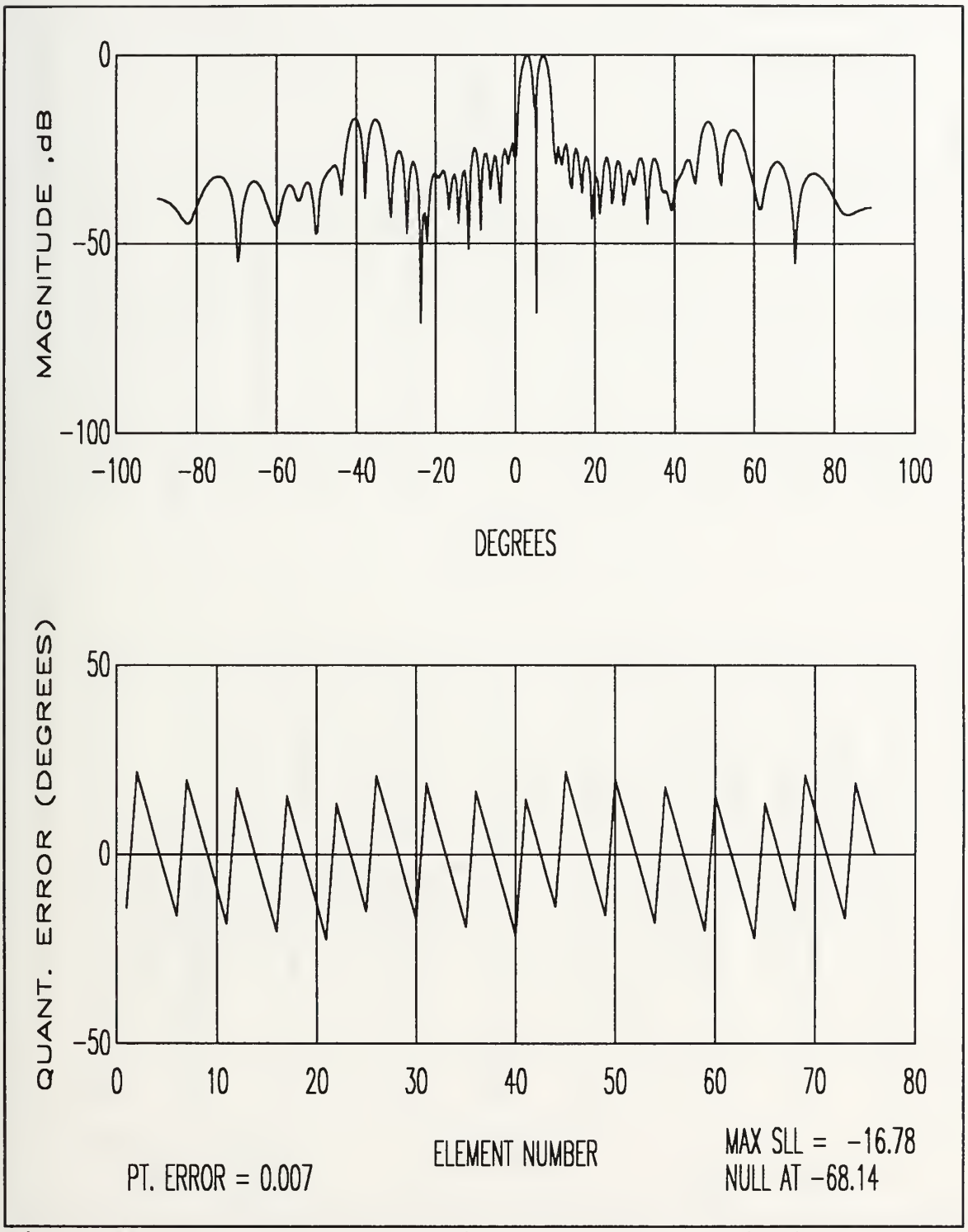

Figure 51. 76 Element Array Difference Beam Radiation Pattern for a 3 Bit Phase Shifter using Regular Roundoff

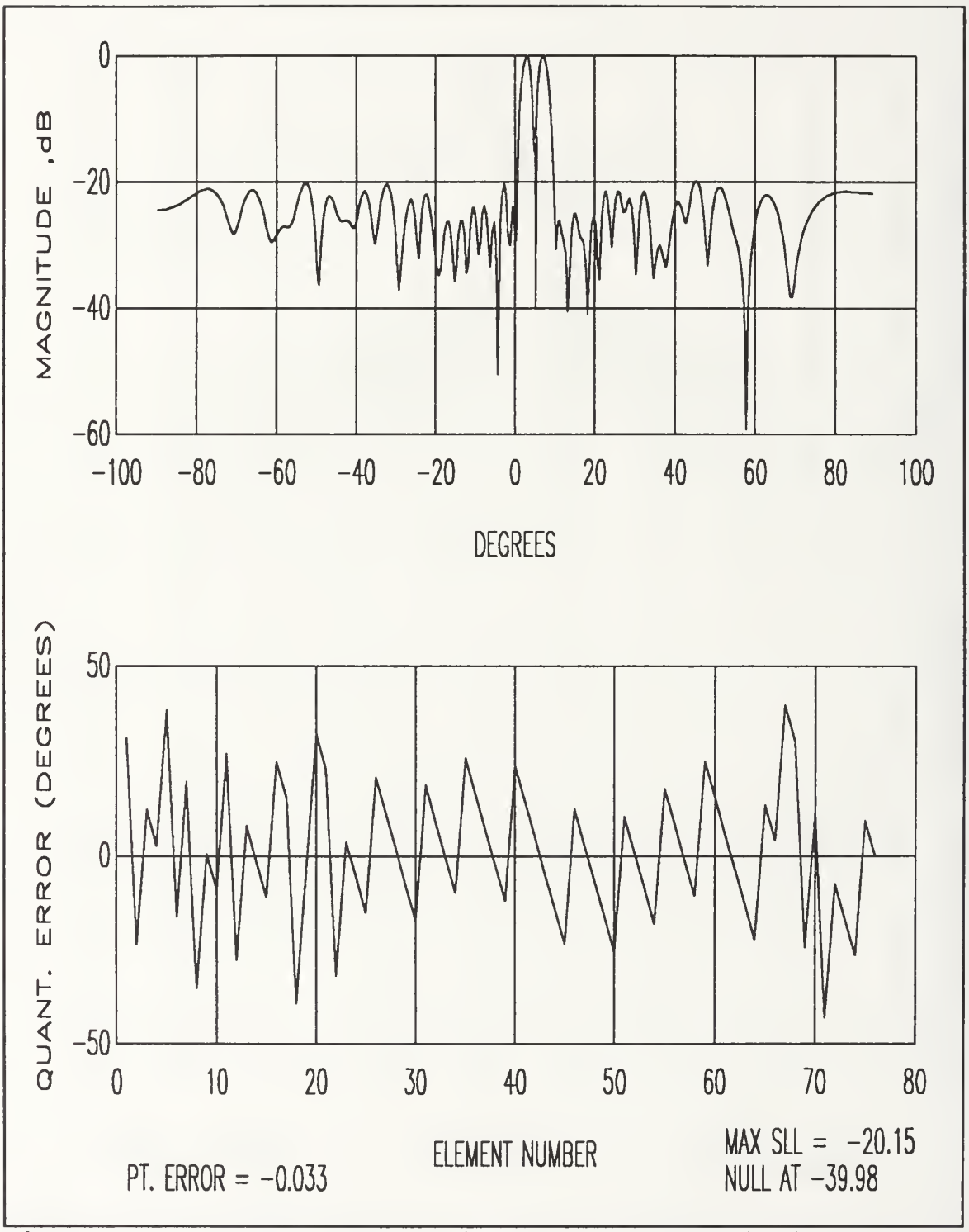

Figure 52. 76 Element Array Difference Beam Radiation Pattern for a 3 Bit Phase Shifter using Weighted Random Roundoff

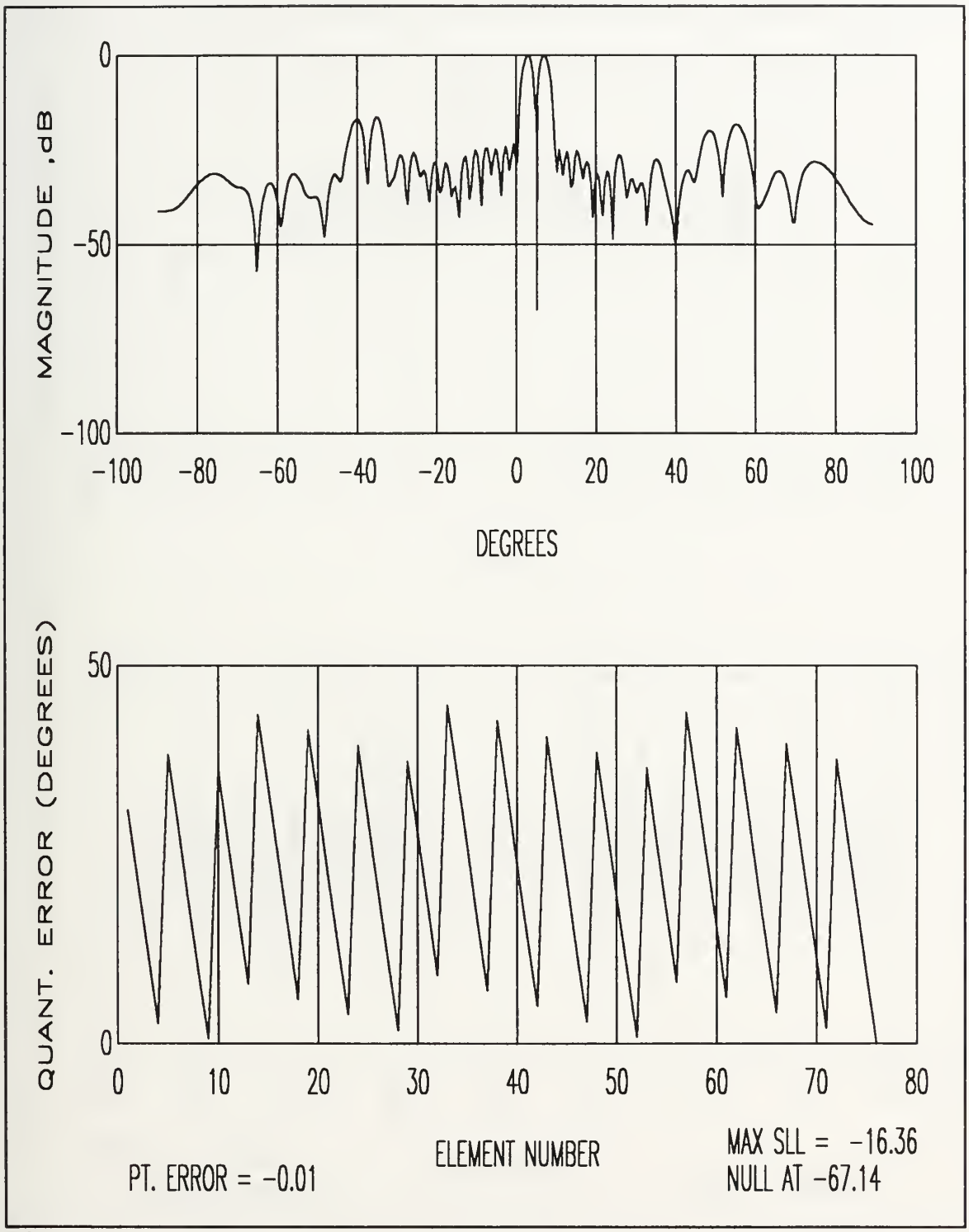

Figure 53. 76 Element Array Difference Beam Radiation Pattern for a 3 Bit Phase Shifter using Running Sum Roundoff

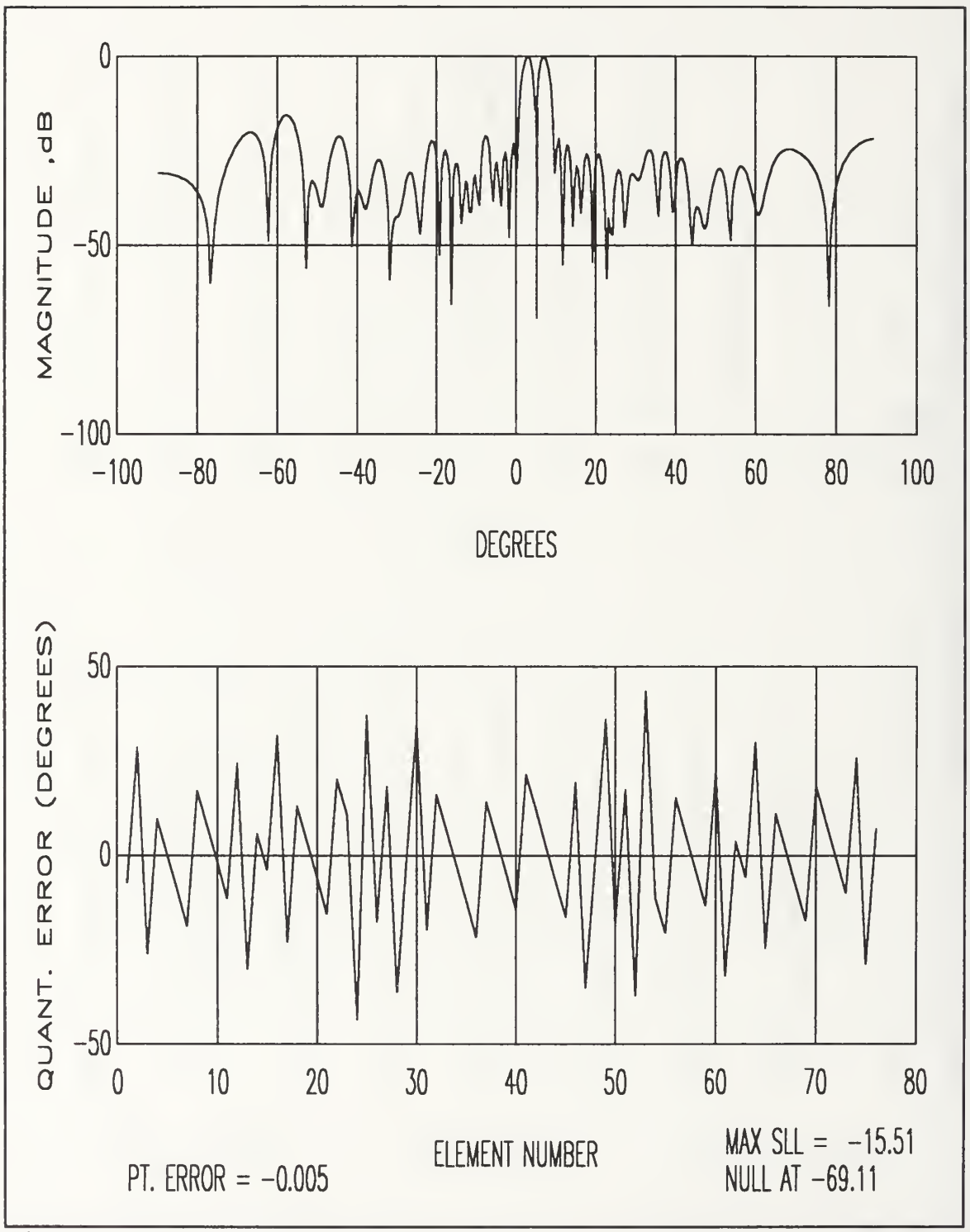

Figure 54. 76 Element Array Difference Beam Radiation Pattern for a 3 Bit Phase Shifter using Symmetric Running Sum Roundoff

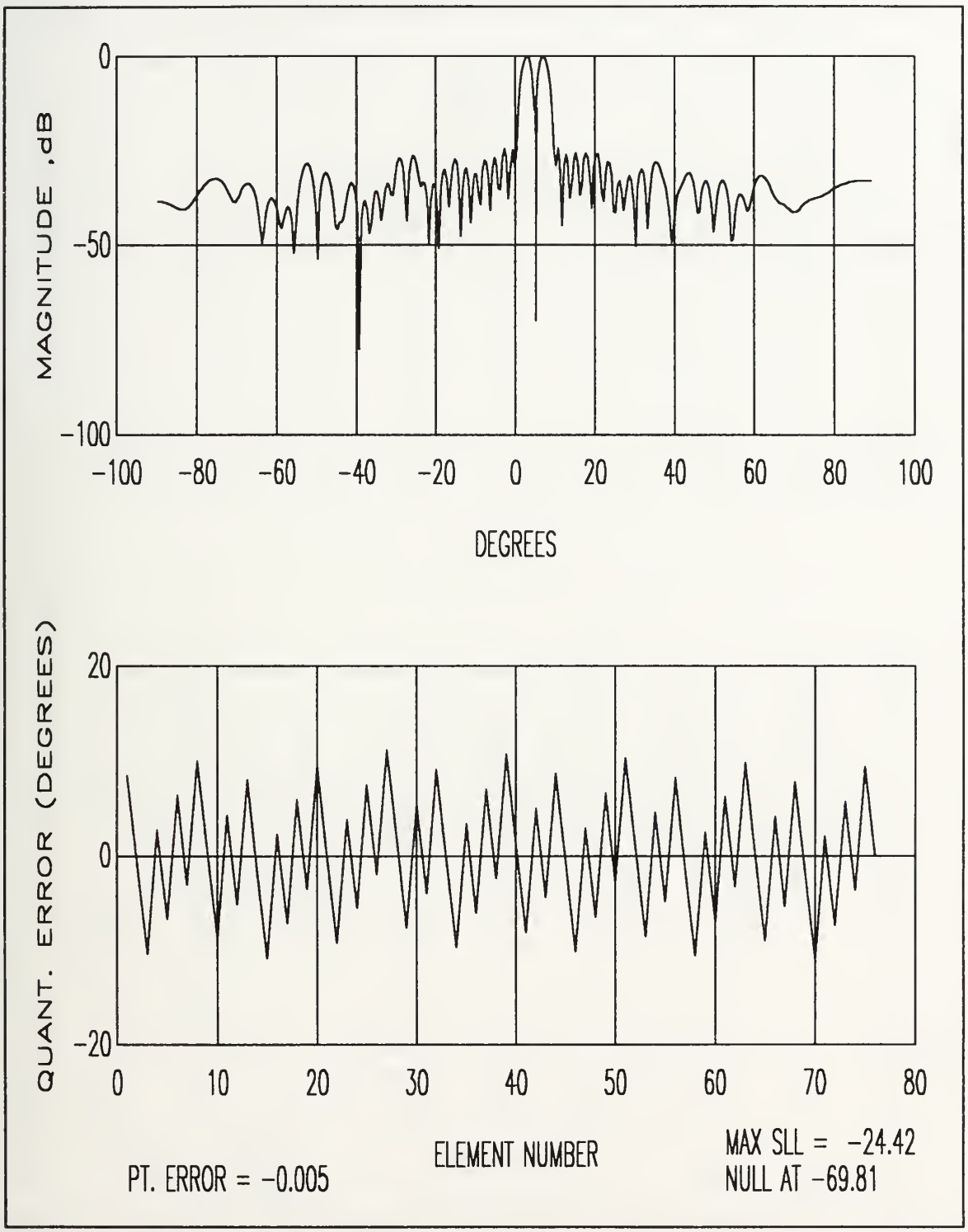

Figure 55. 76 Element Array Difference Beam Radiation Pattern for a 4 Bit Phase Shifter using Regular Roundoff

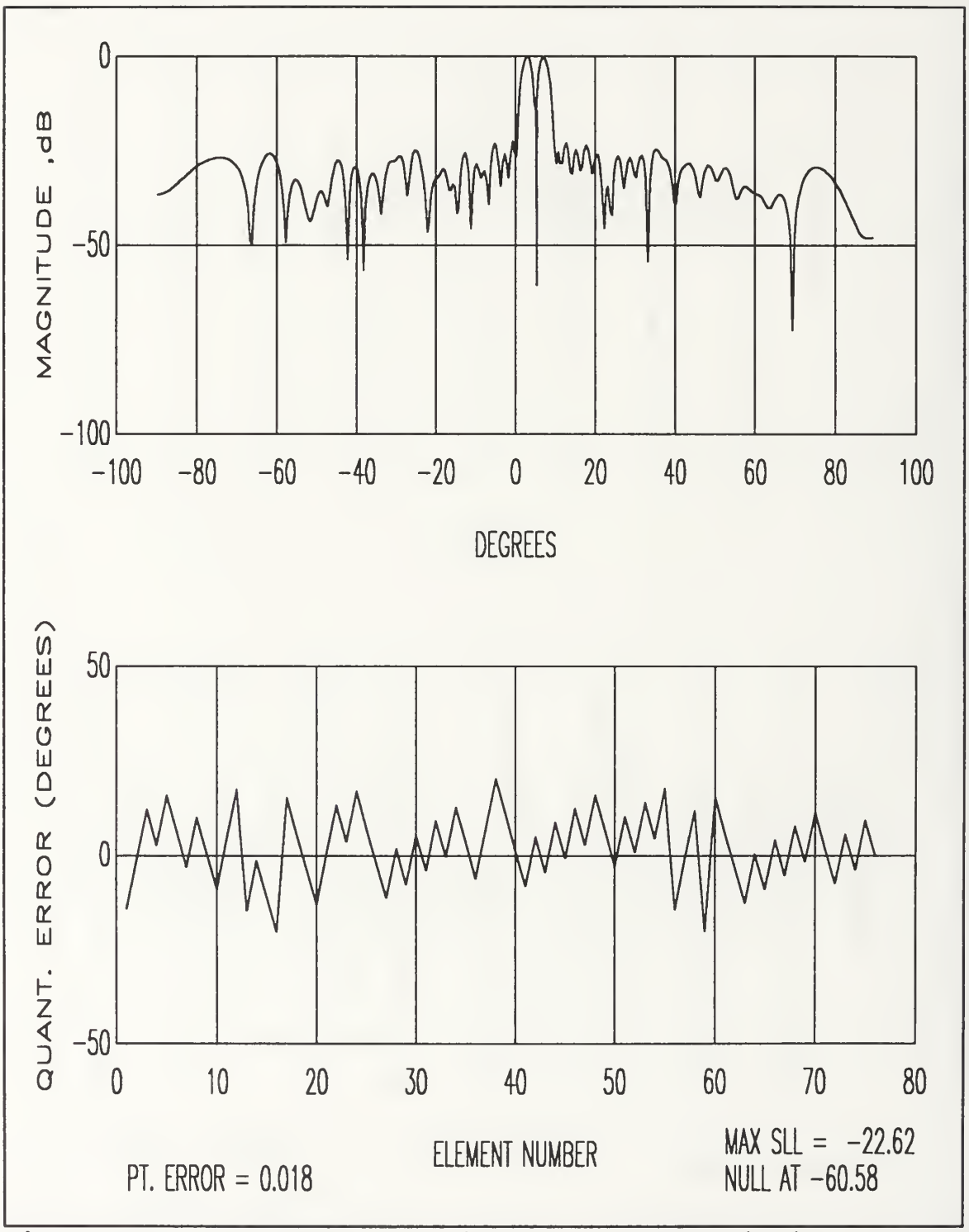

Figure 56. 76 Element Array Difference Beam Radiation Pattern for a 4 Bit Phase Shifter using Weighted Random Roundoff

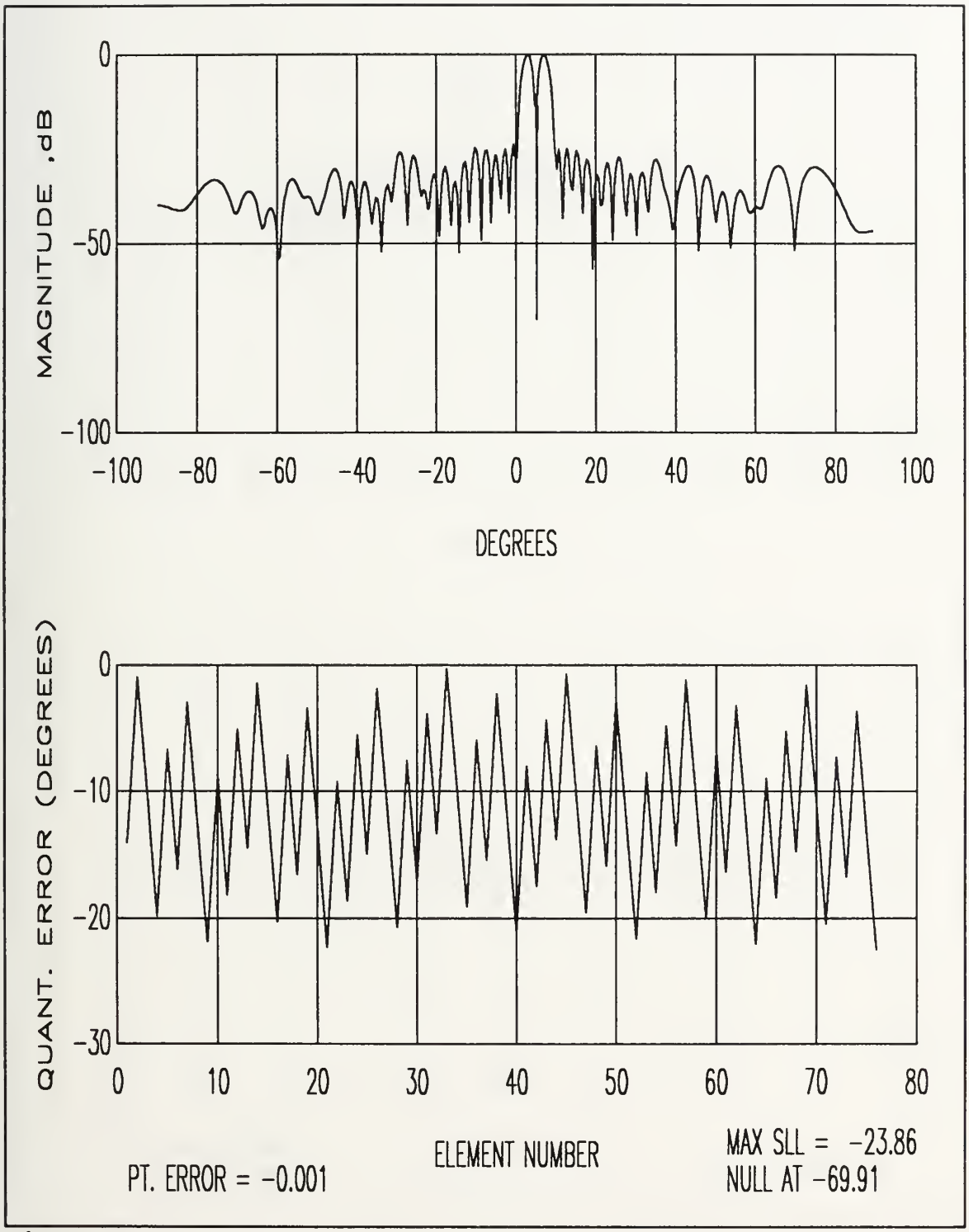

Figure 57. 76 Element Array Difference Beam Radiation Pattern for a 4 Bit Phase Shifter using Running Sum Roundoff

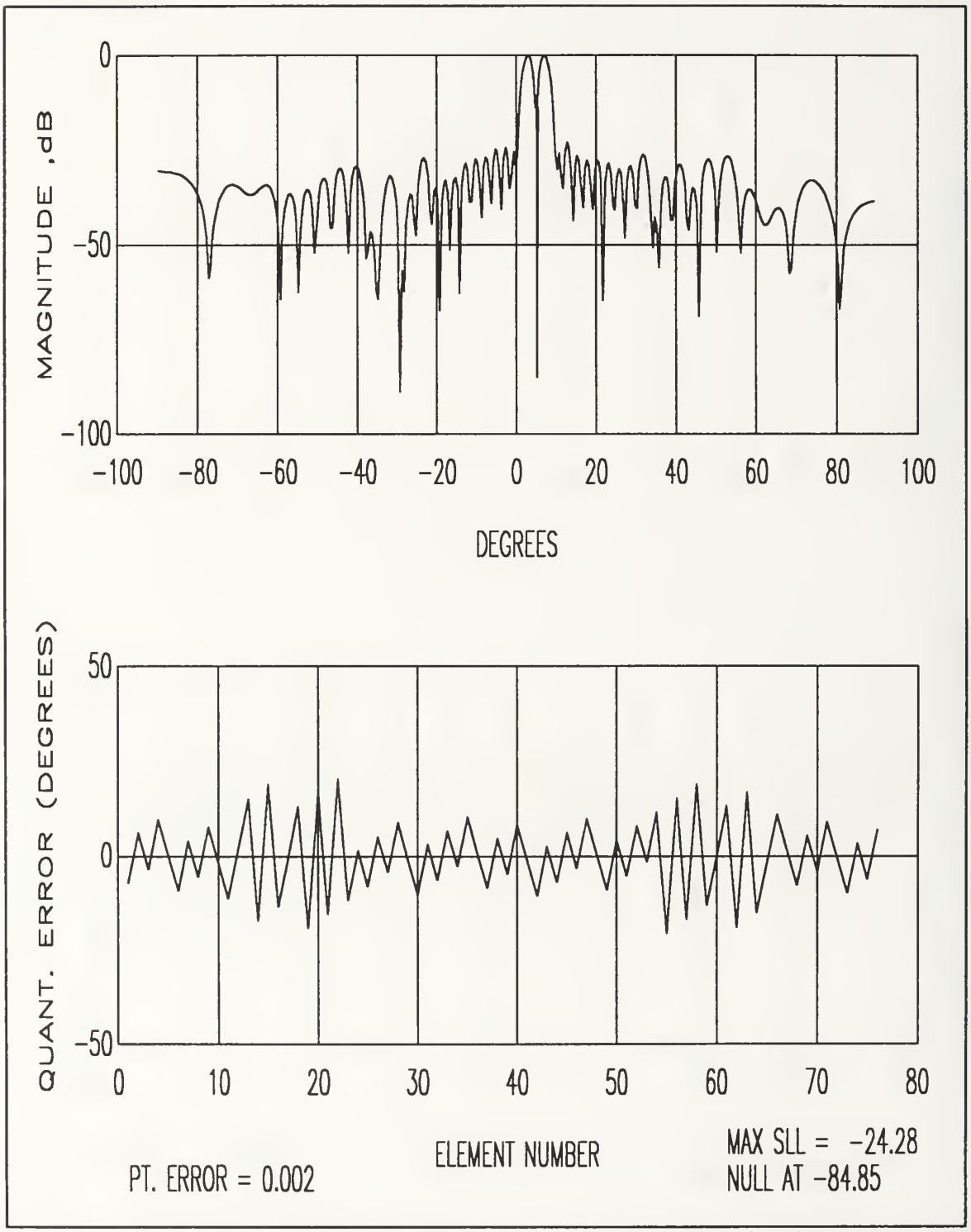

Figure 58. 76 Element Array Difference Beam Radiation Pattern for a 4 Bit Phase Shifter using Symmetric Running Sum Roundoff

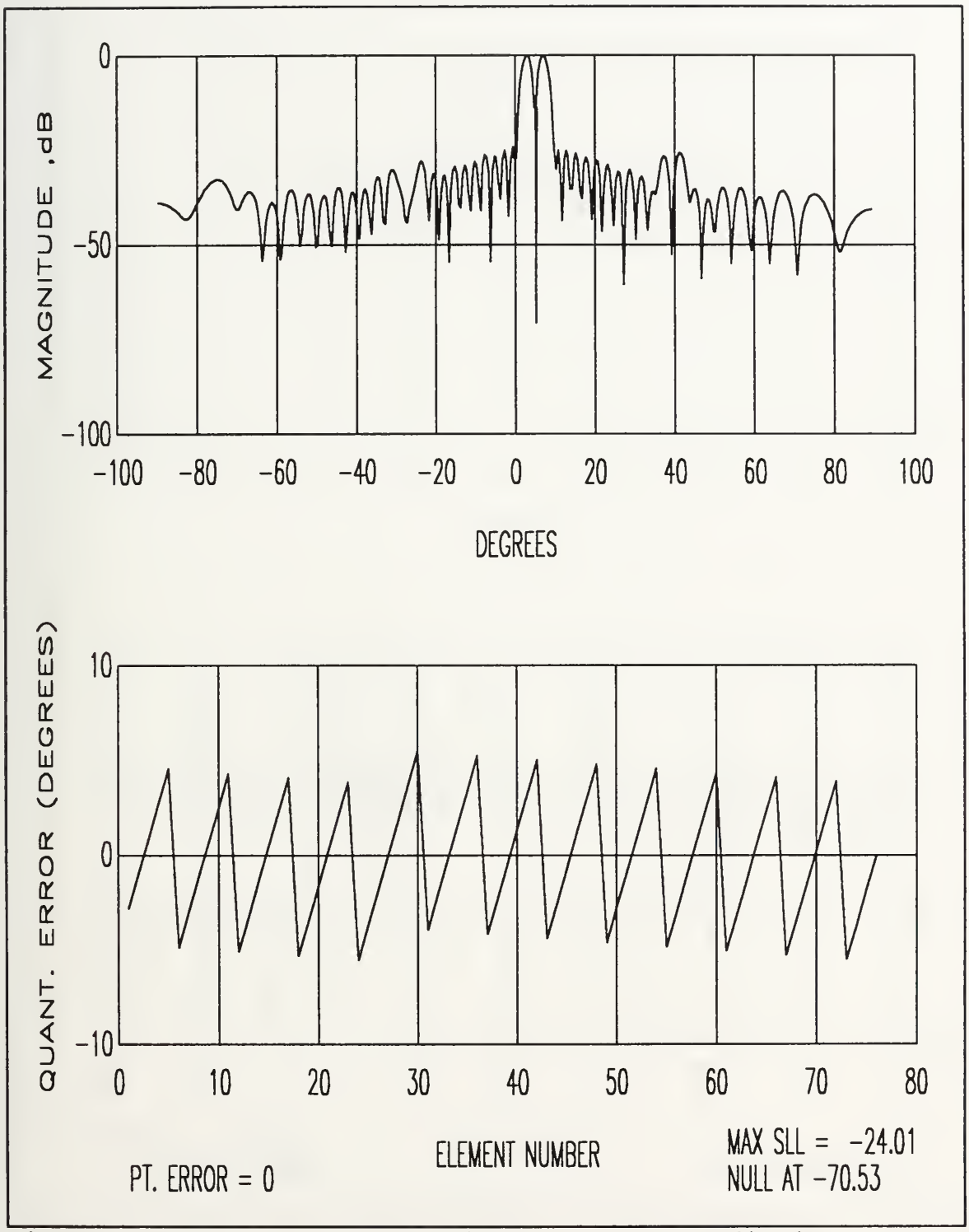

Figure 59. 76 Element Array Difference Beam Radiation Pattern for a 5 Bit Phase Shifter using Regular Roundoff

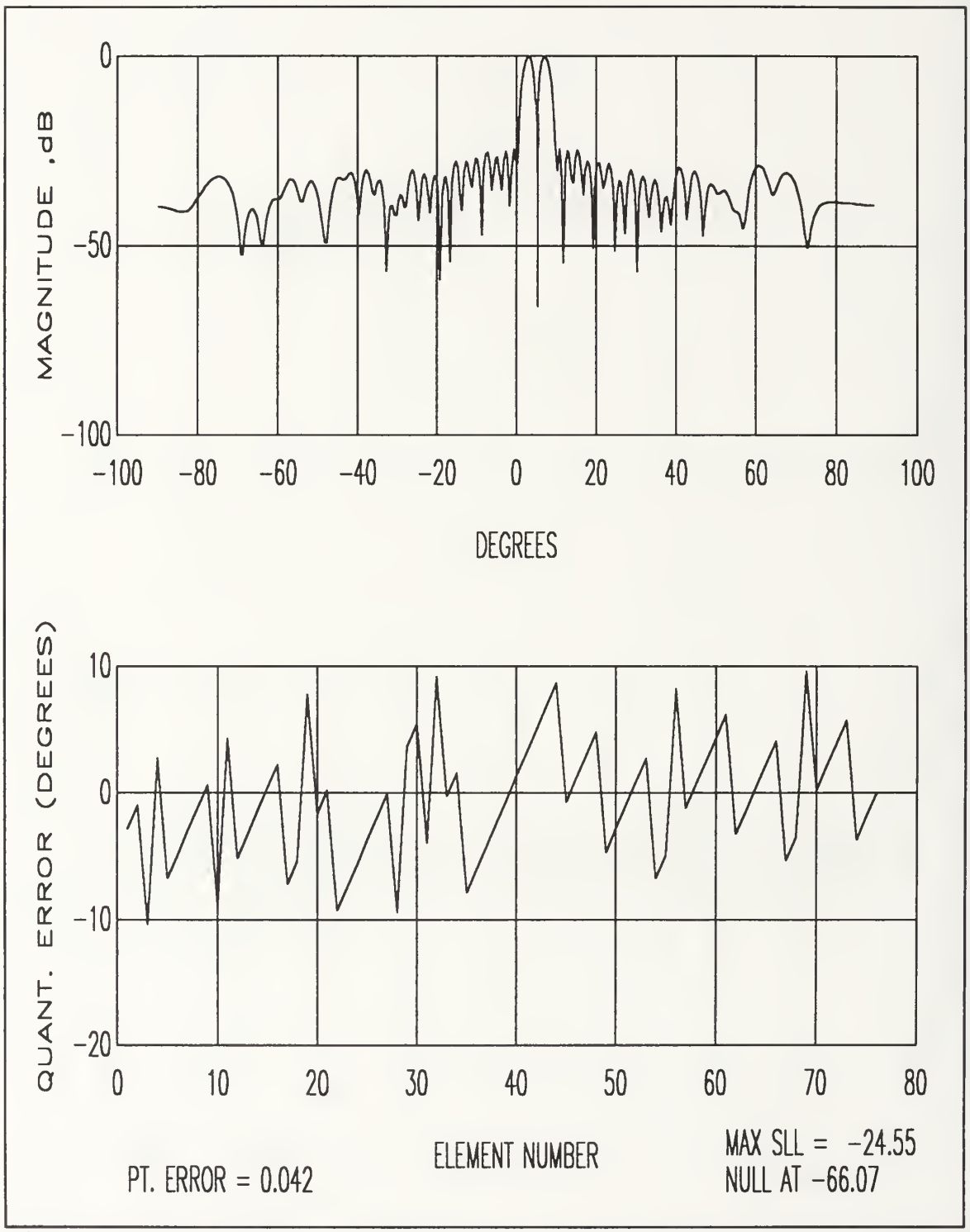

Figure 60. 76 Element Array Difference Beam Radiation Pattern for a 5 Bit Phase Shifter using Weighted Random Roundoff

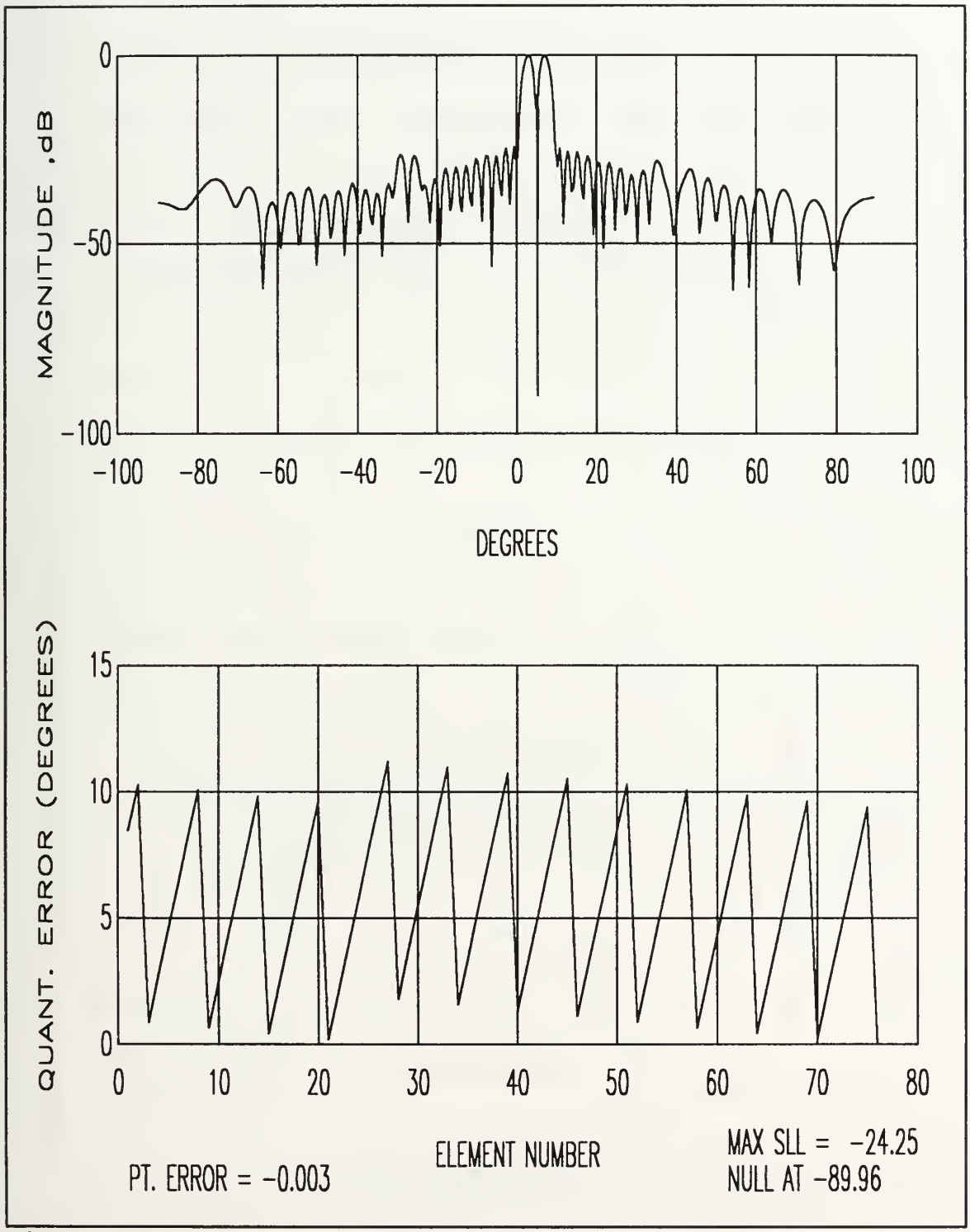

Figure 61. 76 Element Array Difference Beam Radiation Pattern for a 5 Bit Phase Shifter using Running Sum Roundoff

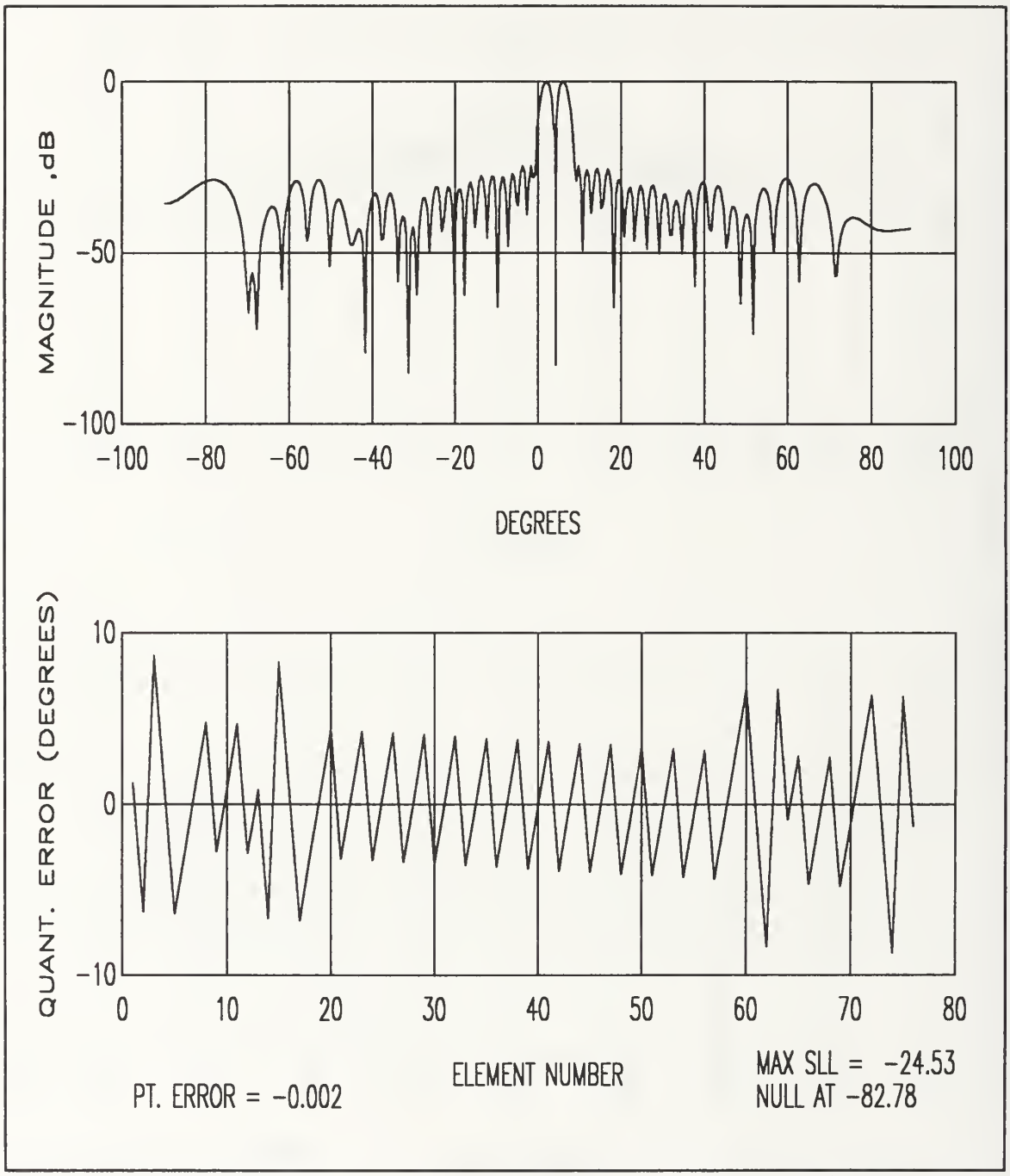

Figure 62. 76 Element Array Difference Beam Radiation Pattern for a 5 Bit Phase Shifter using Symmetric Running Sum Roundoff

APPENDIX B - RADIATION PATTERN CHARACTERISTICS

This section will allow the reader to examine the radiation pattern characteristics for scan angle from 0 to 60 degrees. The plots of the radiation pattern characteristics are grouped by array size, each using the same roundoff algorithm. In each figure the performance of 3,4, and 5 bit phase shifters is compared, in that order from top to bottom. The data is presented in figures 63 through 98.

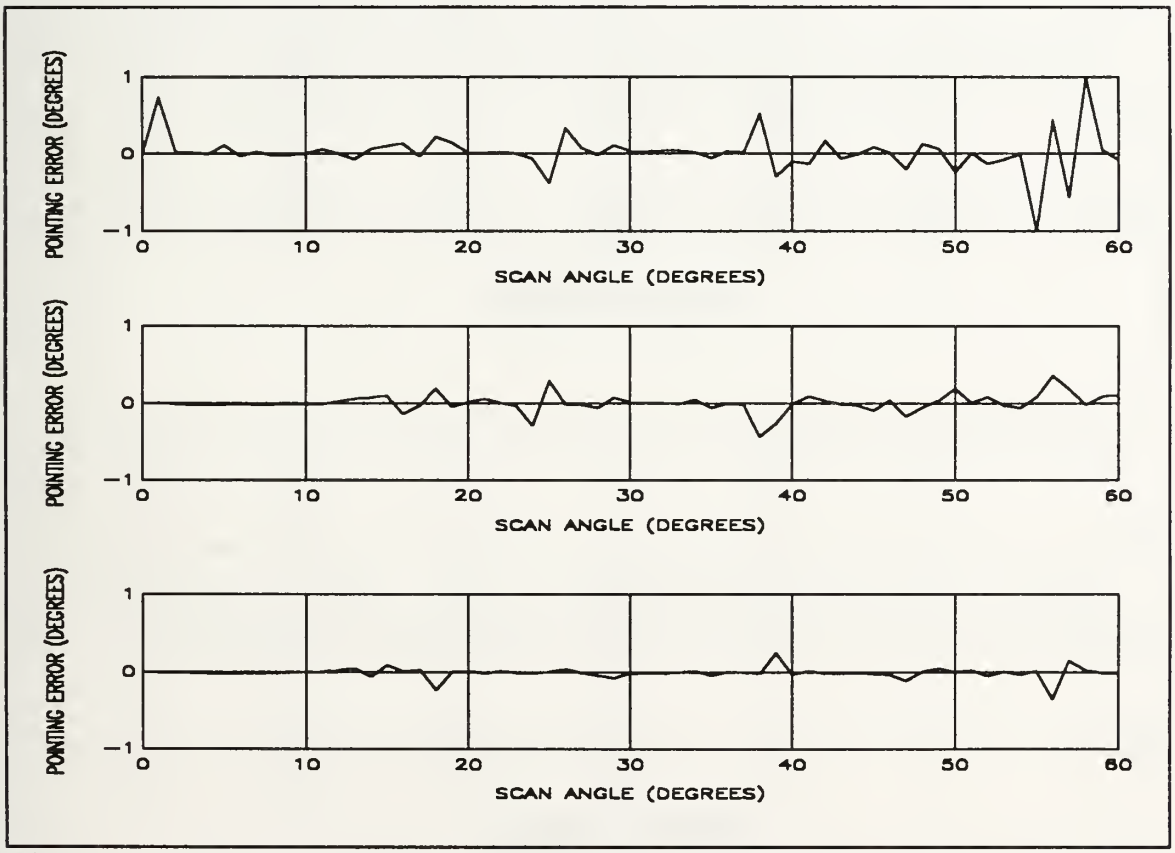

Figure 63. Pointing Error versus Scan Angle for 26 Element Arrays with 3, 4, and 5 Bit Phase Shifters using Regular Roundoff

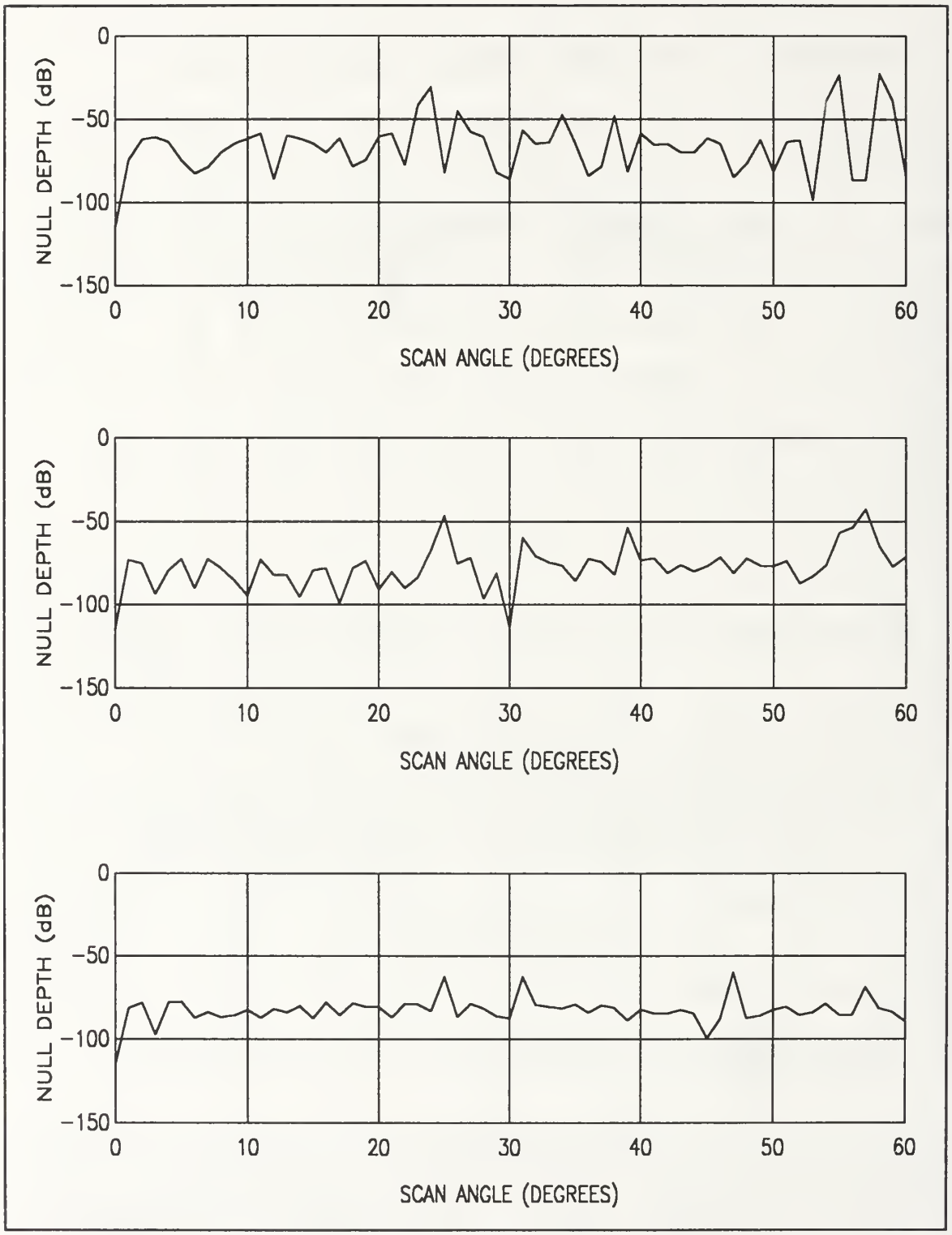

Figure 64. Null Depth versus Scan Angle for 26 Element Arrays with 3, 4, and 5 Bit Phase Shifters using Regular Roundoff

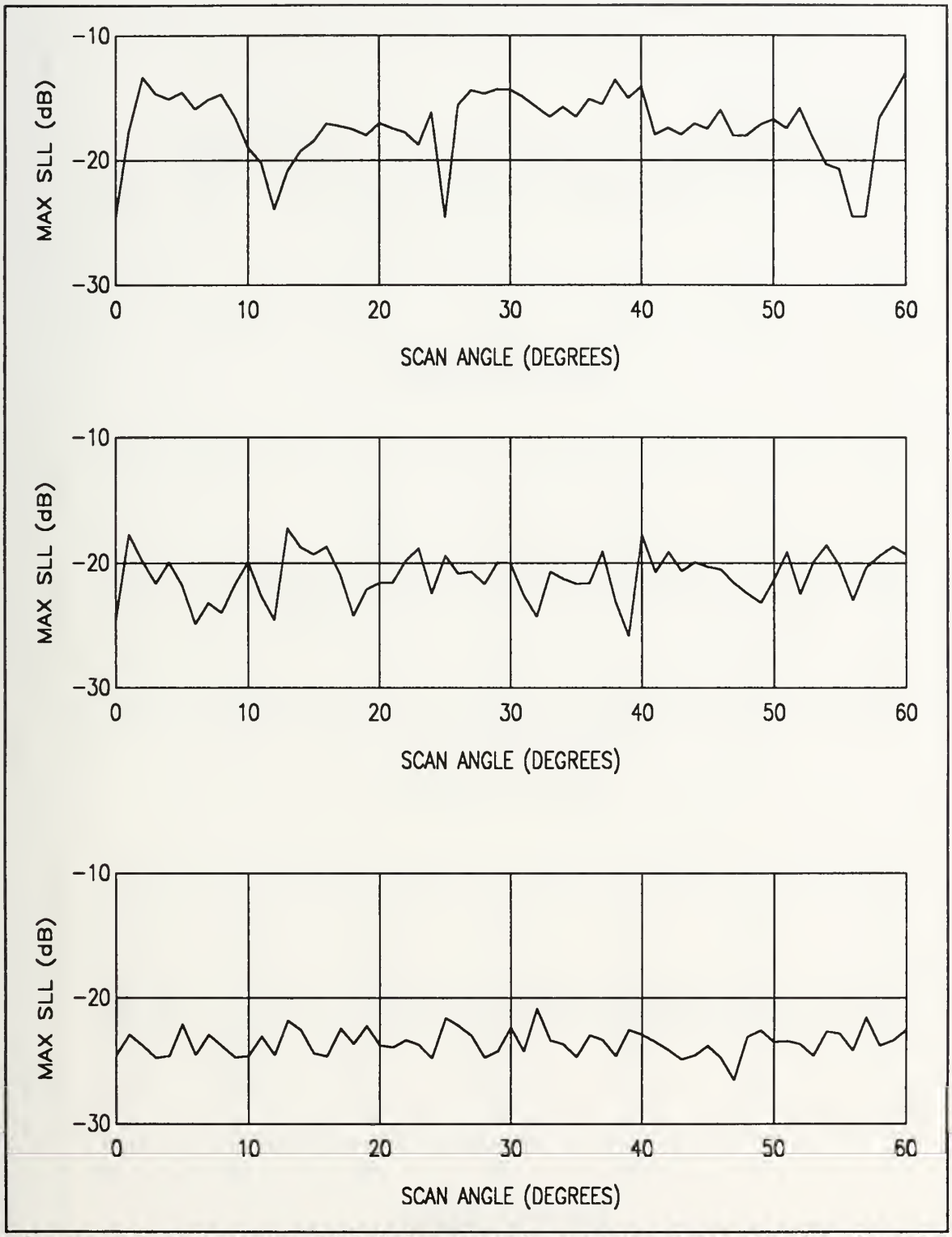

Figure 65. Maximum Sidelobe Level versus Scan Angle for 26 Element Arrays with 3, 4, and 5 Bit Phase Shifters using Regular Roundoff

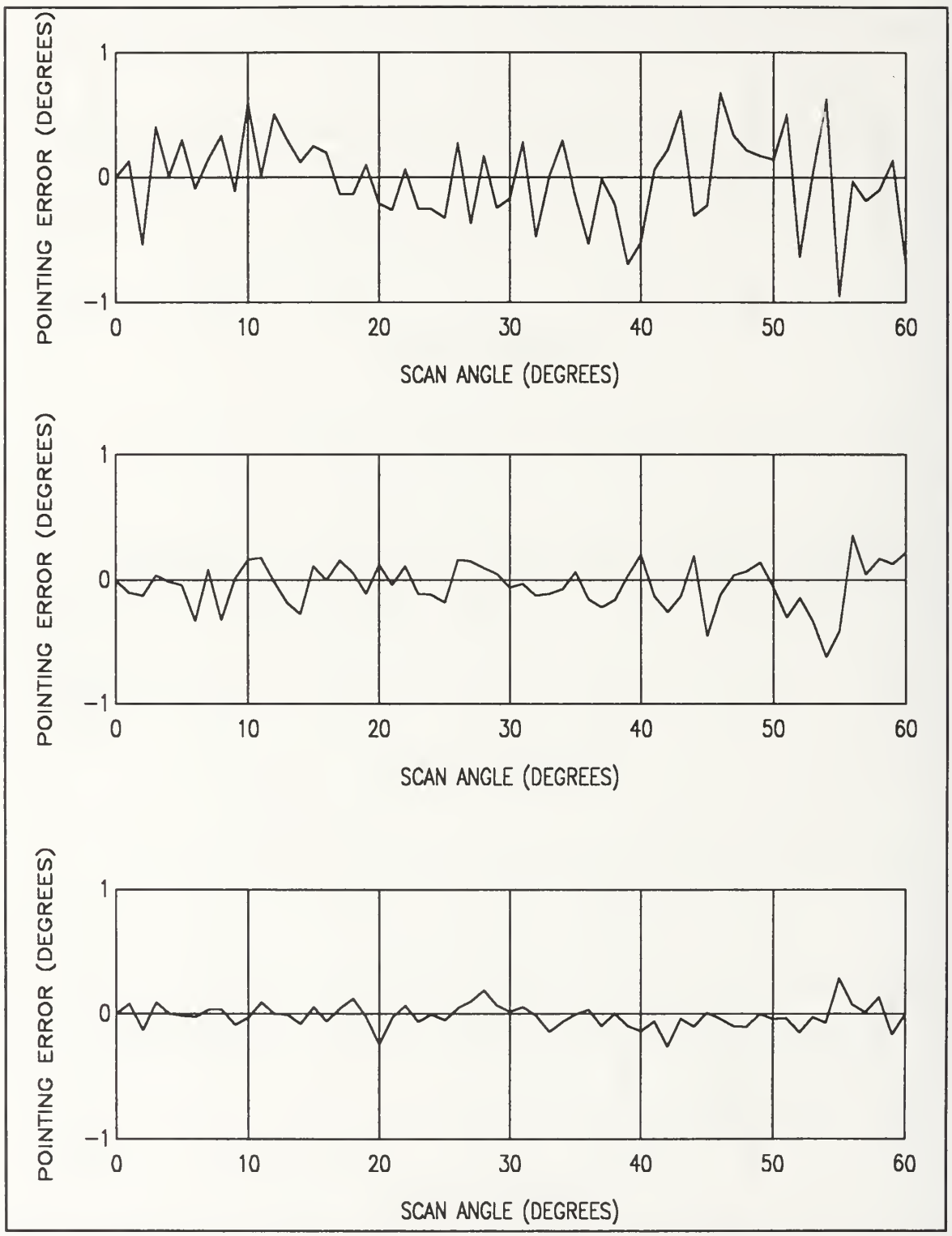

Figure 66. Point Error versus Scan Angle for 26 Element Arrays with 3, 4, and 5 Bit Phase Shifter using Weighted Random Roundoff

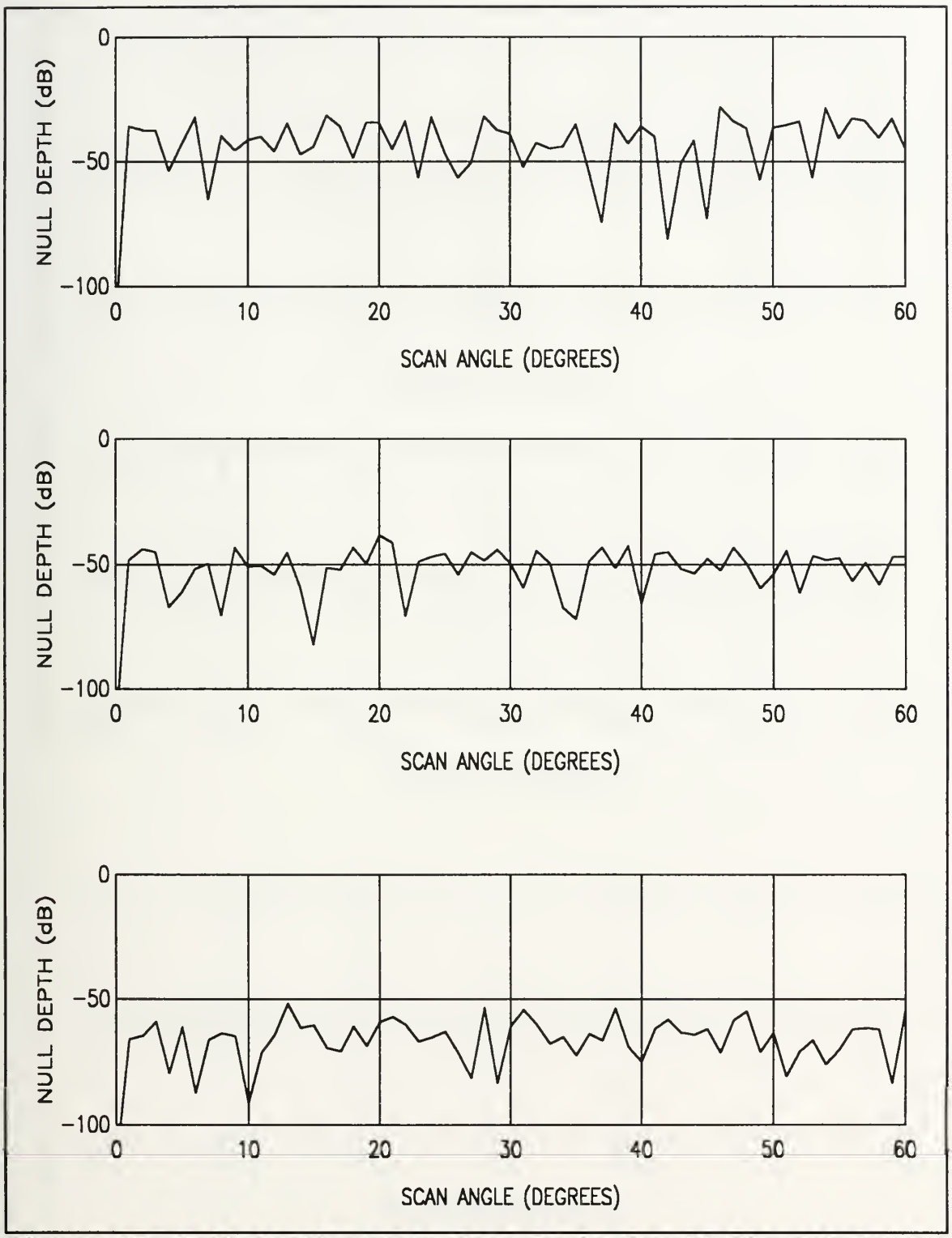

Figure 67. Null Depth versus Scan Angle for 26 Element Arrays with 3, 4, and 5 Bit Phase Shifters using Weighted Random Roundoff

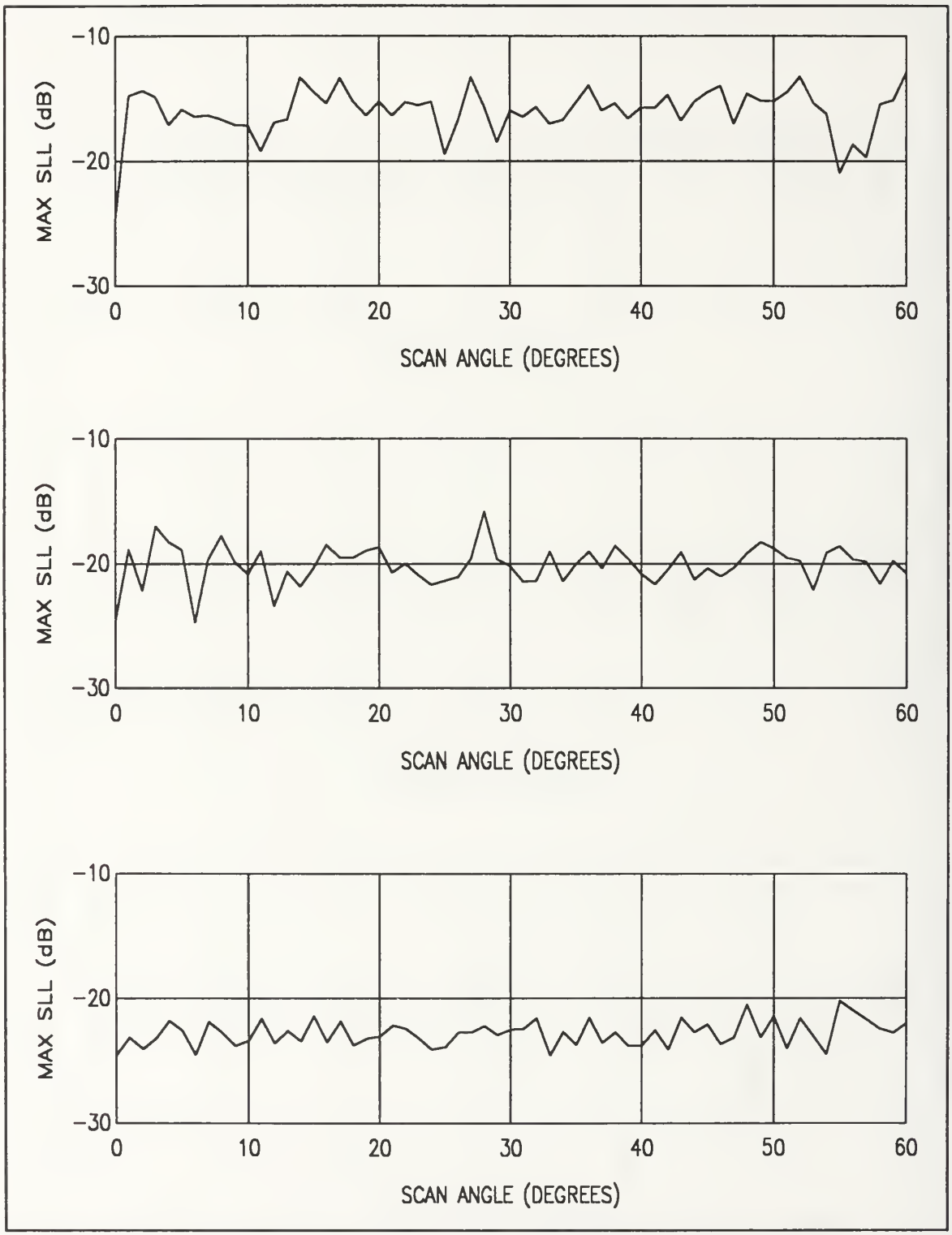

Figure 68. Maximum Sidelobe Level versus Scan Angle for 26 Element Arrays with 3, 4, and 5 Bit Phase Shifters using Weighted Random Roundoff

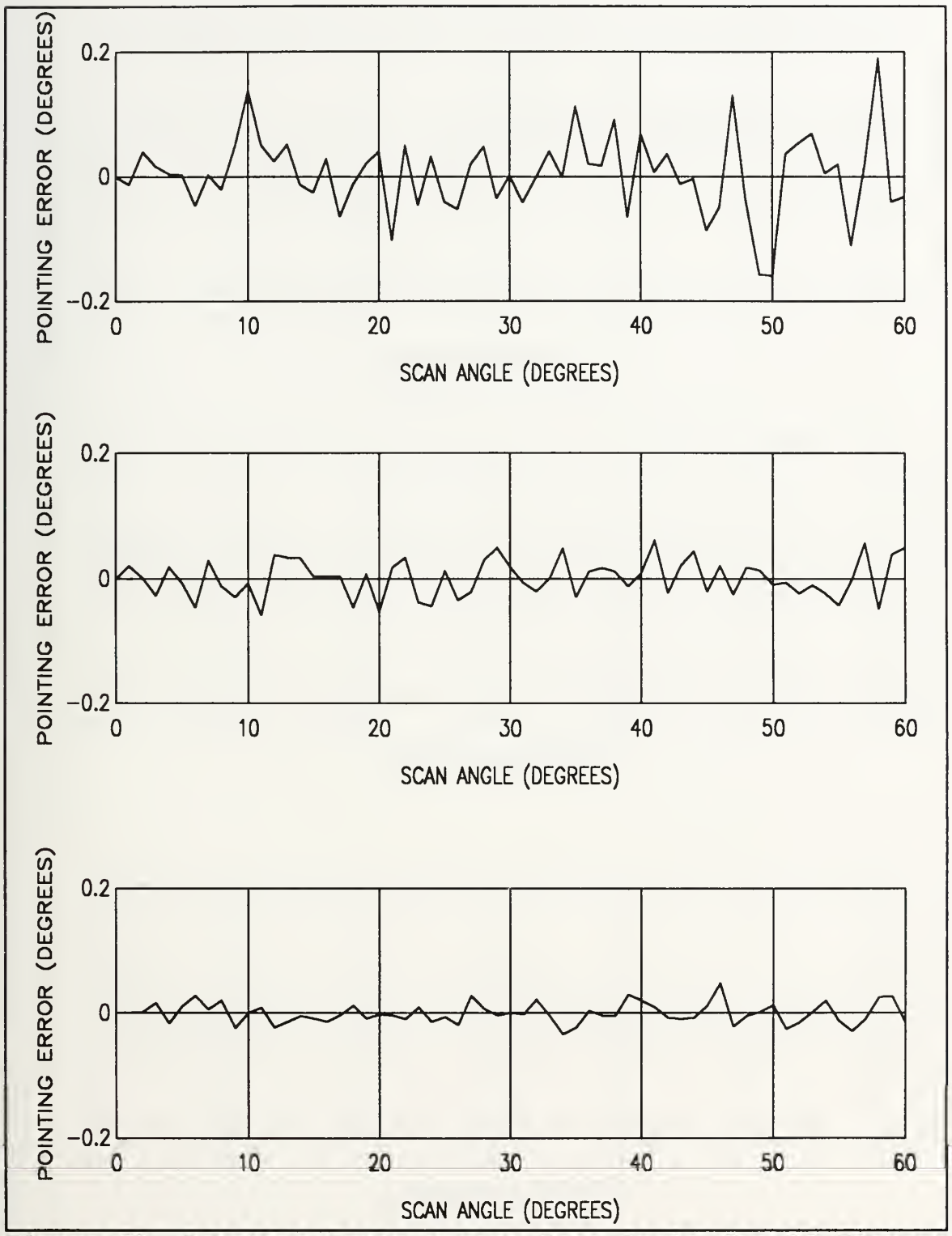

Figure 69. Pointing Error versus Scan Angle for 26 Element Arrays with 3, 4, and 5 Bit Phase Shifters using Running Sum Roundoff

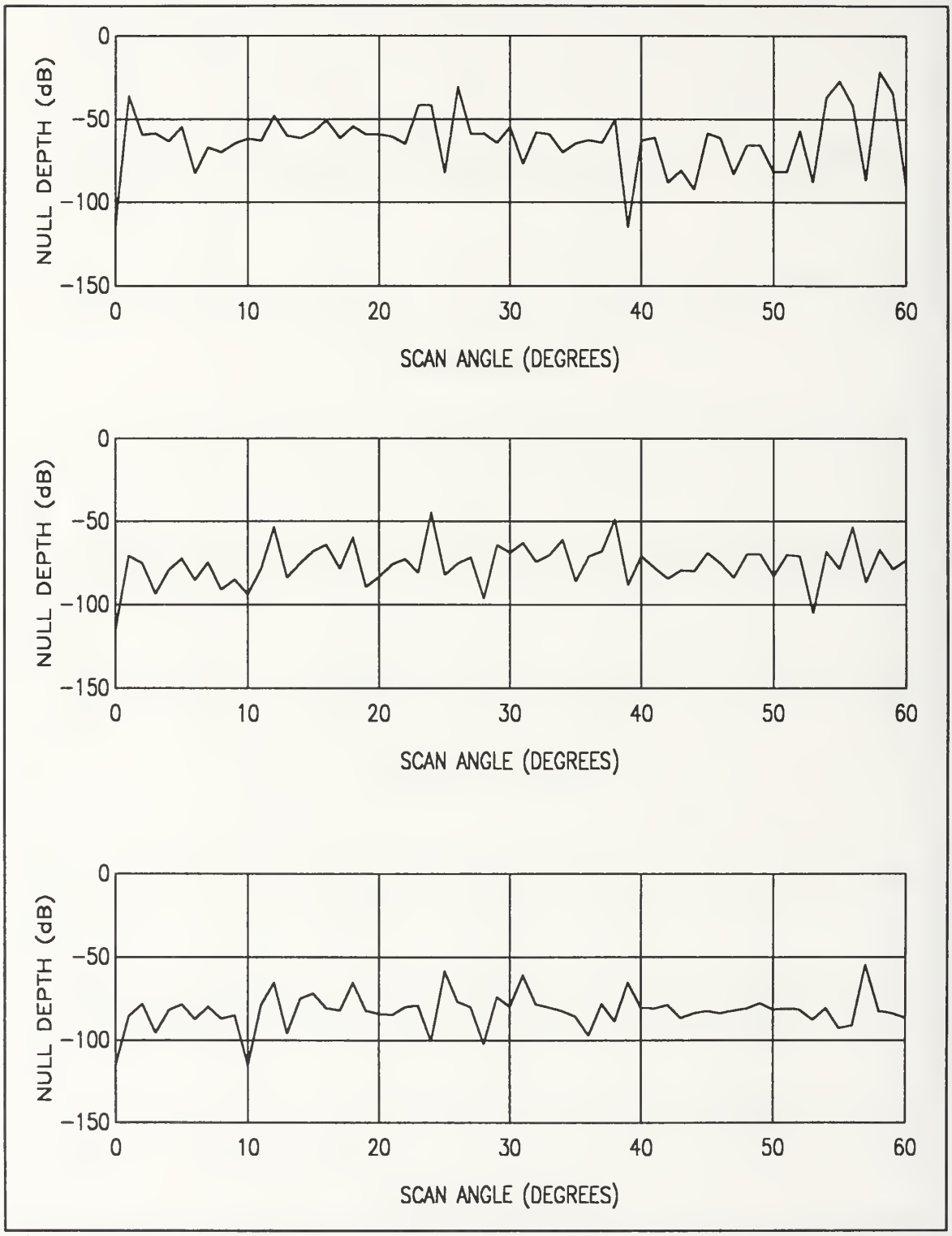

Figure 70. Null Depth versus Scan Angle for 26 Element Arrays with 3, 4, and 5 Bit Phase Shifters using Running Sum Roundoff

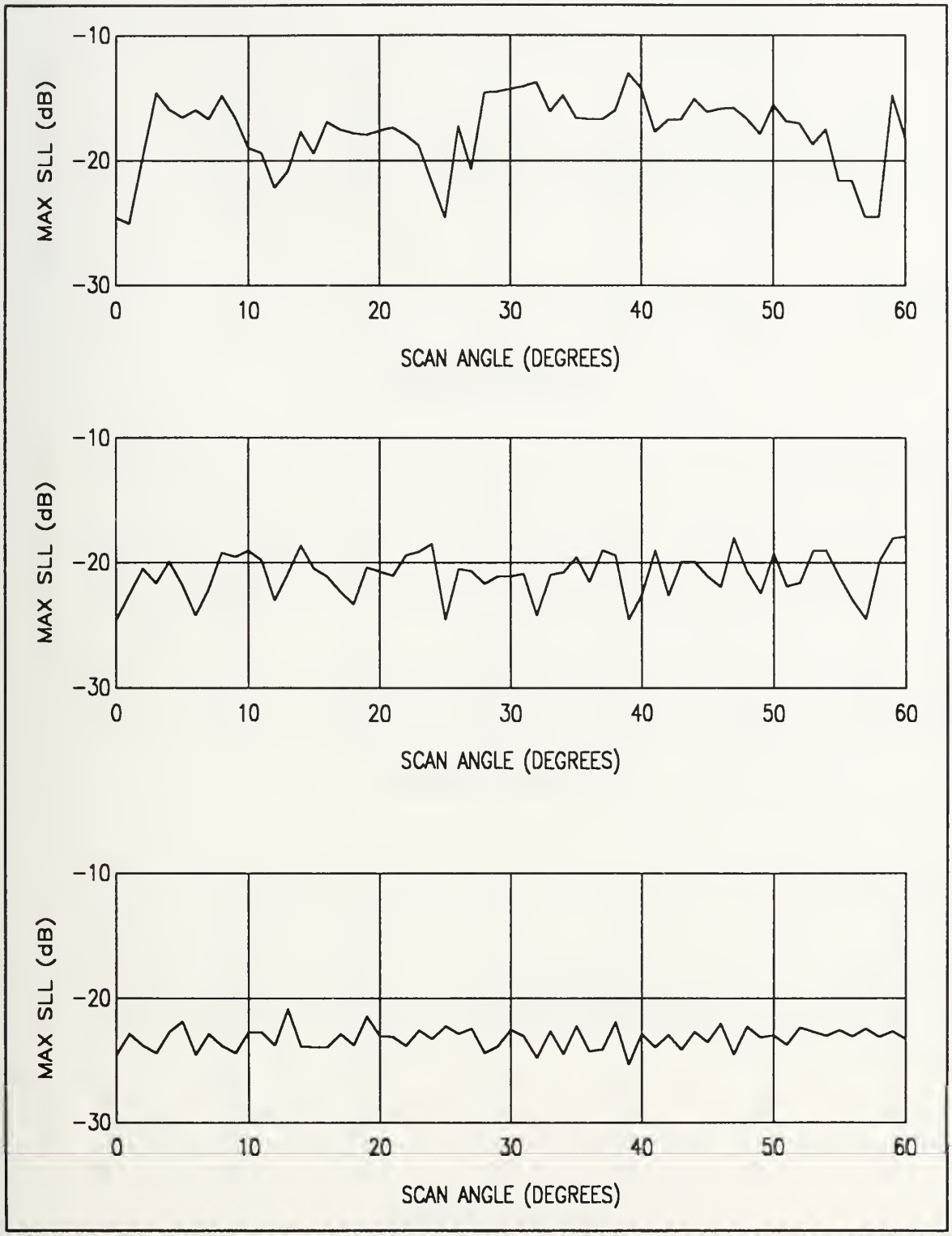

Figure 71. Maximum Sidelobe Level versus Scan Angle for 26 Element Arrays with 3, 4, and 5 Bit Phase Shifters using Running Sum Roundoff

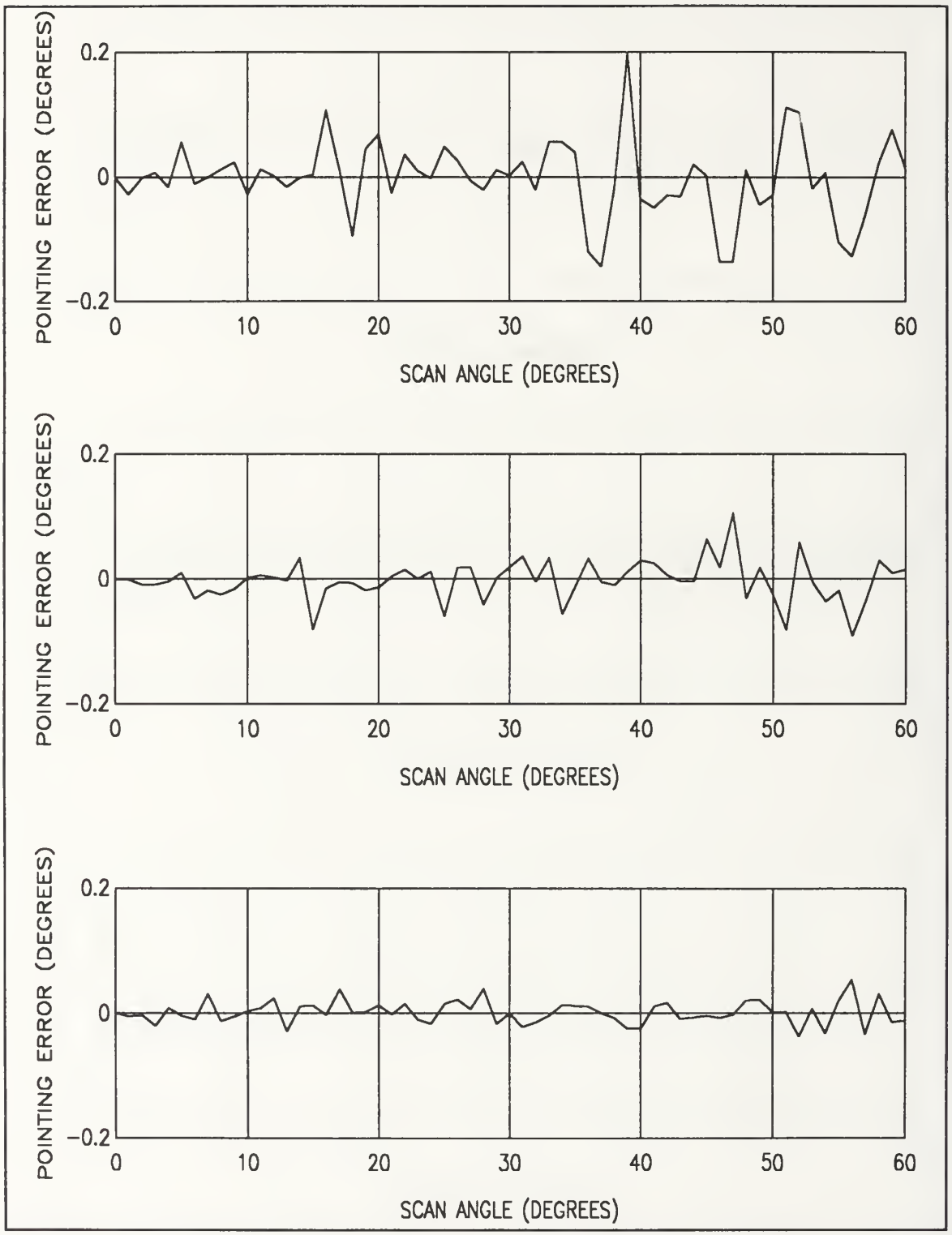

Figure 72. Pointing Error versus Scan Angle for 26 Element Arrays with 3, 4, and 5 Bit Phase Shifters using Symmetric Running Sum Roundoff

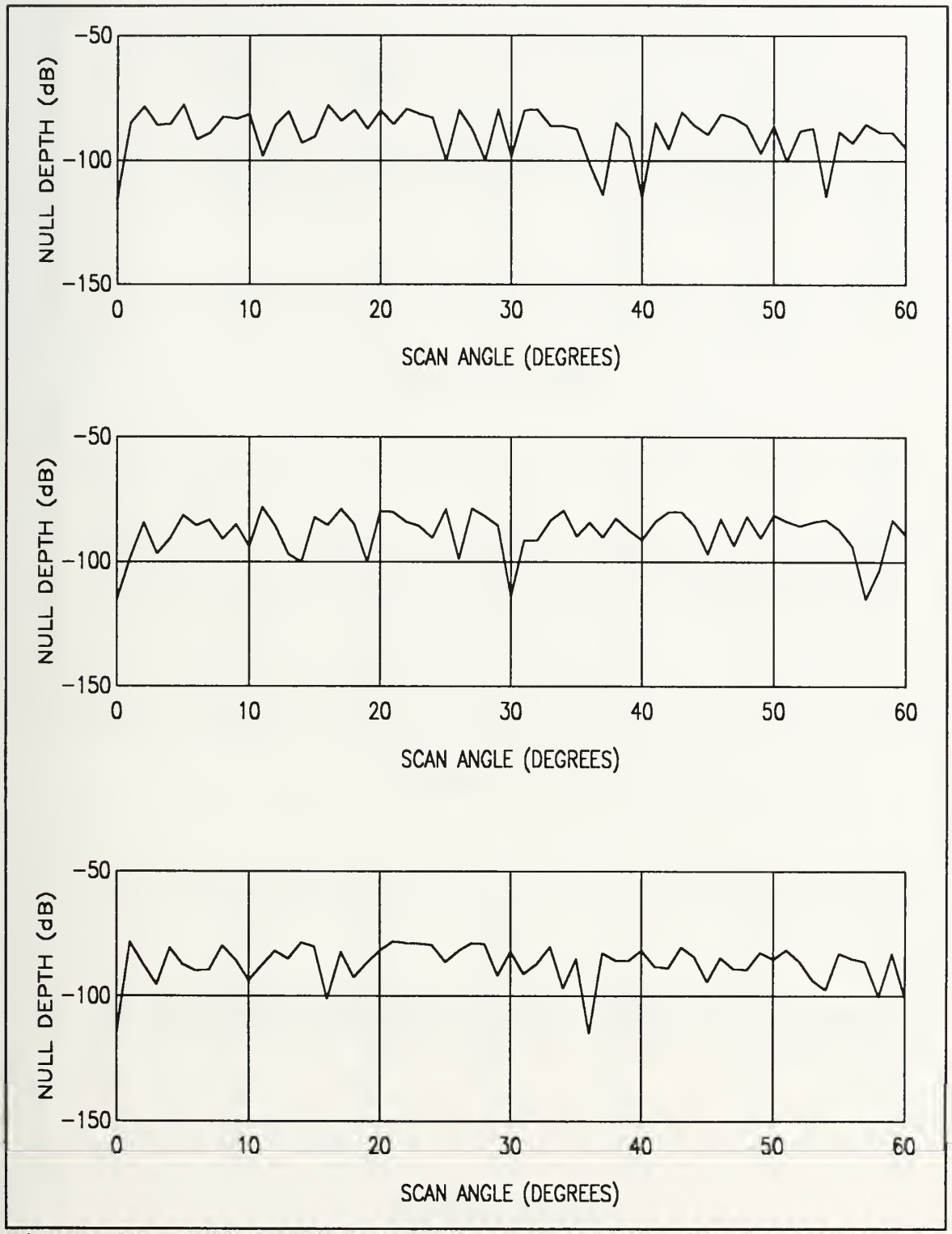

Figure 73. Null Depth versus Scan Angle for 26 Element Arrays with 3, 4, and 5 Bit Phase Shifters using Symmetric Running Sum Roundoff

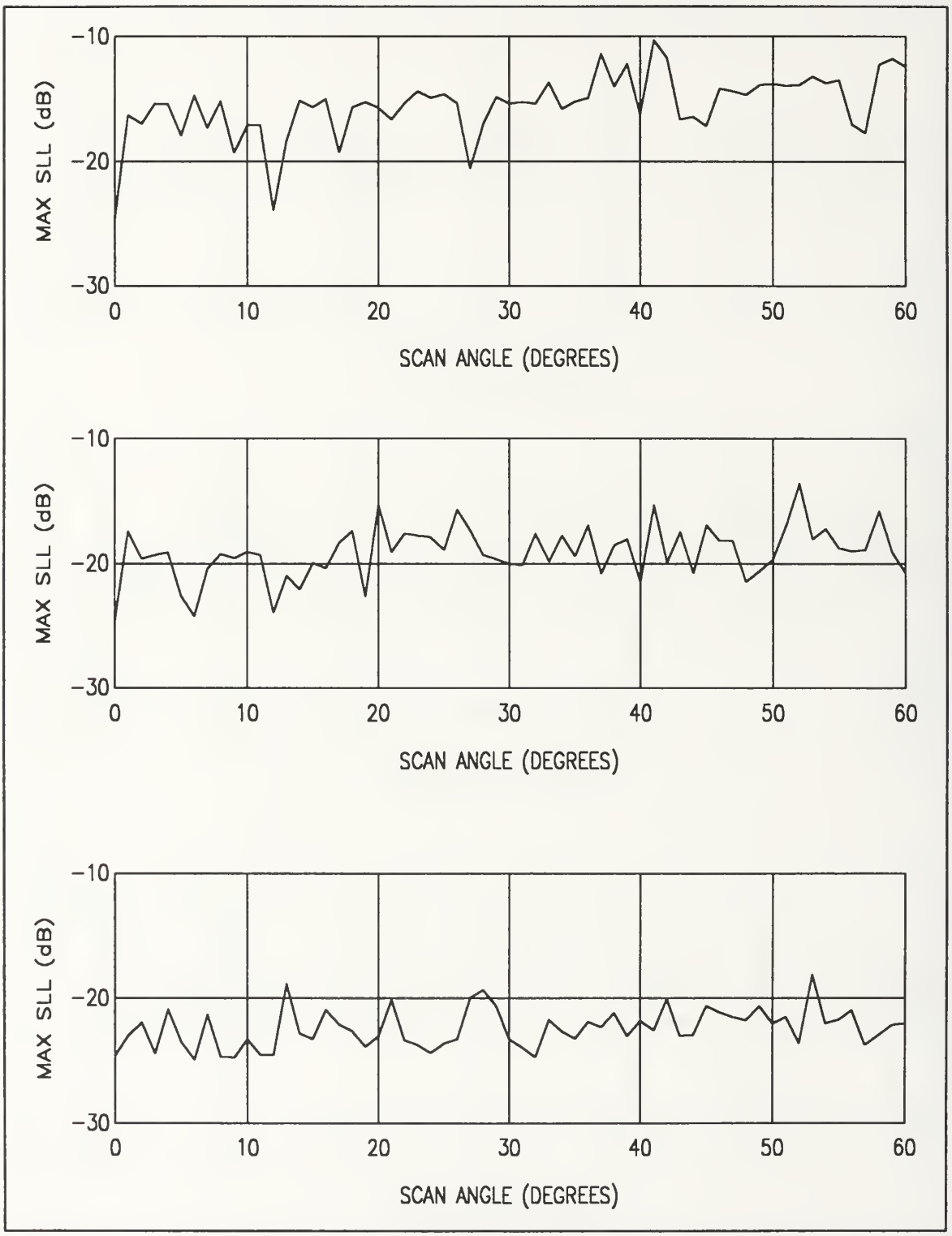

Figure 74. Maximum Sidelobe Level versus Scan Angle for 26 Element Arrays with 3, 4, and 5 Bit Phase Shifters using Symmetric Running Sum Roundoff

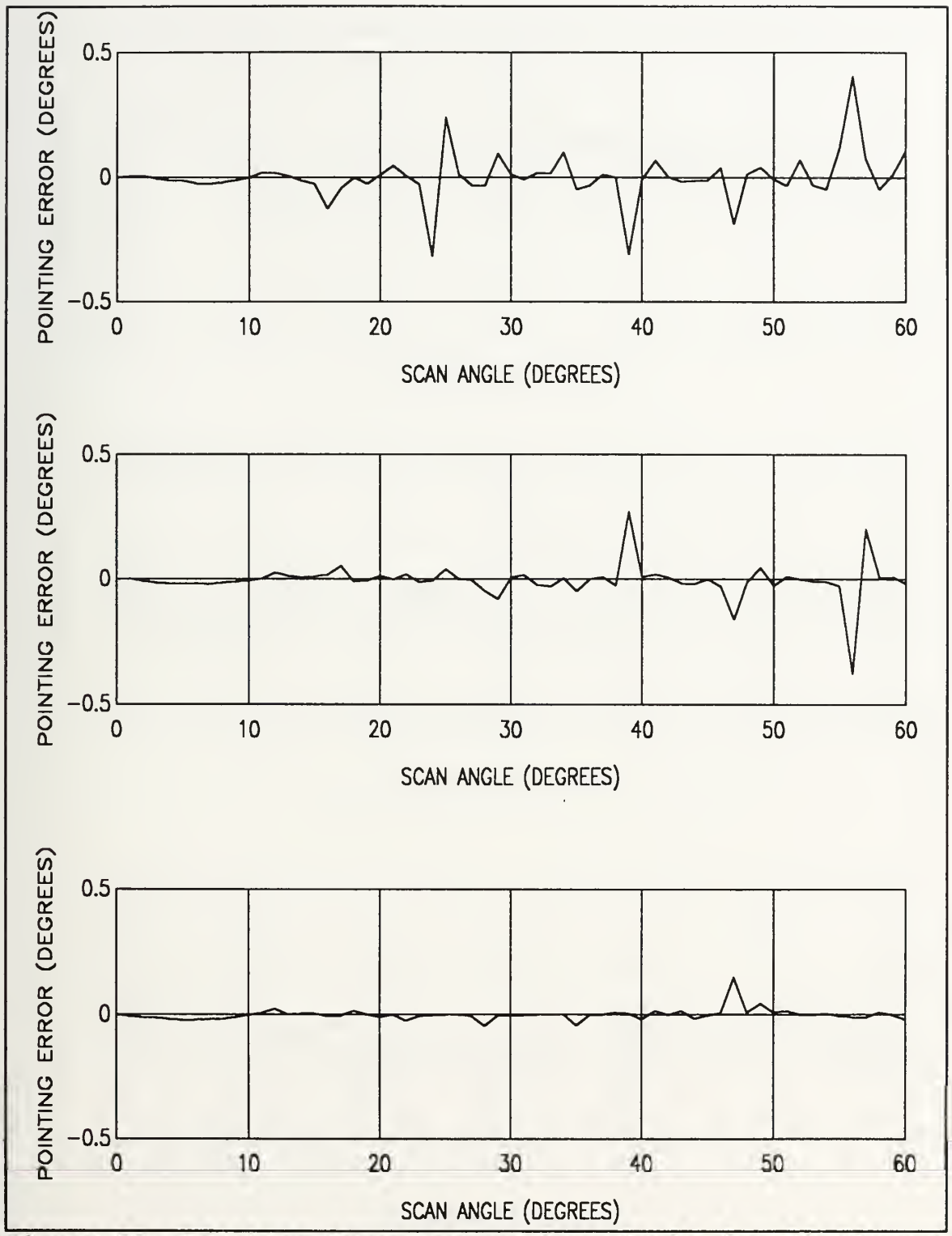

Figure 75. Pointing Error versus Scan Angle for 50 Element Arrays with 3, 4 and 5 Bit Phase Shifters using Regular Roundoff

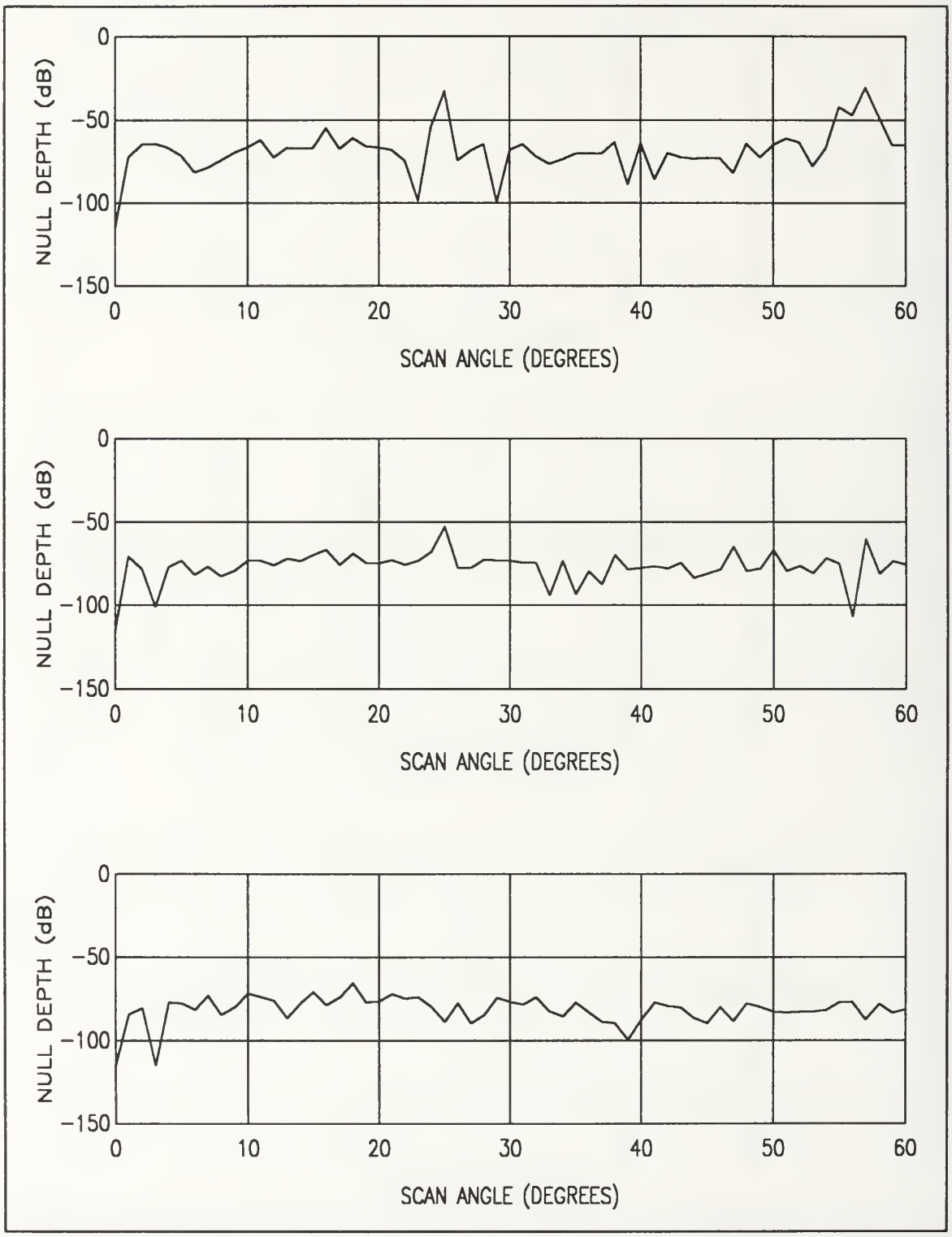

Figure 76. Null Depth versus Scan Angle for 50 Element Arrays with 3, 4, and 5 Bit Phase Shifters using Regular Roundoff

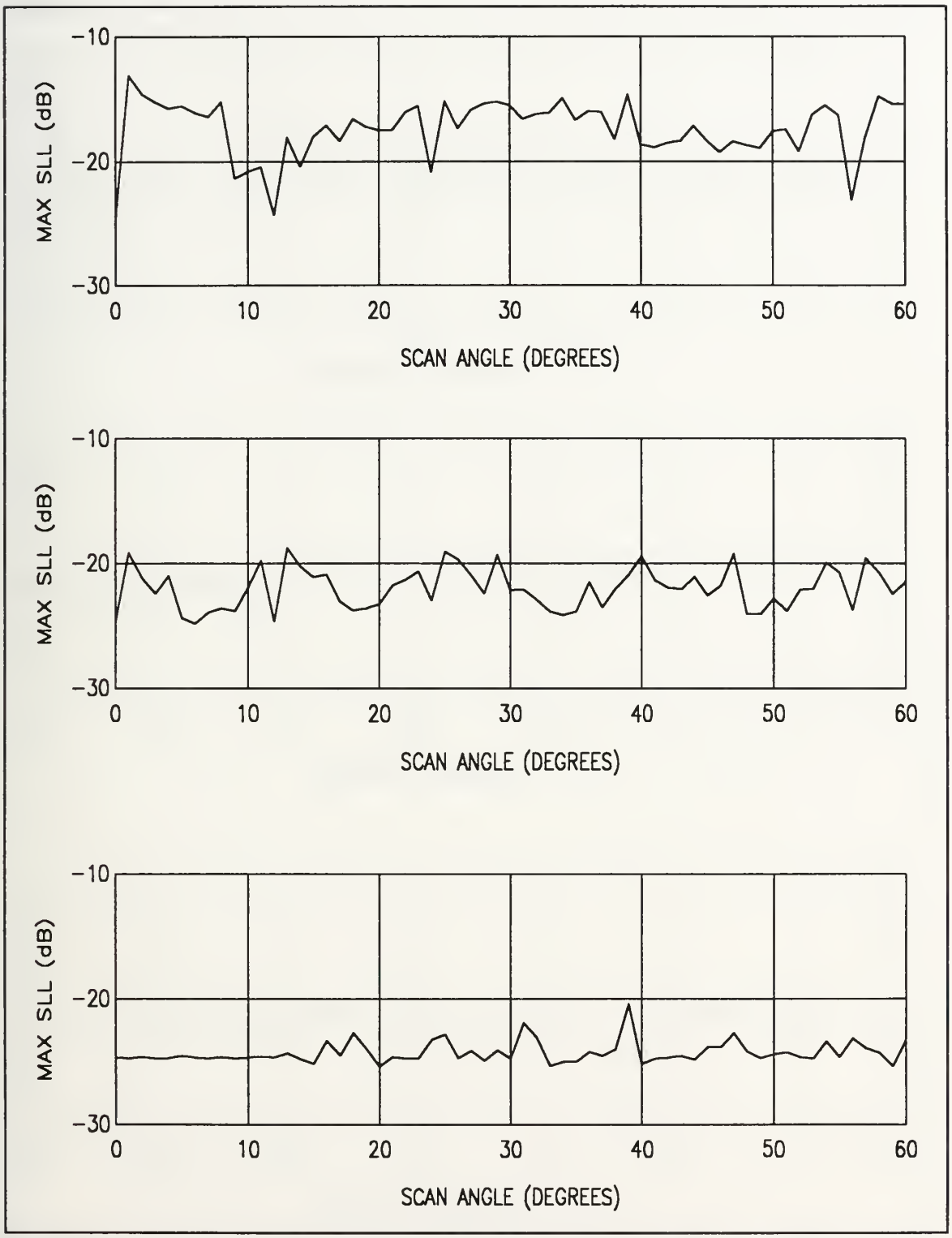

Figure 77. Maximum Sidelobe Level versus Scan Angle for 50 Element Arrays with 3, 4, and 5 Bit Phase Shifters using Regular Roundoff

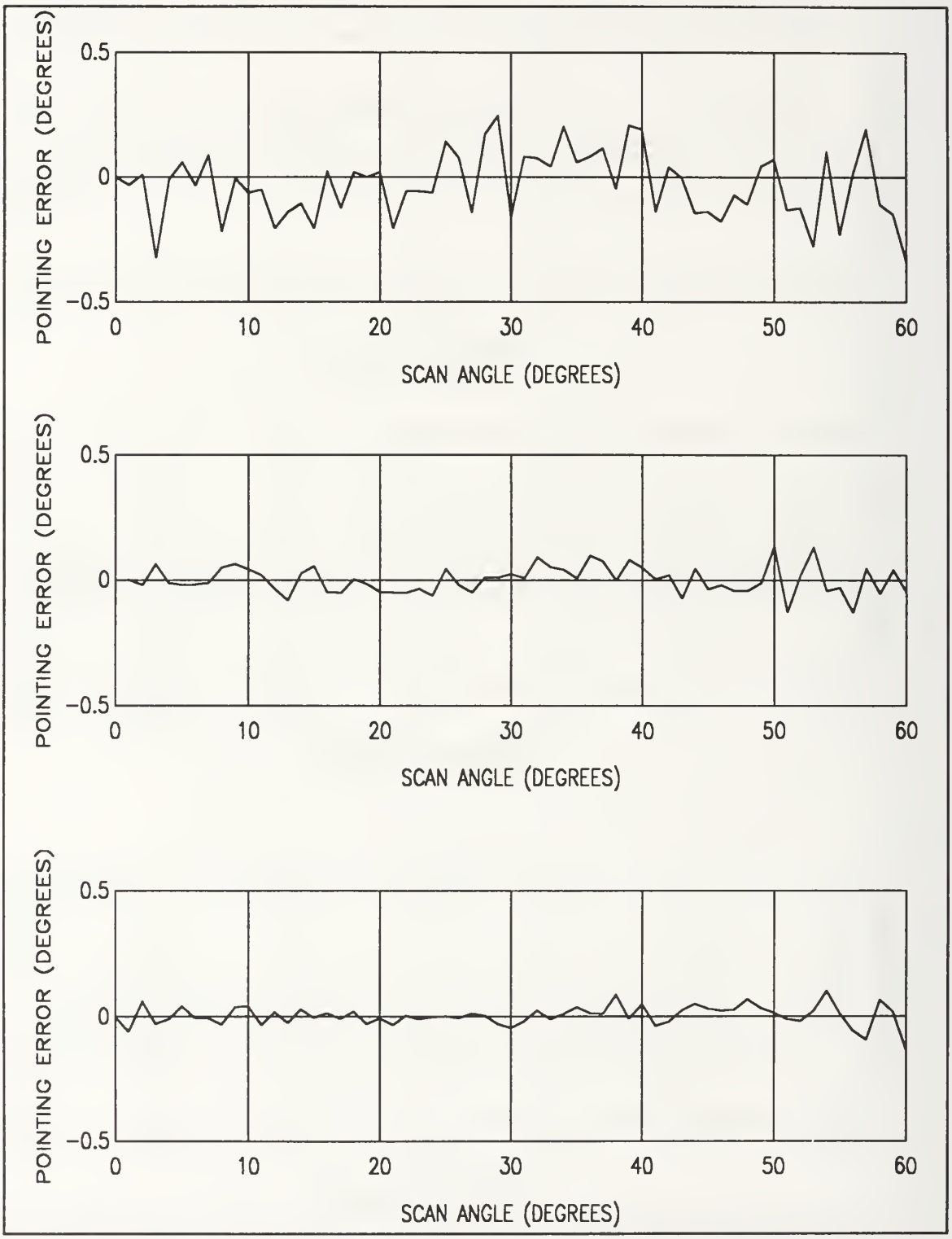

Figure 78. Pointing Error versus Scan Angle for 50 Element Arrays with 3, 4, and 5 Bit Phase Shifters using Weighted Random Roundoff

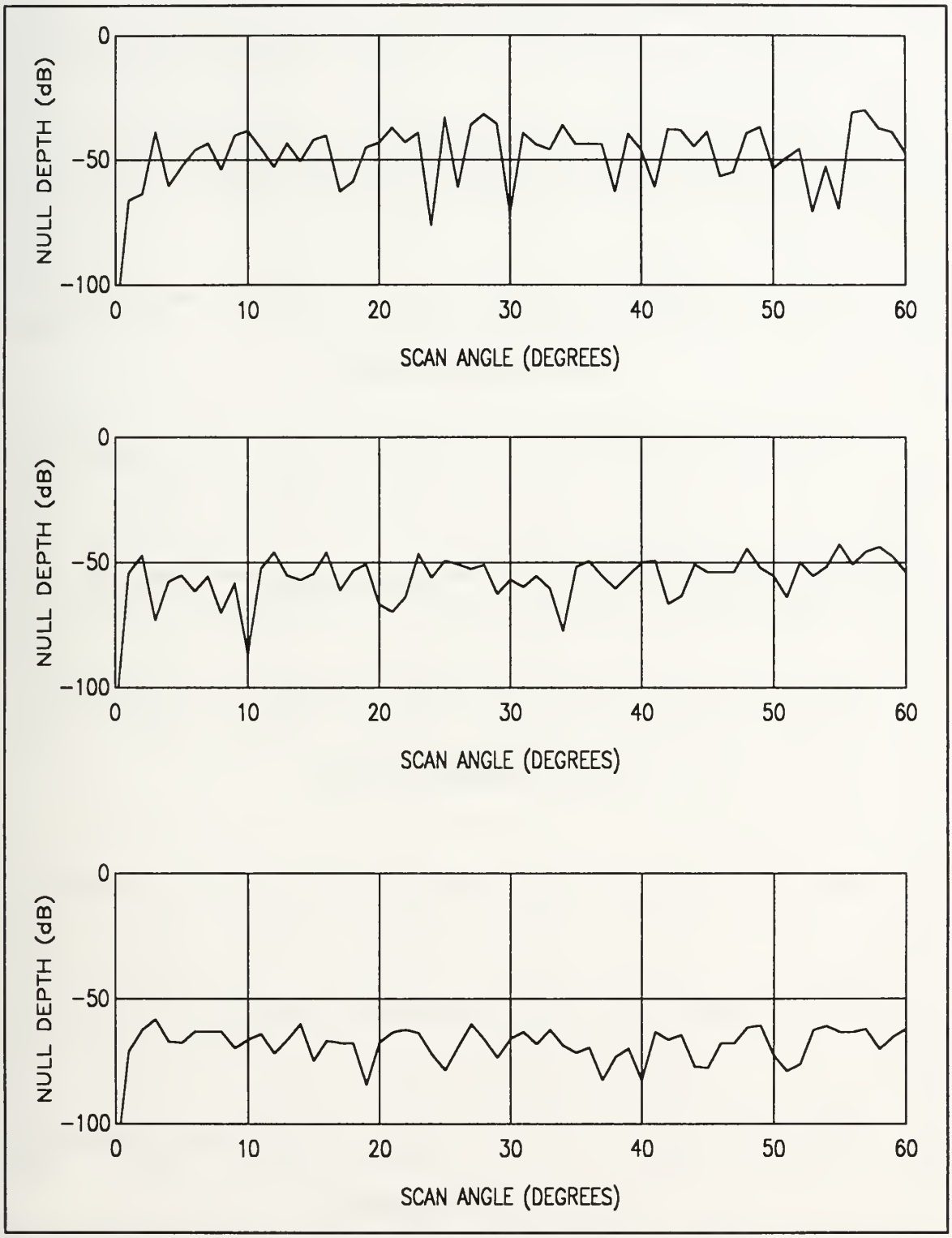

Figure 79. Null Depth versus Scan Angle for 50 Element Arrays with 3, 4, and 5 Bit Phase Shifters using Weighted Random Roundoff

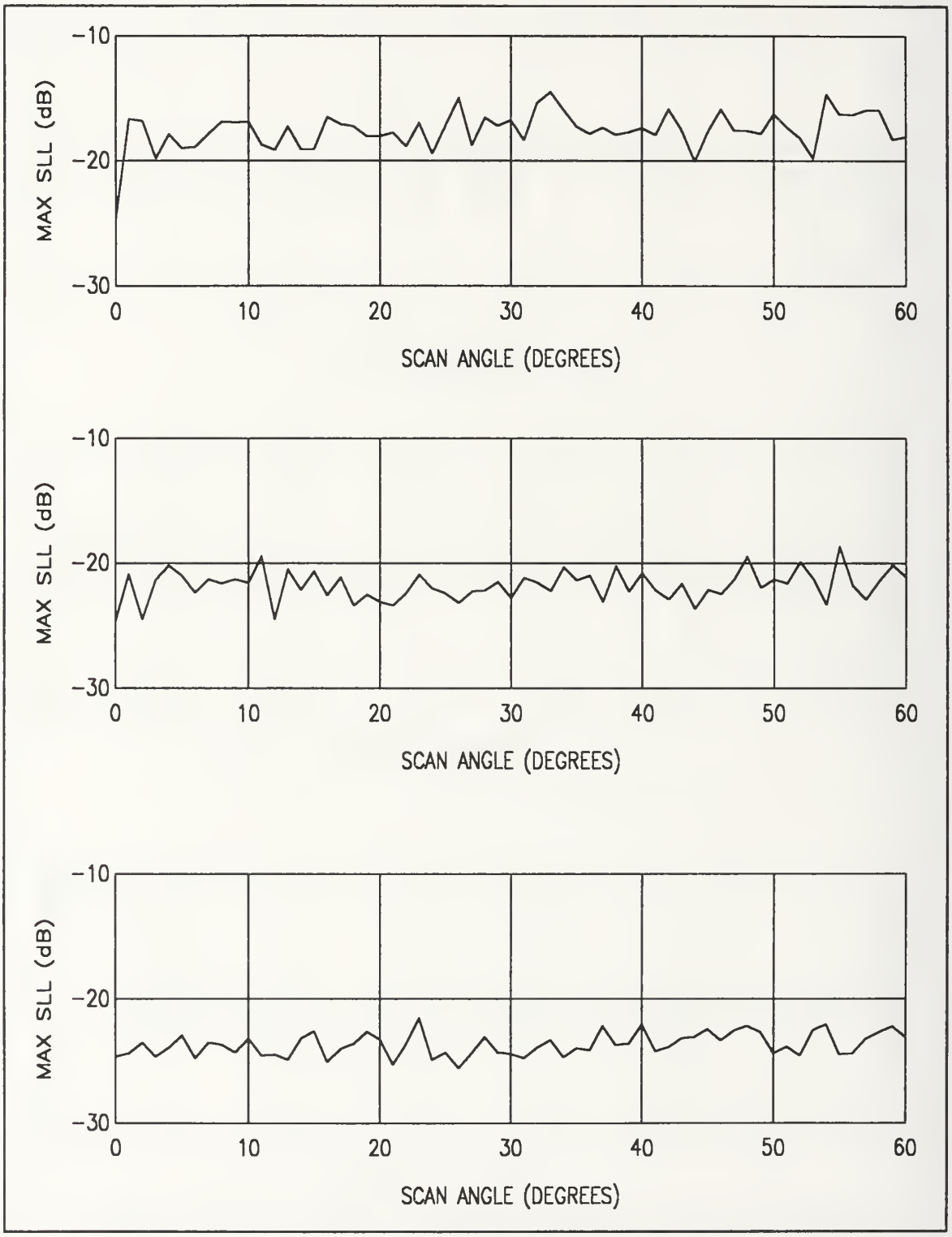

Figure 80. Maximum Sidelobe Level versus Scan Angle for 50 Element Arrays with 3, 4, and 5 Bit Phase Shifters using Weighted Random Roundoff

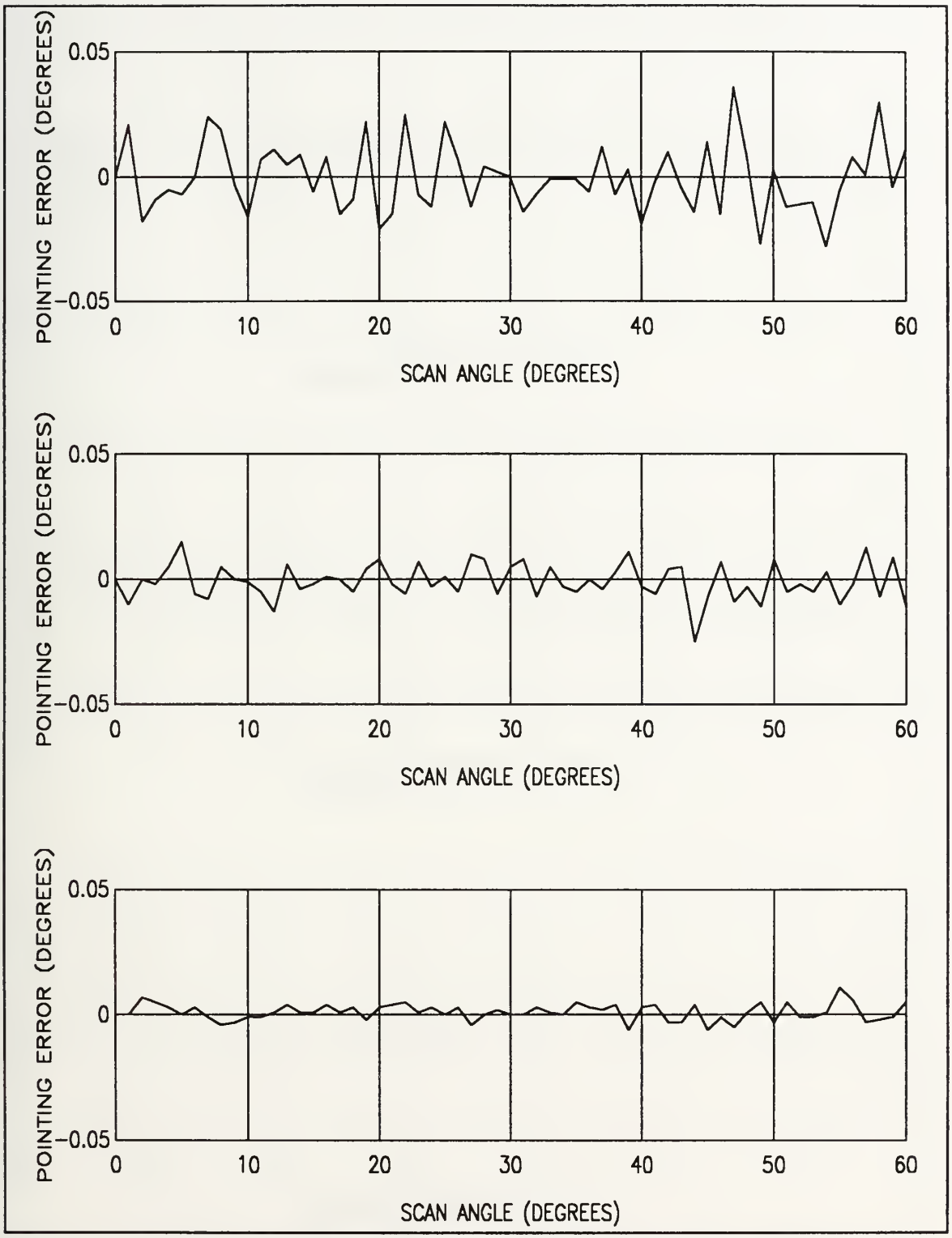

Figure 81. Pointing Error versus Scan Angle for 50 Element Arrays with 3, 4, and 5 Bit Phase Shifters using Running Sum Roundoff

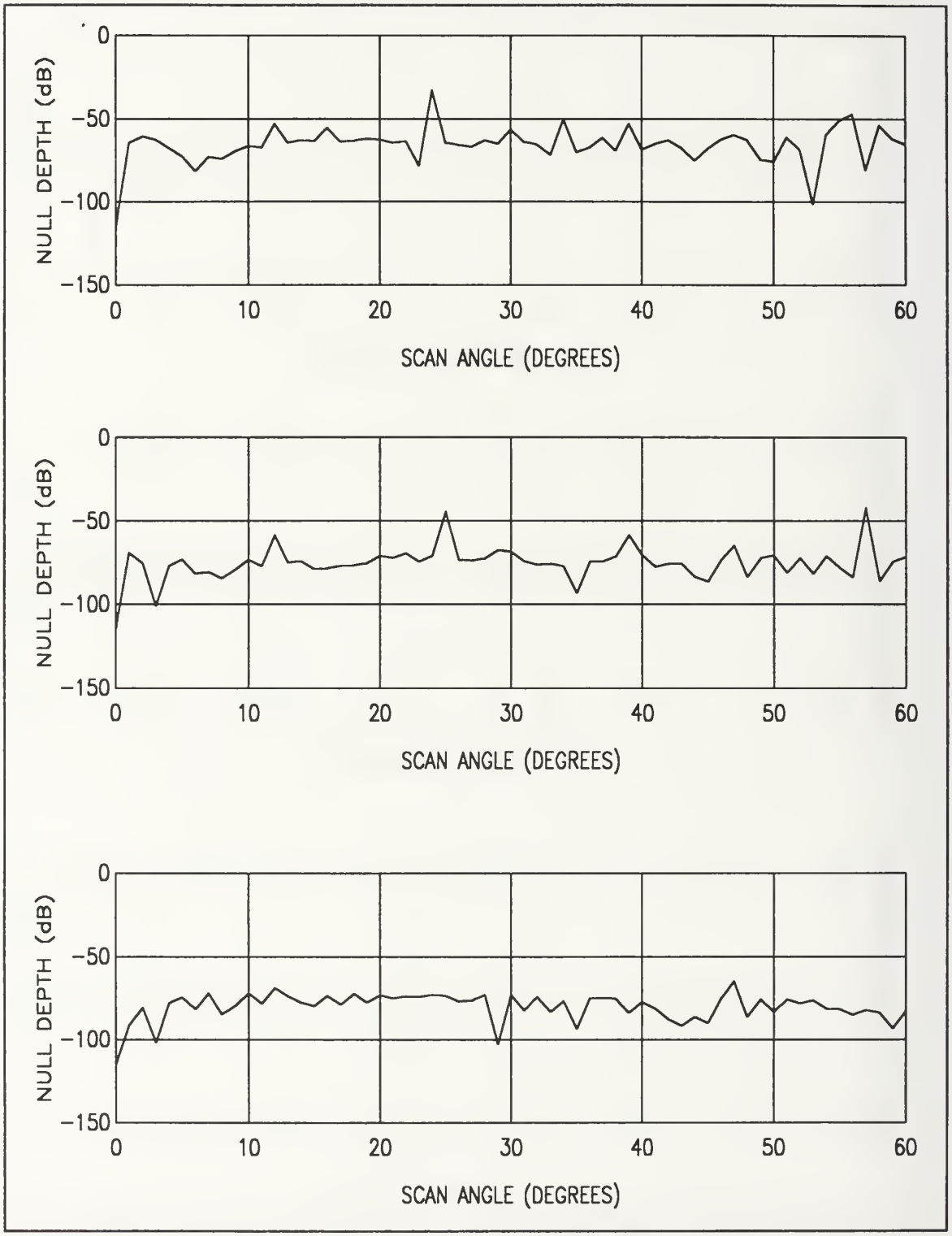

Figure 82. Null Depth versus Scan Angle for 50 Element Arrays with 3, 4, and 5 Bit Phase Shifters using Running Sum Roundoff

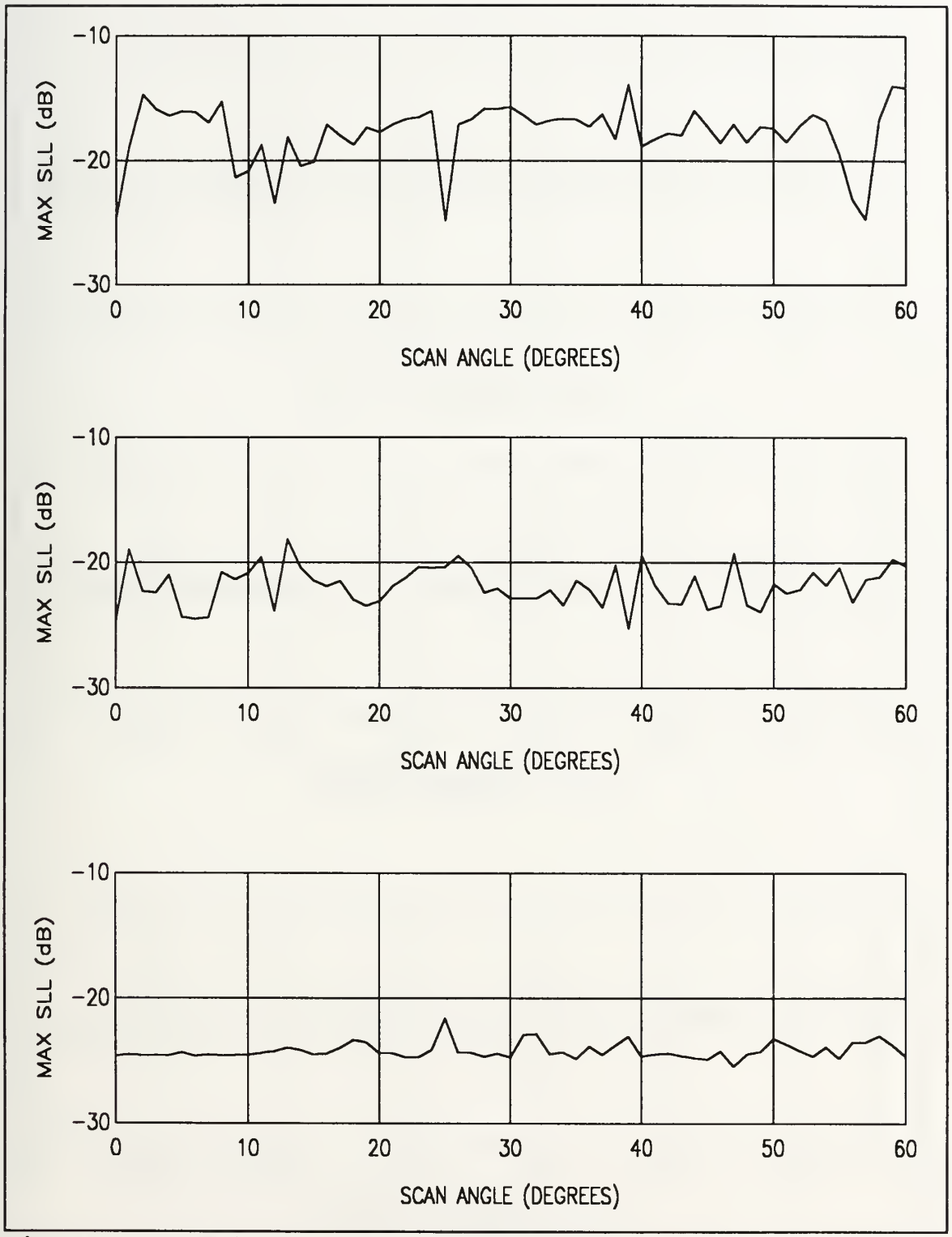

Figure 83. Maximum Sidelobe Level versus Scan Angle for 50 Element Arrays with 3, 4, and 5 Bit Phase Shifters using Running Sum Roundoff

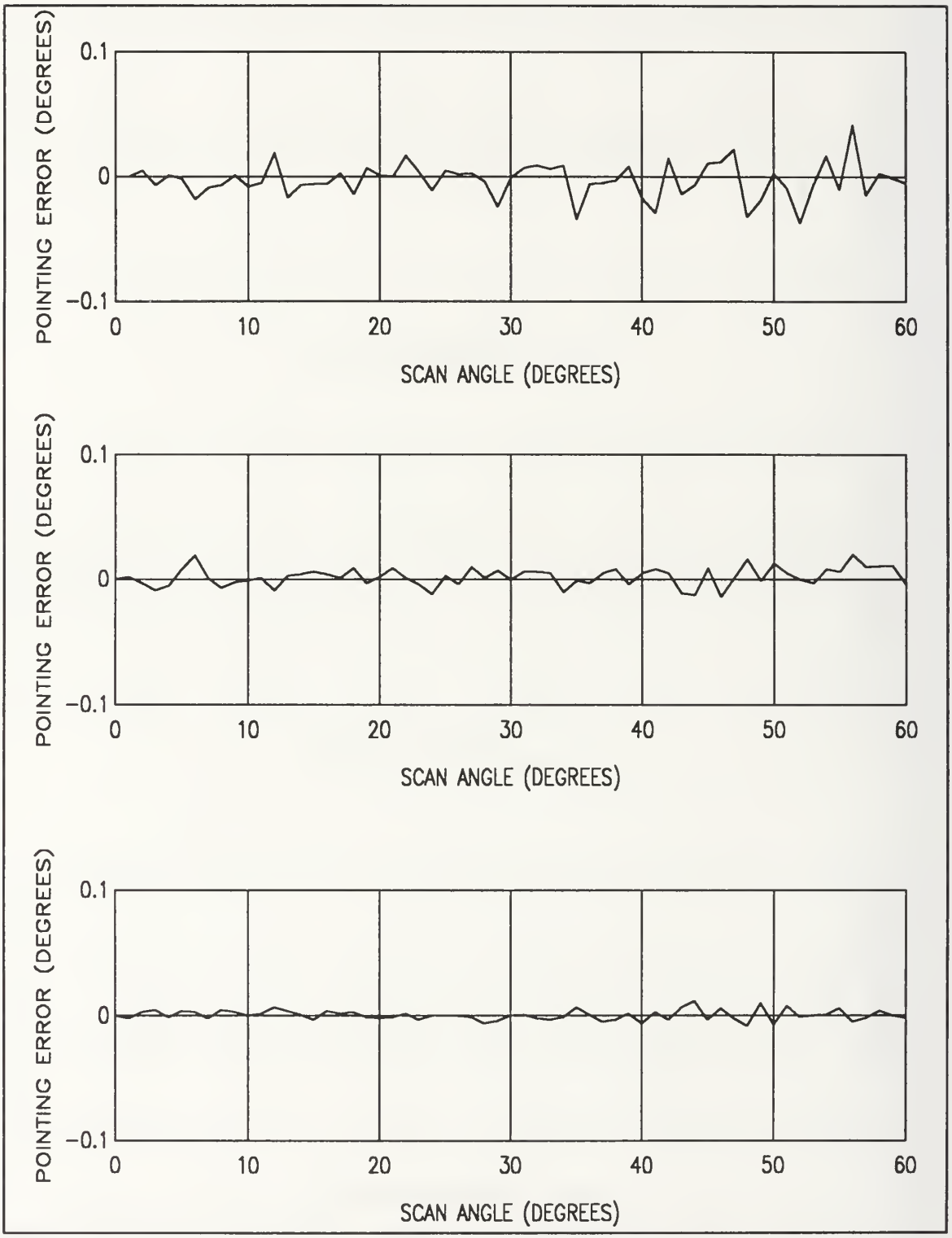

Figure 84. Pointing Error versus Scan Angle for 50 Element Arrays with 3, 4, and 5 Bit Phase Shifters using Symmetric Running Sum Roundoff

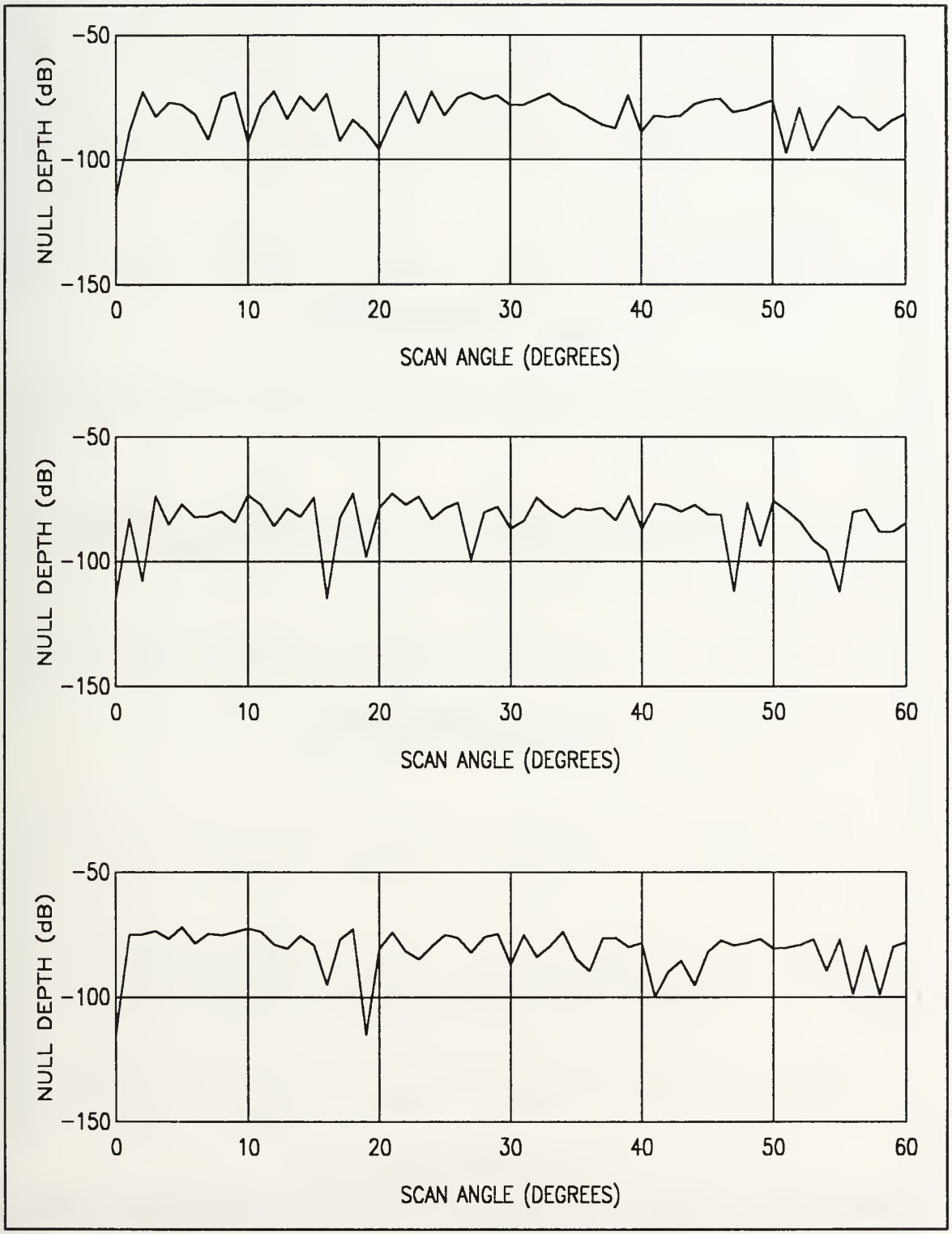

Figure 85. Null Depth versus Scan Angle for 50 Element Arrays with 3, 4, and 5 Bit Phase Shifters using Symmetric Running Sun Roundoff

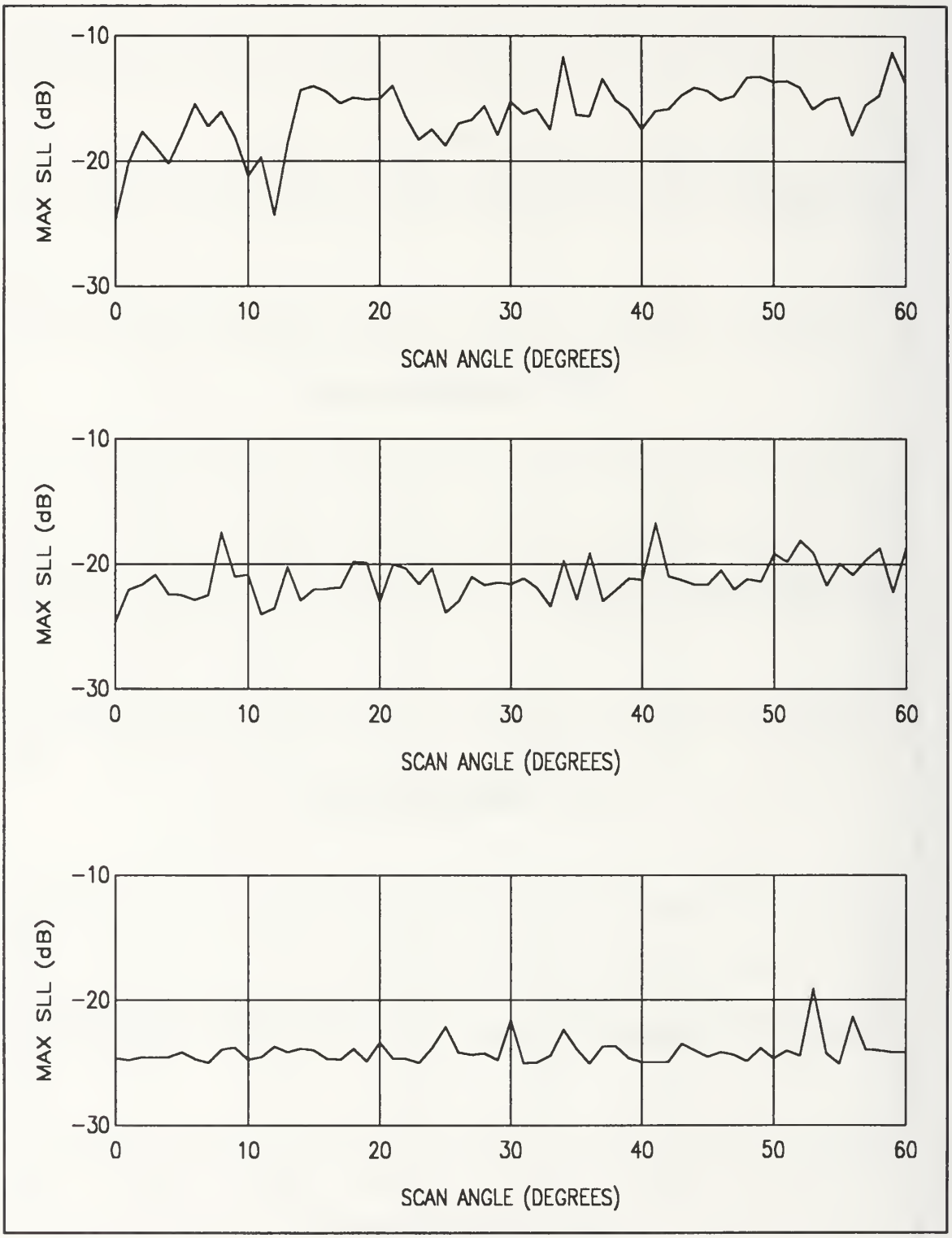

Figure 86. Maximum Sidelobe Level versus Scan Angle for 50 Element Arrays with 3, 4, and 5 Bit Phase Shifters using Symmetric Running Sum Roundoff

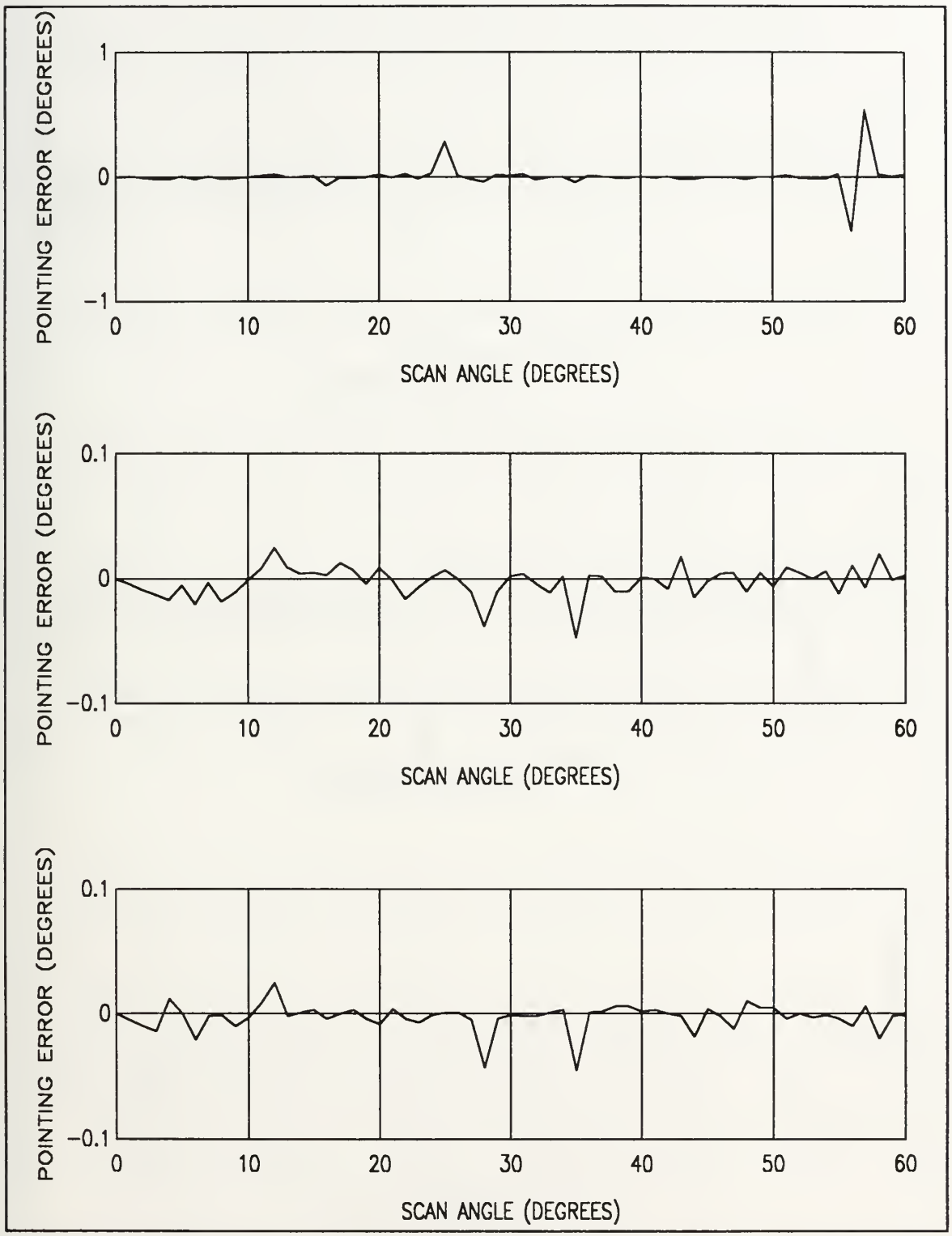

Figure 87. Pointing Error versus Scan Angle for 76 Element Arrays with 3, 4, and 5 Bit Phase Shifters using Regular Roundoff

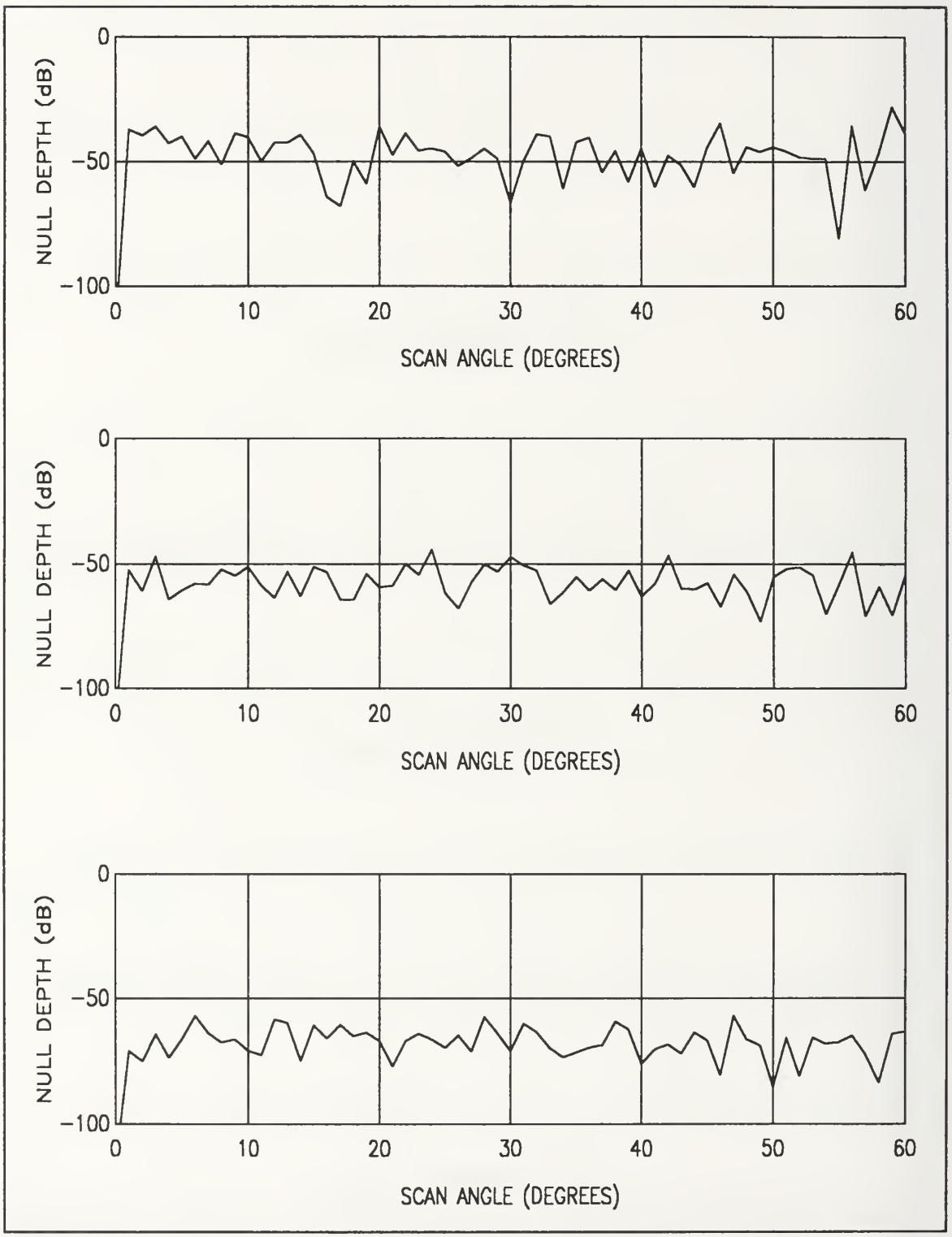

Figure 88. Null Depth versus Scan Angle for 76 Element Arrays with 3, 4, and 5 Bit Phase Shifters using Regular Roundoff

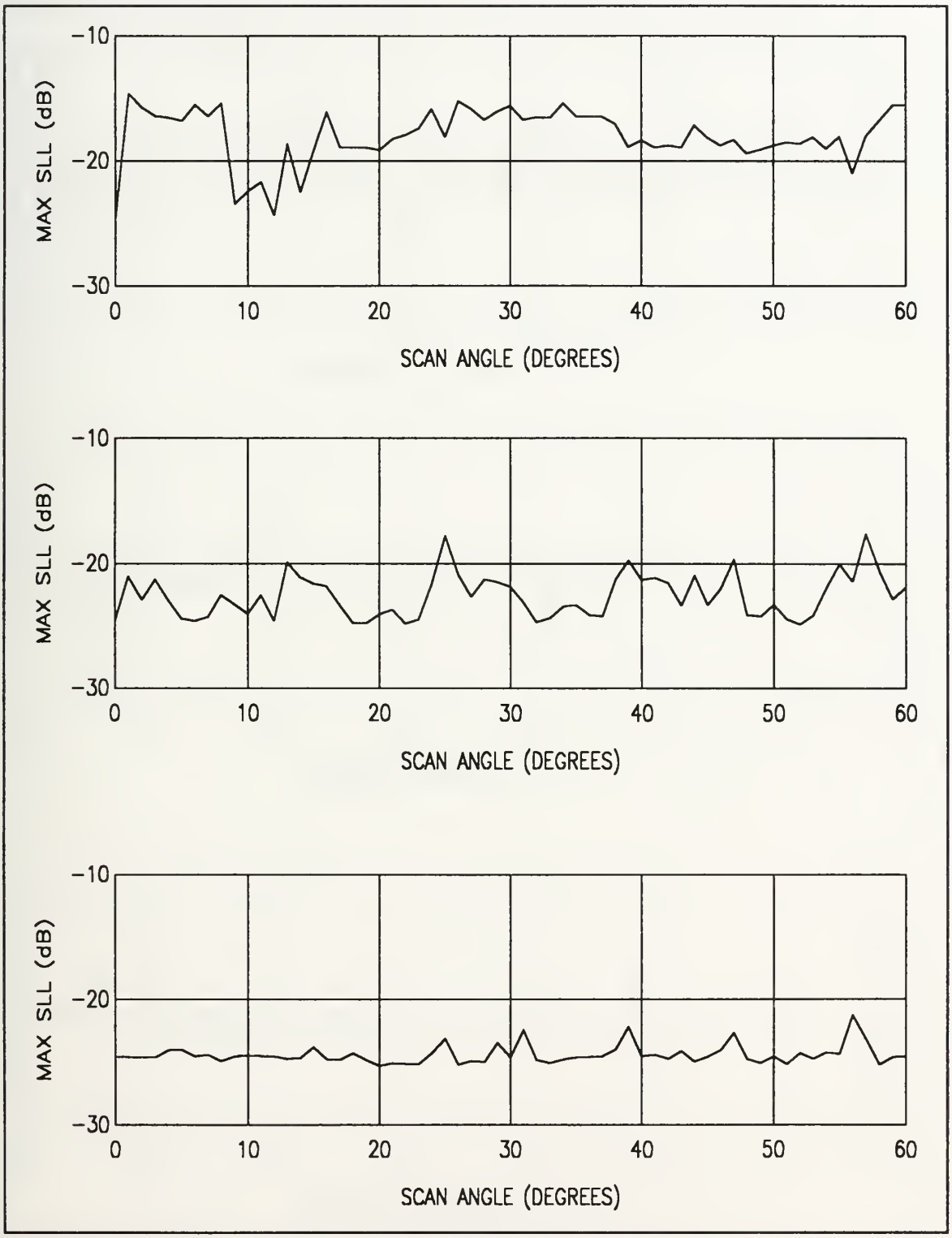

Figure 89. Maximum Sidelobe Level versus Scan Angle for 76 Element Arrays with 3, 4, and 5 Bit Phase Shifters using Regular Roundoff

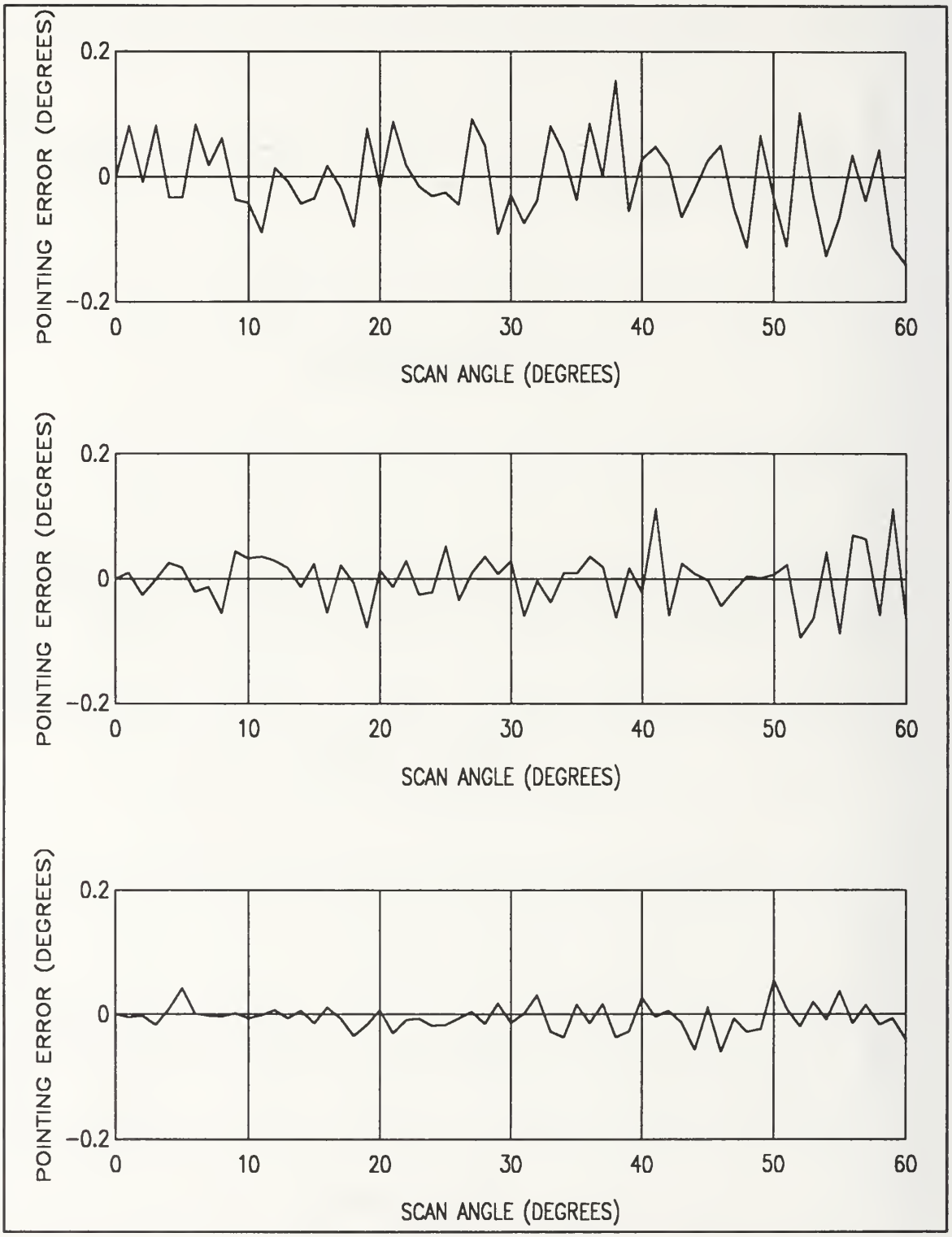

Figure 90. Pointing Error versus Scan Angle for 76 Element Arrays with 3, 4, and 5 Bit Phase Shifters using Weighted Random Roundoff

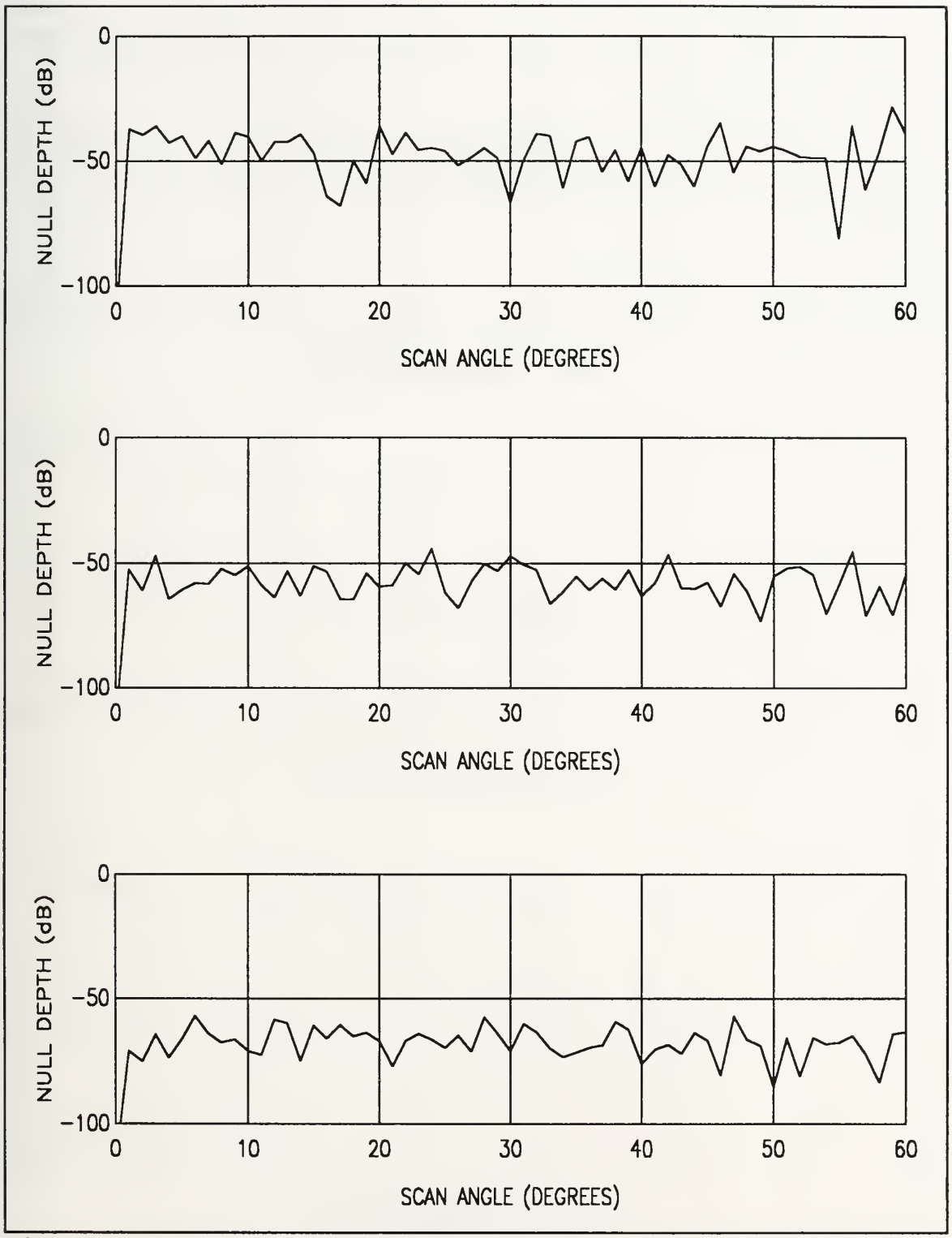

Figure 91. Null Depth versus Scan Angle for 76 Element Arrays with 3, 4, and 5 Bit Phase Shifters using Weighted Random Roundoff

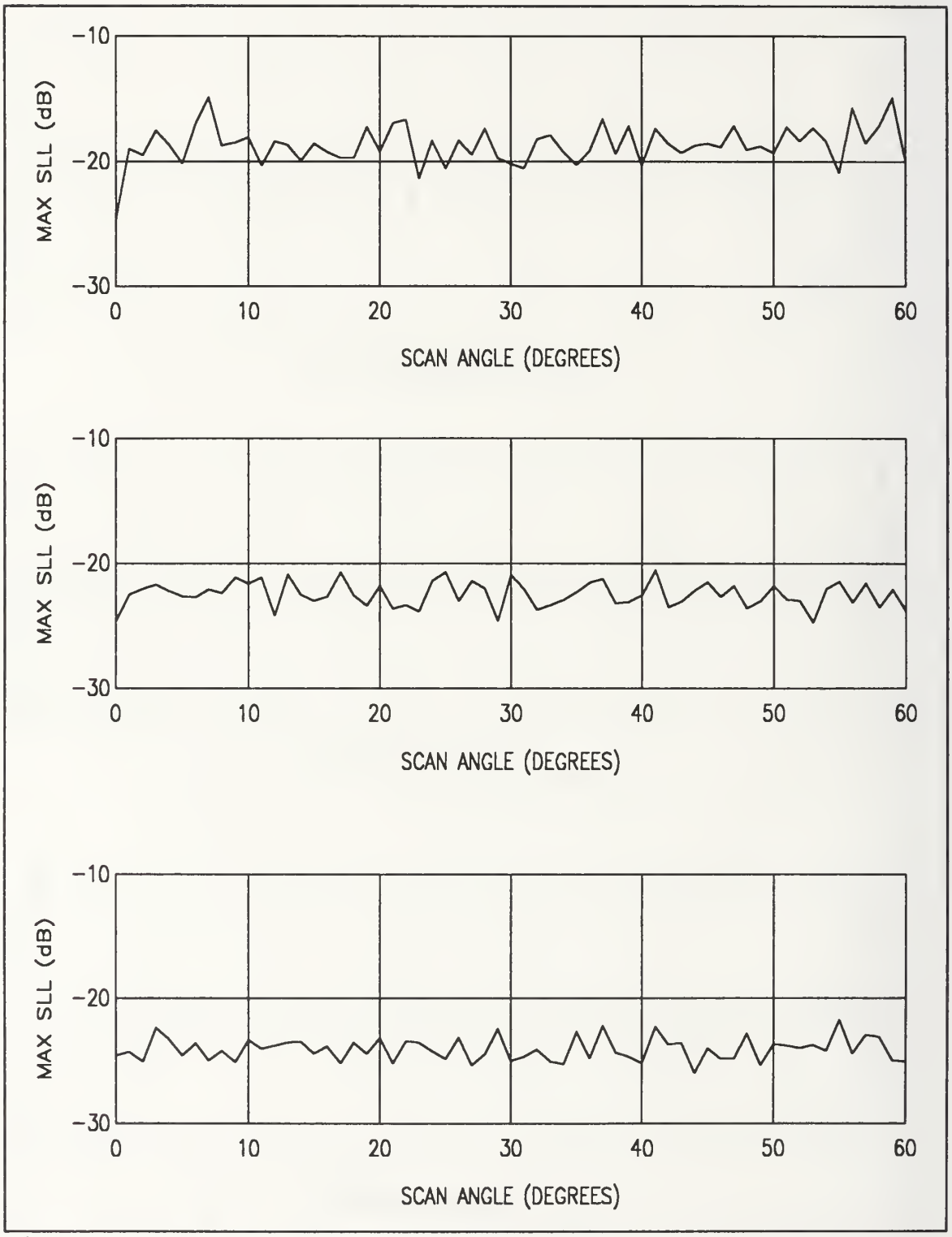

Figure 92. Maximum Sidelobe Level versus Scan Angle for 76 Element Arrays with 3, 4, and 5 Bit Phase Shifters using Weighted Random Roundoff

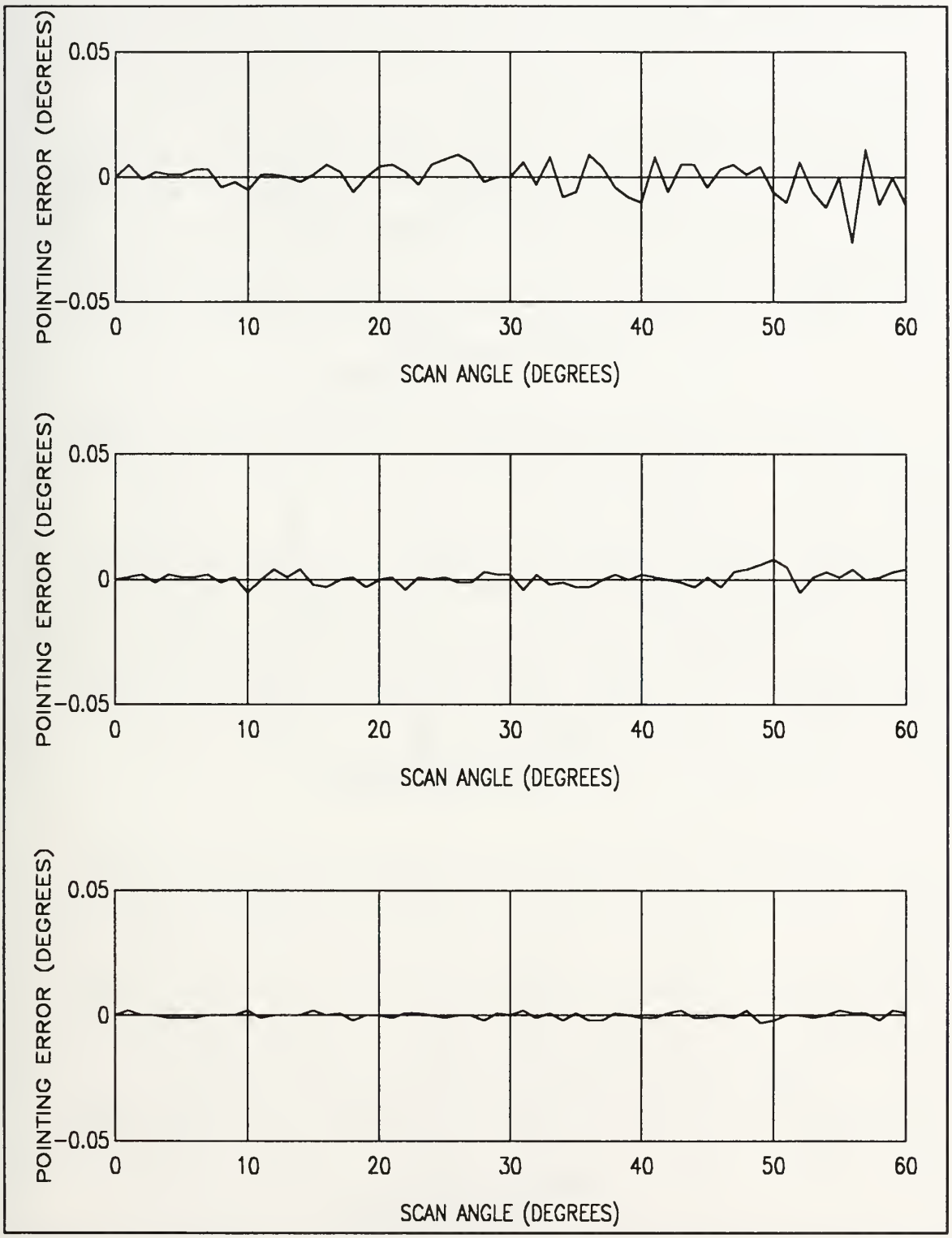

Figure 93. Pointing Error versus Scan Angle for 76 Element Arrays with 3, 4, and 5 Bit Phase Shifters using Running Sum Roundoff

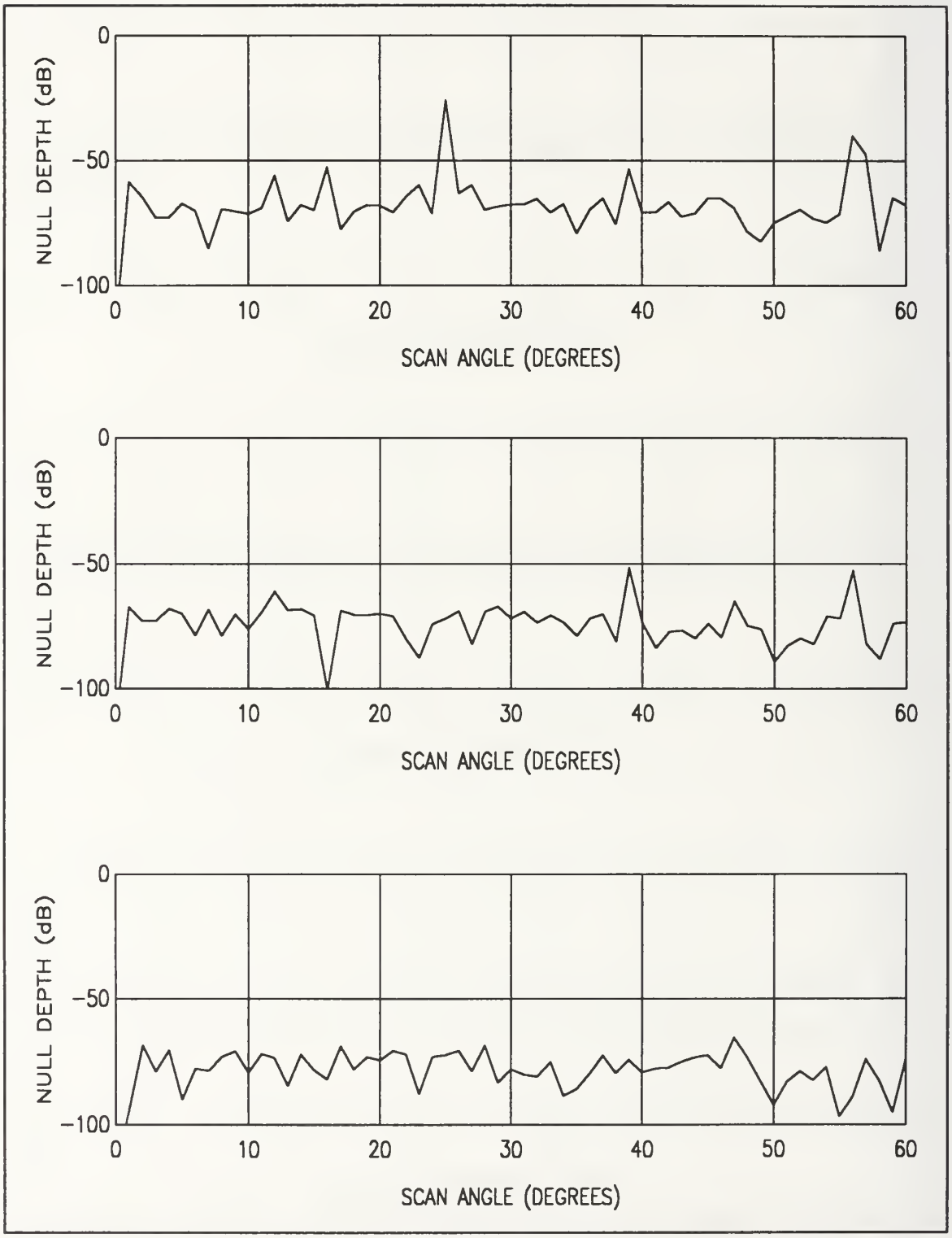

Figure 94. Null Depth versus Scan Angle for 76 Element Arrays with 3, 4, and 5 Bit Phase Shifters using Running Sum Roundoff

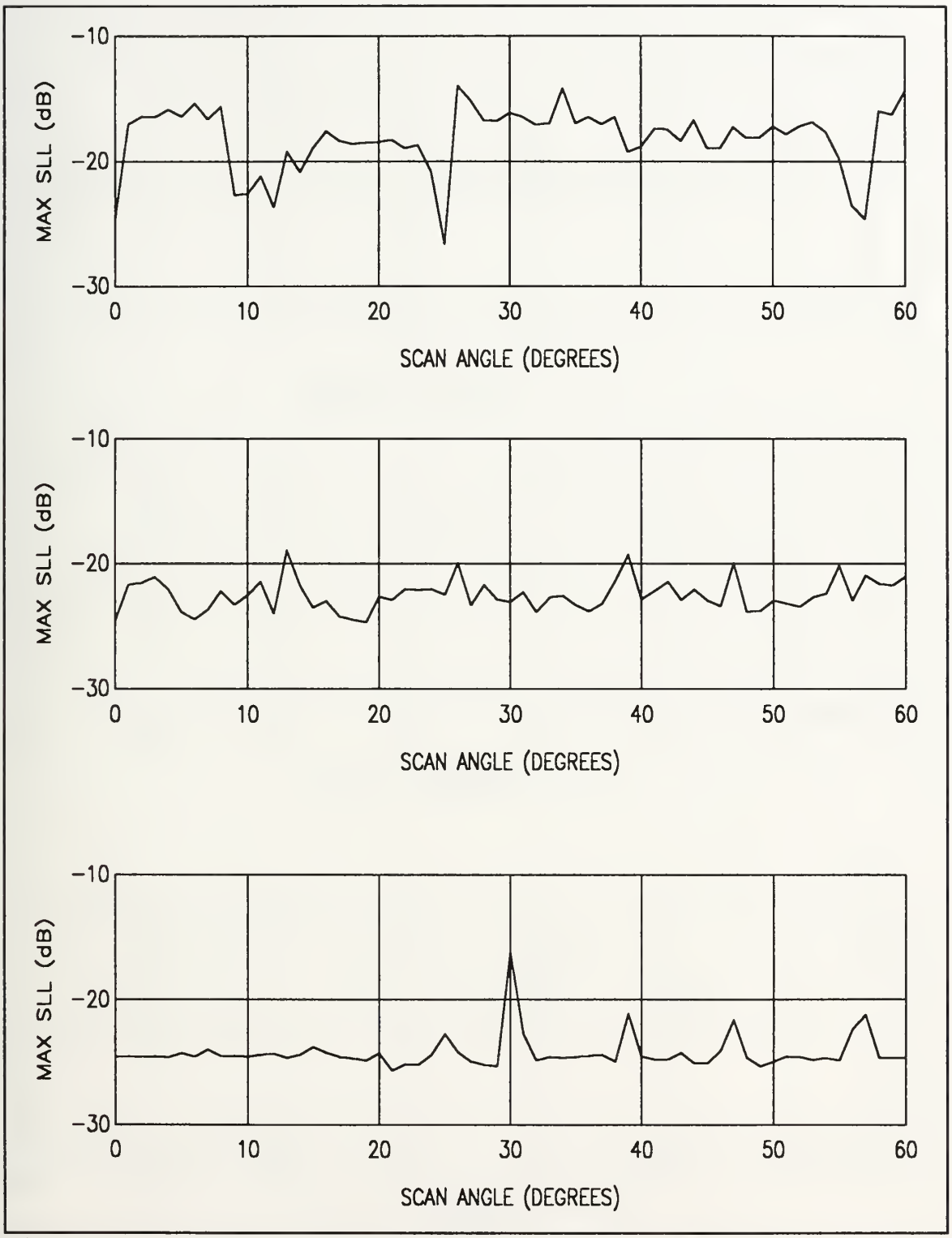

Figure 95. Maximum Sidelobe Level versus Scan Angle for 76 Element Arrays with 3, 4, and 5 Bit Phase Shifters using Running Sum Roundoff

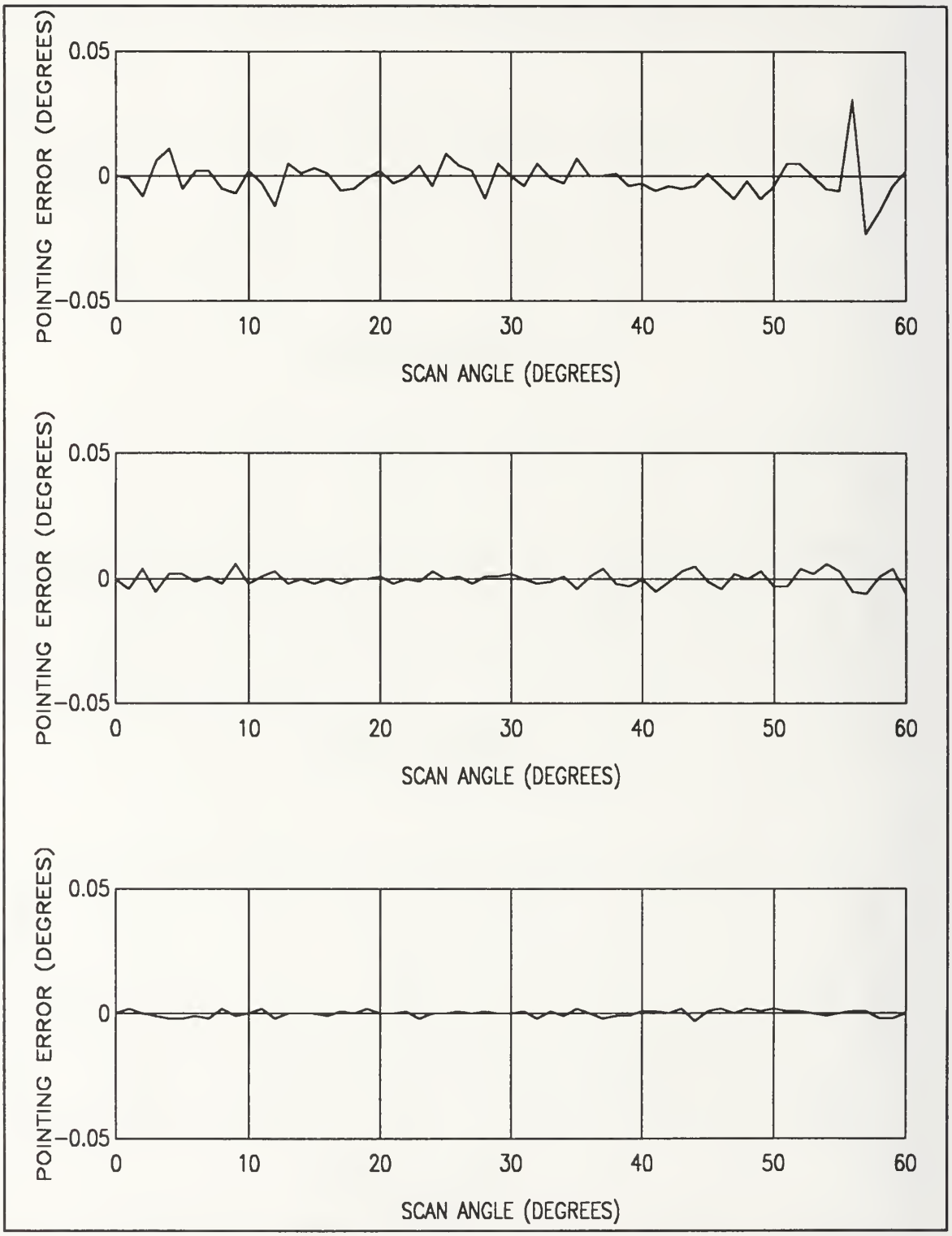

Figure 96. Pointing Error versus Scan Angle for 76 Element Arrays with 3, 4, and 5 Bit Phase Shifters using Symmetric Running Sum Roundoff

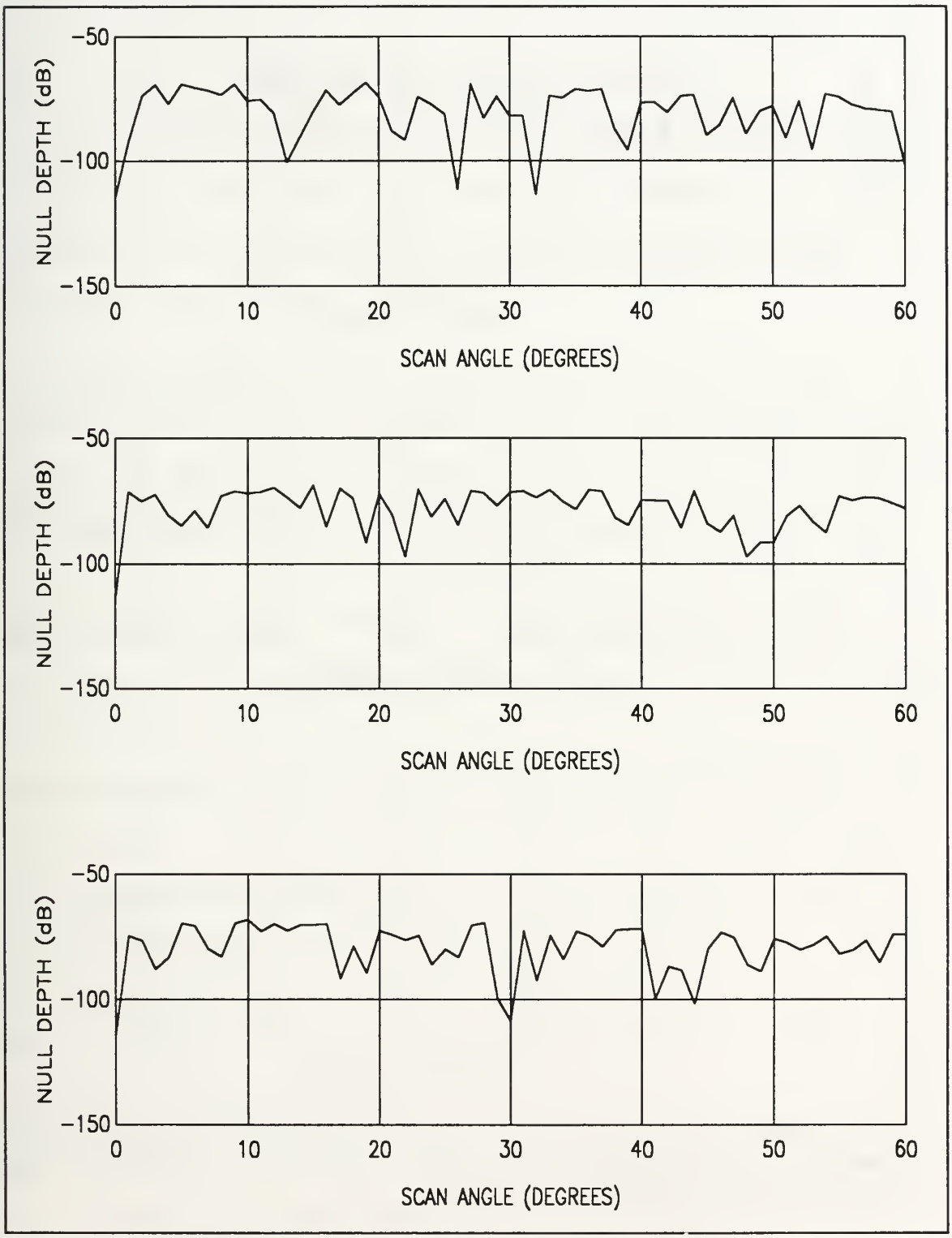

Figure 97. Null Depth versus Scan Angle for 76 Element Arrays with 3, 4, and 5 Bit Phase Shifters using Symmetric Running Sum Roundoff

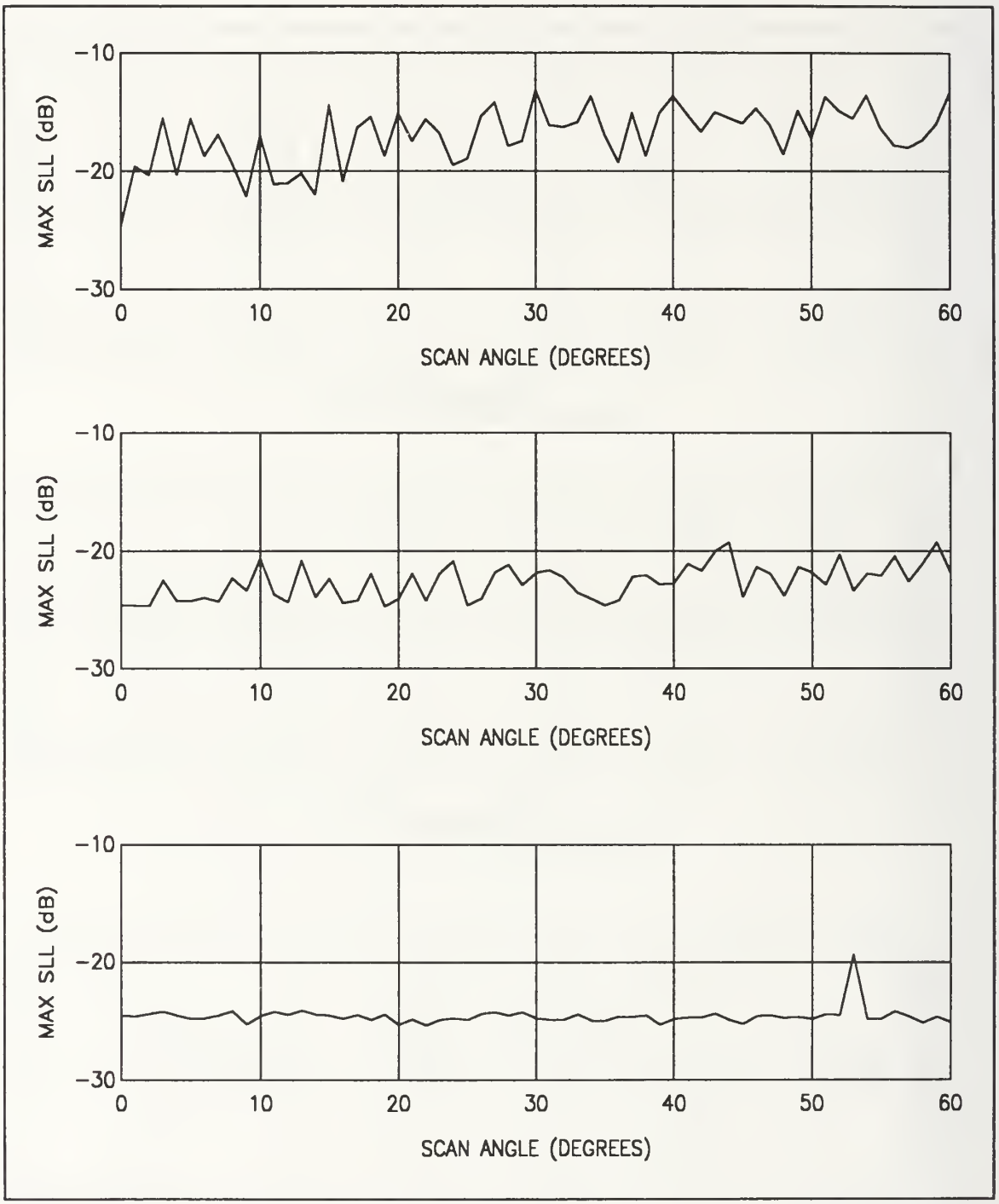

Figure 98. Maximum Sidelobe Level versus Scan Angle for 76 Element Arrays with 3, 4, and 5 Bit Phase Shifters using Symmetric Running Sum Roundoff

APPENDIX C - COMPUTER PROGRAMS

This section includes all the major programs used in compiling the data for this thesis. The programs for plotting and saving the data are not included in this appendix. All programs were written in MATLAB.

A. MAIN PROGRAM

Computes the Radiation pattern of a linear array with either a Bayliss, Taylor, or a Uniform Distribution using any size of Antenna Array with any Bitsize Phase Shifter.

```
begin_scan_angle=0;              % Initializing the initial
end_scan_angle=60;               % conditions for the program
start_angle=-90;
stop_angle=90;
delta=.5;
num_elements=[26 50];
phase_algorithm=1;
bit_size=[3 4 5];
selection=7;
spacing_per_wavelength=.3;
theta_step=1;
w1=1; w2=1; w3=1; w4=1; w5=0;
d1=0; d2=1; d3=0;
```

```
r1=0; r2=1; r3=0; r4=0;
desired_algorithms=[2];
sll=25;
nbar=5;
elem_counter=0;
w6=[];
w7='no';
mainmenu  % Calls a pulldown menu program for parameters
          % modifications
clc
bk=2*pi;
r=pi/180;
del=.5;
it=round((stop_angle-start_angle)/delta)+1;
pe=0;
while selection == 6
a1=length(num_elements);      % The "a" varibles are used to
a2=length(bit_size);          % initialize the size of the
a3=length(desired_algorithms);% arrays depending on the
                              % selections
a4=a1*a2*a3;                  % made for the particular
                              % simulation
a5=length(begin_scan_angle:theta_step:end_scan_angle);
nel=max(num_elements);
pterr=zeros(a4,a5);        % Point Error Matrix
pred_err=zeros(a4,a5);     % Predicted Pointing Error Matrix
```

```
nulldpth=zeros(a4,a5);      % Null Depth Matrix
sllmax=zeros(a4,a5);        % Maximum Sidelobe Level Matrix
ang=zeros(a5,it);           % Angle Matrix
e=zeros(a5,it);             % E Field Matrix
phss=zeros(a5,16);          % Phase State Matrix
amp=zeros(a5,nel);          % Element Amplitude Matrix
xsi=zeros(a5,nel);          % Phase Matrix
qph=zeros(a5,nel);          % Quantized Phase Matrix
trunc=zeros(a5,nel);        % Quantization Error Matrix
scan=zeros(1,a5);           % Scan Angle Matrix
ang1=zeros(a5,2001);     % Angle Matrix for -1 to +1 degrees
                         % about Scan angle
e1=zeros(a5,2001);       % E field Matrix for -1 to +1
                         % degrees about Scan  Angle
count=0;

for element=num_elements
        elem_counter=elem_counter+1;
for phasemod=desired_algorithms
for nbits=bit_size
count=count+1;
ths_count=0;
plot_counter=1;
for ths=begin_scan_angle:theta_step:end_scan_angle
ths_count=ths_count+1;
min1=0;                  % Initializing Variables to Determine
```

```
max1=-120;                  % Pointing Error, Null Depth, and
sllmax1=-120;               % Maximum Sidelobe Level
sllmax2=-120;
scan(ths_count)=ths;

% BAYLISS Coefficients for Difference Beams

if d1 == 1                              % Calling the Appropriate
        taylor                          % program for the Selected
        elseif d2 == 1                  % Distribution
        bayliss
                elseif d3 == 1
                uniform2
end

% Determining the maximum Amplitude to Normalize the
% Amplitudes
am=max(abs(amp(ths_count,1:num_elements(elem_counter))));

if am == 0
am =1;
end
amp(ths_count,:)=amp(ths_count,:)/am;

% Scan Angles in Degrees
```

```
us=sin(ths*r);
psis=bk*spacing_per_wavelength*us;

% Generate exact Phase Required at Each Element. When
% PHASEMOD =0, the Phase is exact and the Phase Slope is
% Continuous ( no Modulo 360 or  2pi. Note that Positive
% Scan Corresponds to Increasing Phase Lag with Increasing
% n.

for i=1:num_elements(elem_counter)
if sym == 1 & phasemod == 3
xsi(ths_count,i)=(-1)*(2*i-(num_elements(elem_counter)+1))/2
                                                    *psis;
else
xsi(ths_count,i)=(-1)*(i-1)*psis;
end
end

if xsi(ths_count,1)
                < xsi(ths_count,num_elements (elem_counter))
       xmin=xsi(ths_count,1);
       else
       xmin=xsi(ths_count,num_elements(elem_counter));
end

% Normalize to the Most Negative Phase so that all xsi(i)> 0
```

```
xsi(ths_count,:)=xsi(ths_count,:)-xmin;
qph(ths_count,:)=xsi(ths_count,:);

% number of BITS is nbit; Number of Phase States is
% 2^(nbit); Each Bit is 360/(2^nbit) Degrees

if phasemod > 0
nstates=2^(nbits);
bitsize=2*pi/nstates;

for i=1:nstates
phss(ths_count,i)=bitsize*(i-1);
end

if phasemod == 1                % Calling the Desired
truncate                        % Roundoff Algorithm
        elseif phasemod == 2
        roundoff
                elseif phasemod == 3
                runround
                        elseif phasemod == 4
                        other
end
end

% Determining the Quantization Error
```

```
trunc(ths_count,:)=qph(ths_count,:)-xsi(ths_count,:);

% Begin Pattern Loop
for i=1:it
th=start_angle+(i-1)*delta;
ang(ths_count,i)=th;
u=sin(th*r);
psi=bk*spacing_per_wavelength*u;
sum=0;
% sum to get Array Factor
for nn=1:num_elements(elem_counter)
q_phase=qph(ths_count,nn);
       if (nn > (num_elements(elem_counter)/2)) & (d2 == 1)
       q_phase=q_phase+pi;
       end

sum=sum+amp(ths_count,nn)*exp(j*(psi*(nn-1)+q_phase));
end

% Normalize the Pattern to the Number of Elements
ev=abs(sum)/num_elements(elem_counter);
e(ths_count,i)=ev^2;
e(ths_count,i)=10*log10(e(ths_count,i));
end

if d2 == 1                          % Refining the Radiation
```

```
        nuldepth                    % increment to .001 Degrees
        elseif d1 ==1 ¦ d3 ==1      % to determine the Point
                max_lobe            % Error, Null Depth, and
end                                 % Maximum Sidelobe Level

pterr(count,ths_count)=pe;          % Saving the Pointing Error
nulldpth(count,ths_count)=min1-max1; % and Null Depth to the
                                        % appropriate Matrix

err_pred                            % Determining the Predicted
                                    % Pointing Error

plot_no1                    % Calling the Plotting Program
                            % for the Radiation Pattern and
                            % Quantization Error
end

plot_no0                    % Calling the Plotting Program
                            % for the predicted versus
                            % calculated pointing Error

mat_save                    % Saving the data to plot the
                            % various combinations of
                            % pointing error, null depth, and
                            % Max. Sidelobe level vs. Scan
                            % Angle
```

```
plot(0:60,pterr(count,:)), grid, xlabel('SCAN ANGLE(DEG)'),
ylabel('POINTING ERROR (DEGREES)'),title(label1)
meta scantot
plot(0:60,nulldpth(count,:)),grid,xlabel('SCAN ANGLE(DEG)'),
ylabel('NULL DEPTH (dB)'),title(label1)
meta scantot
plot(0:60,sllmax(count,:)),grid,xlabel('SCAN ANGLE (DEG)'),
ylabel('MAXIMUM SLL (dB)'),title(label1)
meta scantot
!gpp scantot
!del scantot.met

savefile                                % Saving the data

end
end
end

if w3 == 1
plotcomp        % Plotting the the data save by "matsave"
end

selection =7;
end
```

B. DETERMINATION OF THE POINTING ERROR

This program determines the pointing error, null depth, and maximum sidelobe level for a Taylor Distribution and normalizes the radiation pattern to 0 decibels.

```
del=.5;
it2=-1*(start_angle+1);
it3=-1*(start_angle-1);
for i=((it2+ths)/del):.002:((it3+ths)/del)
th=start_angle+i*del;
angl(ths_count,(i-((it2+ths)/del))*500+1)=th;
u=sin(th*r);
psi=bk*spacing_per_wavelength*u;
sum=0;

% sum to get Array Factor
for n=1:num_elements(elem_counter)
     q_phase=qph(ths_count,n);
     if (n > (num_elements(elem_counter)/2))
     q_phase=q_phase+pi;
     end

sum=sum+amp(ths_count,n)*exp(j*(psi*(n-1)+q_phase));
end

% Normalize the Pattern to the Number of Elements
```

```
ev1=abs(sum)/num_elements(elem_counter);
dummy=ev1*ev1;

if abs(dummy) < 1e-9
     dummy=1e-9;
     end

e1(ths_count,(i-((it2+ths)/del))*500+1)=10*log10(dummy);
ev1=0;
dummy=0;

% Determining the pointing error and null depth

if (e1(ths_count,(i-((it2+ths)/del))*500+1)) < (min1)
min1=e1(ths_count,(i-((it2+ths)/del))*500+1);
theta=th;
pe=theta-ths;
end
end

for i=1:it                          % Determining the location
  if e(ths_count,i) > max1          % of the first maximum
  max1=e(ths_count,i);              % of the differenece beam
  thetamax=ang(ths_count,i);        % radiation pattern
  k=i;
  end
```

```
end

m=k;
max2=max1;

% Determining the location of max null if the maximum of the
% radiation pattern lies on the positive side of the null

if thetamax > theta
        for i=m:-1:1
                if e(ths_count,i) <= max2
                max2=e(ths_count,i);
                k1=i;
                else
                break
                end
        end
b2=k;

% Determining the location of the second maximum of the
% difference beam radiation pattern

        for i=k1:-1:1
                if abs(max2) >= abs(e(ths_count,i))
                max2=e(ths_count,i);
                k2=i;
```

```
                else
                break
                end
        end
b1=k2;
end

% Determining the location of maximum null if the max of the
% radiation pattern lies on the negative side of the null

if theta > thetamax

        for i=m:it
                if e(ths_count,i) <= max2
                max2=e(ths_count,i);
                k1=i;
                else
                break
                end
        end
b1=k;

% Determining the location of the second maximum of the
% difference beam radiation pattern

        for i=k1:it
```

```
                if abs(max2) >= abs(e(ths_count,i))
                max2=e(ths_count,i);
                k3=i;
                else
                break
                end
        end
b2=k3;
end

amax=0;
for i=(b1-2):-1:1                % Determining the location
 if e(ths_count,i) < amax        % of the first null on the
 amax=e(ths_count,i);            % negative side of the scan
        l=i;                     % angle
        else
        break
        end
end

amax=0;
for i=(b2+2):it                  % Determining the location
 if e(ths_count,i) < amax        % of the first null on the
 amax=e(ths_count,i);            % positive side of the scan
        l1=i;                    % angle
        else
```

```
        break
 end
end

for i=1:l                          % Determining the maximum
 if e(ths_count,i) > sllmax1       % sidelobe level on the
 sllmax1=e(ths_count,i);           % negative side of the
 end                               % scan angle
end
for i=l1:it                        % Determining the maximum
 if e(ths_count,i) > sllmax2       % sidelobe level; on the
 sllmax2=e(ths_count,i);           % positive side of the
 end                               % scan angle
end

if (abs(amax)+3) >= abs(sllmax2)
        sllmax2=-1000;
end

if sllmax1 > sllmax2                % Determining the maximum
sllmax(count,ths_count)=sllmax1-max1;  % sidelobe level
else
sllmax(count,ths_count)=sllmax2-max1;
end
```

```
e(ths_count,:)=e(ths_count,:)-max1;  % Normalizing the
                                     % Radiation
yb=min(e1(ths_count,:));             % pattern
if yb <= -89.90
        [xa,xb]=min(e1(ths_count,:));
        e1(count,xb)=-90+max1;
        min1=e1(ths_count,xb);
end
e1(ths_count,:)=e1(ths_count,:)-max1;

x=((it2+ths)/del)+1;
y=((it3+ths)/del)+1;
```

C. BAYLISS DISTRIBUTION

```
Computes Linear BAYLISS Coefficients for Difference Beams
mu=zeros(1,11);
z=zeros(1,10);
b=zeros(1,10);

% Linear Bayliss Distribution

nbar1=nbar-1;
for i=1:11
mu(i)=i-.5;
end
```

```
sll25=sll-25;
z(1)=1.87+sll25*.038;
z(2)=2.5+sll25*.016;
z(3)=3.35+sll25*.019;
z(4)=4.25+sll25*.016;
a=1.45+sll25*.042;

for ns=5:nbar
z(ns)=sqrt(a*a+ns^2);
end

sigma=mu(nbar+1)/z(nbar);

for mms=1:nbar
bb=1;
        for ns=1:nbar1
        bb=bb*(1-(mu(mms)/(sigma*z(ns)))^2);
        end

bbb=1;
        for lls=1:nbar
                if ((lls-mms) < 0) ¦ ((lls-mms) > 0)
                bbb=bbb*(1-(mu(mms)/mu(lls))^2);
                end

        end
```

```
bes=(-1)^(mms);
b(mms)=mu(mms)^2/bes*bb/bbb;
end
for alf=1:(num_elements(elem_counter)/2)
rho=(2*alf-1)/num_elements(elem_counter);

        for lls=1:nbar
        pmu=mu(lls)*pi*rho;
        bes=sin(pmu);
        gg=gg+b(lls)*bes;
        end
amp(ths_count,num_elements(elem_counter)/2+1-alf)=abs(gg);
amp(ths_count,num_elements(elem_counter)/2+alf)=abs(gg);
end
end
```

D. ROUNDOFF ALGORITHMS

1. Regular Roundoff

```
% Computes the Phase at each Array element by Truncation
for i=1:num_elements(elem_counter)
nsteps=round(xsi(ths_count,i)/bitsize);
xs=nsteps*bitsize;
qph(ths_count,i)=xs;
end
```

2. Weighted Regular Roundoff

```
% Program Quantizes Phase Slope using Random Roundoff
for i=1:num_elements(elem_counter)
nsteps=fix(xsi(ths_count,i)/bitsize);
plo=nsteps*bitsize;
phi=plo+bitsize;
qph(ths_count,i)=plo;
xn=rand;
% Criteria for Weighted Random Roundoff
        pnorm=(xsi(ths_count,i)-plo)/bitsize;
        rnd=pnorm+xn;
                if (rnd > 1)
                qph(ths_count,i)=phi;
                end
end
```

3. Running Sum Roundoff

```
% Computes the Phase at each Array element by "the Running
Sum Method" and "Symetric Running Sum Method"

s=0;
if sym == 1
nloop=num_elements(elem_counter)/2;
else
nloop=num_elements(elem_counter);
end
```

```
for i=1:nloop
nsteps=fix(xsi(ths_count,i)/bitsize);
phi_lo=nsteps*bitsize;
phi_hi=phi_lo+bitsize;

sone=s+phi_lo-xsi(ths_count,i);
stwo=s+phi_hi-xsi(ths_count,i);
if abs(stwo) < abs(sone)
s=stwo;
qph(ths_count,i)=phi_hi;
if sym == 1
qph(ths_count,num_elements(elem_counter)+1-i)=-phi_hi;
end
end
if abs(sone) < abs(stwo)
s=sone;
qph(ths_count,i)=phi_lo;
if sym == 1
qph(ths_count,num_elements(elem_counter)+1-i)=-phi_lo;
end
end
end
```

LIST OF REFERENCES

1. Skolnik, The Radar Handbook, pp. 11-2,5,6,9,37,38; 12-2,3,4,5; 21-22, Mc Graw Hill Book Co., 1970

2. Jenn, D.C., "A Criterion for Phase Shifter Roundoff that Minimizes Null Shift", Hughes Aircraft Co., Report LCAJDL (5-1.6-4), April 13, 1981

3. MIT Lincoln Labs Report 248, Physical Limitations of Antennas, by John Ruze, October 1952

INITIAL DISTRIBUTION LIST

		No. Copies
1.	Defense Technical Information Center Cameron Station Alexandria, VA 22304-6145	2
2.	Library, Code 52 Naval Postgraduate School Monterey, CA 93943-5002	2
3.	Chairman, Code EC Department of Electrical and Computer Engineering Naval Postgraduate School Monterey, CA 93943-5000	1
4.	Professor D.C. Jenn, Code EC/Jn Department of Electrical and Computer Engineering Naval Postgraduate School Monterey, CA 93943-5000	2
5.	Lieutenant Commander H.J. Rood, Code EC/Ro Department of Electrical and Computer Engineering Naval Postgraduate School Monterey, CA 93943-5000	1
6.	Lieutenant S.E. Engle 2860 Hayloft Way Morgan Hill, CA 95037	4